

1967

# The strength of heavy welded shapes

William A. Cranston  
*Lehigh University*

Follow this and additional works at: <https://preserve.lehigh.edu/etd>



Part of the [Civil Engineering Commons](#)

---

## Recommended Citation

Cranston, William A., "The strength of heavy welded shapes" (1967). *Theses and Dissertations*. 3504.  
<https://preserve.lehigh.edu/etd/3504>

This Thesis is brought to you for free and open access by Lehigh Preserve. It has been accepted for inclusion in Theses and Dissertations by an authorized administrator of Lehigh Preserve. For more information, please contact [preserve@lehigh.edu](mailto:preserve@lehigh.edu).

Welded Built-Up Columns

THE STRENGTH OF HEAVY WELDED SHAPES

by

William A. Cranston

A Thesis

Presented to the Graduate Faculty

of Lehigh University

in Candidacy for the Degree of

Master of Science

Lehigh University

1967

CERTIFICATE OF APPROVAL

This thesis is accepted and approved in partial fulfillment of the requirements of the degree of Master of Science.

12 June 1967

Date

L Tall

Dr. Lambert Tall  
Professor in Charge

Ray S. Beedle

Dr. L. S. Beedle  
Acting Chairman,  
Department of Civil Engineering

## TABLE OF CONTENTS

	<u>Page</u>
ABSTRACT	
1. INTRODUCTION	1
1.1 Background	1
2.2 Program	2
2. EXPERIMENTAL INVESTIGATION	4
2.1 Test and Measurement Procedures	4
1. Tensile Coupon Tests	4
2. Residual Stress Measurements	5
3. Stub Column Tests	7
4. Column Tests	8
2.2 Test Results	11
1. Tensile Coupon Tests	11
2. Residual Stress Measurements	12
3. Stub Column Tests	17
3. THEORETICAL INVESTIGATION	19
3.1 Tangent Modulus Curves	19
1. Brief History	19
2. Curve Construction	20
3.2 Ultimate Strength Analysis	22
1. Assumptions	22
2. Formulation	23
3. Limitations	29

	<u>Page</u>
4. DISCUSSION OF RESULTS	30
4.1 Tangent Modulus Column Curves	30
4.2 Ultimate Strength Curves	32
4.3 Strength Comparisons	33
5. SUMMARY AND CONCLUSIONS	36
6. ACKNOWLEDGEMENTS	39
7. NOMENCLATURE AND DEFINITIONS	40
8. TABLES AND FIGURES	42
9. REFERENCES	88
10. VITA	90

## ABSTRACT

This thesis presents the results of a preliminary investigation of welded H columns of A7, A36, and A441 steels; of primary interest is the effect on the strength characteristics of using component plates which vary in thickness from 1/2" to 2 1/2".

The sections compared include two light shapes (7H28 and 10H62) and one heavy shape (15H290), with both UM and flame-cut component plates.

The experiments reported are tensile coupon tests, residual stress measurements, stub column tests, and full column tests. The results of these tests are used to formulate a tangent modulus analysis, and based on this, the ultimate strength of axially loaded, pinned-end columns is found. These theoretical analyses are performed using the actual residual stress distributions in the shapes, including the variations across the component plate thicknesses.

It is concluded that there is a strength difference in the heavy sections which is dependent on the grade of steel; that flame-cutting of the component plates improves the strength of both light and heavy welded shapes; that there seems to be little difference in strength due to the type of weld used to join the heavy plates.

## 1. INTRODUCTION

### 1.1 Background

Within the past twenty years, extensive research has been devoted to evaluating the effects of residual stress on the strength of axially loaded, pinned-end columns. (A review of the significant contributions prior to this time can be found in a number of other works <sup>1,2,3,4,5</sup>). This research came about at the instigation of the Column Research Council, which in 1949 realized the importance of considering these "locked-in" stresses in the investigation of column strength.<sup>1</sup> The early work was conducted on rolled columns, and was involved principally with the cooling residual stresses. From this study, it was found that these stresses accounted for the, until then, unexplained transition that is found in the column curve for initially straight columns.<sup>6</sup>

A pilot study connected with this early work was concerned with column shapes built up by welding, and in these tests, a reduction in strength from that of the rolled shapes was noted.<sup>6</sup> As a result of these findings, a full investigation into the strength of columns fabricated by welding was conducted. The results of this project confirmed the lower strength for welded H-shapes, while the welded box shapes displayed strengths approaching that of the rolled.<sup>7</sup> The reason for the strength reduction can

be traced, primarily, to the welding residual stress pattern in the H-shapes, as well as to initial out-of-straightness, which tends to be greater in welded than in rolled columns<sup>2,7,8</sup>.

Indications from these programs and from a knowledge of the process of residual stress formation were that an increase in strength could be realized by altering the residual stress pattern in some way: by annealing, flame-cutting of component plates, application of a weld bead to the flange tips of the shape, or some other method<sup>2,8</sup>. Until that time, research had been conducted on plates 3/4" or under. Thus, it was thought that using an increased plate thickness would give greater strength, since the ratio of weld area to total cross-sectional area, and consequently, the relative heat input, would be less than in the light shapes, and the stress pattern would vary across the plate thickness and perhaps be less of an influence<sup>7,8</sup>.

## 1.2 Program

The investigation reported here is a pilot study on welded built-up columns using component plates which were over one inch in thickness. The work involved both UM\* and flame-cut plates welded to form H-shaped columns.

Primarily, three shapes are compared in this report. There are two light shapes, a 7H28, and a 10H62. Both were

\* UM = Universal Mill



fabricated from ASTM A7 steel and joined by fillet welds. The heavy shape (only one was tested) was a 15H290 shape\* of both ASTM A36 and A441 steels, with both full and partial penetration welds. Table 1 and figures 1 and 2 give particulars on these shapes.

The light shapes with UM component plates were tested previously, and the results have been presented in an earlier work.<sup>7</sup> They will be used for comparative purposes with the heavy shape and the other light shapes with flame-cut plates.

---

\* The designation "H" was adopted to denote a welded built-up shape.

## 2. EXPERIMENTAL INVESTIGATION

### 2.1 Test and Measurement Procedures

The investigation took on both a theoretical and experimental aspect. The experimental tests which were performed were: tensile coupon tests, residual stress measurements, stub column tests, and full column tests. It should be noted that there were no full column tests in the series involving the heavy shape, since there were no pinned-end column fixtures of sufficient capacity available.

#### 1. Tensile Coupon Tests

The tensile coupon tests were performed to obtain or verify the mechanical properties of the steels being studied. Most of the tests were performed on the ASTM standard 8 inch flat and 1/2 inch round coupons, while some were on non-standard 8 inch and 2 inch coupons. The non-standard 8 inch coupons were in all respects the same as the standard flat specimens, except that they were not full thickness pieces. The area was reduced in order to utilize a smaller capacity mechanical testing machine which had greater accuracy than the larger hydraulic machines. The non-standard 2 inch coupons were cut from residual stress sectioning specimens and were primarily in the weld areas.

The yield stress, that was used in the computations was the static yield stress level <sup>6,9</sup>. This is the stress level which occurs in the plastic portion of the stress-strain curve at a zero rate of strain. In other words, the movable crosshead of the testing machine is brought to a halt, and allowed to come to equilibrium with the specimen. A drop in load is noted as well as an increase in strain, and when all motion has ceased, the static yield stress level has been reached.

## 2. Residual Stress Measurements

Residual stress measurements were made on all pieces to determine the welding and cooling residual stress patterns in all of the shapes. Only one set of measurements was taken for each specimen used, since it was found previously <sup>6,10,11</sup> that the variation of residual stress along the length of a column is negligible, except for a distance near the ends which is about equal to the depth of the member.

All residual stress measurements were made by the method of sectioning, in which relaxation of stress is accomplished by sawing of the specimen into strips <sup>12</sup>. The procedure is as follows (the letters refer to parts of Fig. 3):

The plate element (a plate, flange, web, etc.) is laid out with a system of gage holes for a measuring apparatus (in this case, a 10 inch Whittemore strain gage), as shown in the figure (A). These holes are on both sides of

the element. A measurement, reading number one, is taken and the plate is cut into strips by sawing along the dashed lines, giving each specimen two sets of gage holes (one on each side) (B). Another reading is taken, reading number two, and the residual strain is found by dividing the difference in the readings by the gage length. For plates under one inch in thickness, the sets of gage holes on each side of the plate should give approximately equal readings, since there is little variation across the thickness of the plate element. Thus the final strain reading will be the average of the two sides.

However, in the heavy shape, plates were up to 2 1/2 inches in thickness, and the readings on each side differed quite significantly; further measurements had to be made. This was accomplished by laying out gage holes on each individual, previously-cut, specimen (C) where again there were gage holes on each side of the element. A measurement (number three) was taken, and the second set of saw cuts was made, whereupon reading number four was taken (D). The variation of residual strain across the plate thickness was then obtained by dividing the difference of these last two readings by the gage length.

The base upon which these variations are superimposed must be an assumed one. In this case, beam-type action was presumed to occur in each specimen after the initial cutting, and previous to the second relaxation, and consequently a

straight line variation of stress would result. Superimposing these last strains on this straight line, we obtain the total residual strain variation across the thickness of the section (E).

A ten inch Whittemore strain gage was used to make these measurements because it gives a reading over a relatively large distance, averaging out most discontinuities and localized disturbances and giving more reproducible results.

### 3. Stub Column Tests

Stub column tests were performed in order to obtain stress-strain curves which would include the effects of residual stresses present in the sections. The tests were conducted according to the Stub Column Test Procedure presented as an appendix to reference 1. In brief, the stub column is a section of a specimen which has a slenderness ratio that is low enough to preclude any general column buckling. In this way it resembles a large compression coupon except that it is not stress relieved.

The test was conducted much like a compression coupon test. The specimen was aligned in the machine geometrically and instrumented. Figure 4 shows two schemes of instrumentation using dial gages. Around the base of the specimen are four gages attached to the top end plate by tight wires, used for attaining and checking alignment.


Next to the column is a gage for measuring crosshead movement. At the mid-height of the column are mounted two 10,000<sup>th</sup> inch dial gages for strain measurement during the test. The upper picture shows these gages fastened by tack welds. The lower shows the gages mounted on a rack arrangement. If desired, some or all of the dials may be replaced with wire-resistance strain gages, but the dials are preferred since they give average values.

When the instrumentation was complete and the white-wash applied, the alignment was performed. (Whitewash is used to show the flaking of mill scale, indicating the progress of yielding.) The specimen was loaded to a point below the proportional limit, and the corner dial gages checked. Only when the gages read to within 5% of the average was the load considered axial. Adjustment was made by tilting the top crosshead of the machine.

The actual test was performed by loading the specimen in increments and taking static readings. The reading was taken after the crosshead dial gage showed that all movement had ceased. A continuing plot of load versus deflection was maintained to check test progress and to aid in choosing the increments of loading.

#### 4. Column Tests

Column tests were conducted to obtain experimental verification of theoretical column strengths; they were conducted only on the lighter shapes.



Next to the column is a gage for measuring crosshead movement. At the mid-height of the column are mounted two 10,000<sup>th</sup> inch dial gages for strain measurement during the test. The upper picture shows these gages fastened by tack welds. The lower shows the gages mounted on a rack arrangement. If desired, some or all of the dials may be replaced with wire-resistance strain gages, but the dials are preferred since they give average values.

When the instrumentation was complete and the white-wash applied, the alignment was performed. (Whitewash is used to show the flaking of mill scale, indicating the progress of yielding.) The specimen was loaded to a point below the proportional limit, and the corner dial gages checked. Only when the gages read to within 5% of the average was the load considered axial. Adjustment was made by tilting the top crosshead of the machine.

The actual test was performed by loading the specimen in increments and taking static readings. The reading was taken after the crosshead dial gage showed that all movement had ceased. A continuing plot of load versus deflection was maintained to check test progress and to aid in choosing the increments of loading.

#### 4. Column Tests

Column tests were conducted to obtain experimental verification of theoretical column strengths; they were conducted only on the lighter shapes.

These tests were performed on columns which were in the pinned-end condition, since this is the basic column of most design specifications and curves. The end condition was achieved by the use of column end fixtures designed at Lehigh University<sup>13</sup>. The principle is that of a cylindrical surface bearing on a horizontal plane, but with the center of curvature of the cylindrical portion located at the base of the specimen so that the slenderness ratio can be determined using the actual length of the column. As these cylinders rotate when the column deflects, the load remains on a line passing through the center of the column base and is still axial. Figure 5 shows this action, as well as a schematic view of the bottom end fixture.

#### Instrumentation

The instrumentation of the specimen consisted of electrical wire-resistance strain gages for strain measurement, dial gages for measurement of deflections, strip scales mounted along the column flange to measure out-of-straightness and lateral deflection, and level bars to measure end fixture rotation.

The electrical strain gages mounted at the mid-height, top, and bottom, and at intermediate points on the column, were used in alignment and to record strain readings. At the mid-height a dial gage was mounted and connected to the column by a tight wire to measure mid-height deflection of



the column during the test. Another dial gage recorded crosshead movement and was used to indicate at what point load stabilization had taken place. The strip scales, attached at the mid-height, ends, and intermediate points, were read with a surveying transit to record lateral deflection at a number of points along the specimen. A point on the laboratory floor served as a reference for readjusting the transit when it was disturbed, and a scale on the machine crosshead indicated lateral machine movement. The end rotation level bars were precision levels mounted on brackets which were welded to the base plates of the column. By turning a micrometer screw, the level could be brought to the horizontal position, and the amount of adjustment could be determined from an attached dial gage on a 20 inch lever arm. As a further check on strain readings, gage holes on a 10" gage length were drilled at the column mid-height for a Whittemore strain gage. All of these instruments and their locations are shown in Fig. 6.

#### Alignment

Once the specimen had been erected in the testing machine, geometrically aligned, instrumented, and white-washed, the alignment was performed. The column was loaded to a point well below the proportional limit and the strain was read on the corner strain gages at the mid-height and ends. If these were not equal, the crosshead was tilted, or the column shifted in the fixtures, and then reloaded.

The alignment was considered satisfactory when all readings were within 5% of the average at each of the three gage points.

### Test

The column was given an initial load of about  $40^k$  and a zero reading was made on all dials and gages. The initial eccentricity of the column was read through the transit. When these preliminaries were completed, the column was loaded in increments and static readings were taken as in the stub column test when the crosshead dial gage indicated that all movement had ceased. Readings were taken until after the ultimate load had been reached and passed, after local buckling was observed. The specimen was then unloaded, and the permanent set was noted.

## 2.2 Test Results

### 1. Tensile Coupon Tests

The results of the tensile coupon tests are found in Table 2. An interesting point in the tensile tests was that in the heavier 15H290 shapes, some of the coupons displayed a total lack of a yield plateau (Fig. 7). Upon reaching the stress at which yield would be expected to occur, strain hardening commenced and continued until ultimate load. This same type of curve was found in the stub column tests. This has a definite effect on one assumption

for the tangent modulus concept, that is: the material is perfectly elastic-plastic. Since not all of the coupons showed this phenomenon (and those which did were all flange coupons), the total effect on the column strength cannot be readily evaluated until more work is done.

## 2. Residual Stress Measurements

### Shapes Composed of U.M. Plates

The residual stresses that are discussed in this report are principally due to the plastification of all or a part of a section from thermal action. The part of the section to cool last is usually the part that will contain the tensile stress, this being balanced by the compressive stress set up in the parts away from the weld or molten area<sup>14</sup>. Thus, if a part of the section can be maintained in the molten state after the rest has cooled, tensile stress can be induced, and depending on the location, the strength of the column may be increased.

In a rolled H-shape, the last part to cool will be the area around the junction of web and flange, and it will contain the tensile stress; Fig. 8 for the 8WF31 section. The tensile stresses are not the critical ones; the location and magnitudes of the compressive stresses are the controlling influences on the amount of strength reduction that will occur in a compression member. The pattern in the 8WF31 shape (Fig. 8) shows compressive

stresses in the flange tips, at the maximum distance from the axis of bending (weak axis), and upon yielding the result will be the greatest possible reduction in the load-carrying capacity of the column.

For the light welded shapes composed of universal mill plates, the residual stress pattern is shown in Fig. 9. The distribution resembles that of the rolled shape in that the compressive stresses are in the flange tips, but the magnitudes are higher. Therefore, when the column is loaded, the outer portions of the flanges will yield sooner, and the loss in strength compared to the rolled shape will be greater.

Looking next at the heavy shapes, the rolled 14WF426 is the heaviest rolled section to be tested to date.<sup>15</sup> The stress distribution is shown in Fig. 10. Again there is the same general distribution, except that there is also a variation across the plate thicknesses. (No measurements were made at the time to find the type of variation). Note the high stress due to cooling alone.

Comparing this with the heavy welded shape composed of Universal Mill plates, fillet welded, of A36 steel (Fig. 11) there is again a similar distribution, with the compressive stress in the flange tip. However, even though the ratio of weld area to total cross-sectional area is smaller than for the light shapes (for example,  $\frac{1}{170}$  for the heavy shape versus  $\frac{1}{115}$  for the 7H28), the compressive stresses are quite high,

approaching seventy-five percent of the yield value in some places. The explanation of this can be found in the initial stresses present in the plate prior to welding. It was found from past tests that the residual stress distribution due to cooling in plates of one inch in thickness could be significant. For example, Fig. 12 shows the cooling residual stresses in a plate 20" x 1". The stresses attain a magnitude of 23 ksi. at one edge or approximately  $\frac{2}{3}$  the yield stress<sup>16</sup>. Thus, in the heavy shapes with plates up to 2 1/2 inches thick, the cooling stresses will tend to be quite high, while the welding process will contribute relatively little to this<sup>17</sup>; that is, the source of the high stresses in the shape is principally the initial cooling stresses in the plate.

Figure 13 shows the variation of residual stress across the thickness of the component plates for the mild steel, fillet welded specimen. The variation is either slightly parabolic or straight line in nature in the area away from the weld. If the parabolic shape could be accentuated, or in other words, if tension could be retained in the center of the plate elements, there would be a "core" of stiffer material to sustain the column after the external fibers had yielded. But, in this case, the welding process has erased these tensile stresses. One advantage is that it may be possible to predict the stress in the plate interior with merely a knowledge of the surface measurements

and a straight line interpolation between. There are some non-destructive testing techniques (x-ray, for example) which can measure these surface values quite accurately. However, more work, and more shapes, are needed before this can be said with certainty.

Figures 14, 15, and 16 show the stress distribution in the other shapes composed of UM plates. The A36 specimen with groove welds is quite similar to the previous section, but the A441 steel sections show a somewhat lower compressive stress magnitude in the edges of the flanges, which is in agreement with the earlier findings that the residual stress magnitudes will vary inversely with the parent metal yield stress <sup>17</sup>.

The variations through the thickness of the plates for these specimens are basically the same as that for the A36, fillet welded, specimen.

#### Shapes Composed Of Flame-Cut Plates

The flame-cutting of the component plates can be expected to give a more favorable stress distribution, due to the fact that the flange edges will have been in the molten state subsequent to any other part of the plate prior to welding. As mentioned previously, tensile stress should occur in this area. In narrow plates, this tensile stress would be completely erased by a center weld. However, the plates used here can be considered wide, and the tensile

stress in the edges will remain after welding, although decreased somewhat in magnitude<sup>8</sup>.

Figure 17 gives the stress distribution for the light shapes composed of flame-cut plates. The distribution has been altered considerably by the cutting process, and thus an increase in column strength should be expected.

The distribution for the heavy shape composed of A36 steel, with partial penetration fillet weld is shown in Fig. 18. Again, there are tensile stresses in the flange tips but of a smaller magnitude. The reason for the smaller magnitude is not known, since details of the flame-cutting operation were not obtained at the time of rolling and fabrication. The variation of this stress across the plate thickness (Fig. 19) is similar to that in the shapes composed of UM plates, with either slightly parabolic or straight line variation.

The distribution for the mild steel specimen with full penetration weld (Fig. 20) is similar to that for the fillet welded specimen.

The sections composed of A441 steel, however, show a somewhat different pattern (Figs. 21 and 22). The very high stress in the flange tips of both shapes is readily evident, exceeding the yield stress in some places. Since only one heat of this steel was tested for the flame-cut

plates, and only one cutting operation was involved, the reproducibility of these very high stress magnitudes cannot be certain until more work is conducted on heavy shapes of high strength steel.

### 3. Stub Column Tests

Stub column test results are shown in Figs. 23 and 24 for the shapes composed of UM plates, and in Figs. 25 and 26 for those of flame-cut plates. Checking these curves with the residual stress distributions, the dependence of the proportional limit on the residual stress magnitudes can be seen. For example, in the 7H28 shape composed of flame-cut plates (Figs. 17 and 25) the proportional limit is about 12 ksi, and the maximum residual stress value is about 24 ksi, which total up to the yield stress of 36 ksi found from this same stub column test.

The yield stress levels were found by taking the stress at the 0.5% strain as recommended in Appendix B of reference 1. Although this method has been found to give results that are high <sup>18</sup>, in the specimens tested here, there is good agreement with the yield stress obtained from the tensile coupon tests.

It is evident on all the curves that they lack a "plastic" portion, that is, there is continual strain hardening once the knee of the curve has been passed, much like some of the tensile coupons. This is probably due primarily



plates, and only one cutting operation was involved, the reproducibility of these very high stress magnitudes cannot be certain until more work is conducted on heavy shapes of high strength steel.

### 3. Stub Column Tests

Stub column test results are shown in Figs. 23 and 24 for the shapes composed of UM plates, and in Figs. 25 and 26 for those of flame-cut plates. Checking these curves with the residual stress distributions, the dependence of the proportional limit on the residual stress magnitudes can be seen. For example, in the 7H28 shape composed of flame-cut plates (Figs. 17 and 25) the proportional limit is about 12 ksi, and the maximum residual stress value is about 24 ksi, which total up to the yield stress of 36 ksi found from this same stub column test.

The yield stress levels were found by taking the stress at the 0.5% strain as recommended in Appendix B of reference 1. Although this method has been found to give results that are high<sup>18</sup>, in the specimens tested here, there is good agreement with the yield stress obtained from the tensile coupon tests.

It is evident on all the curves that they lack a "plastic" portion, that is, there is continual strain hardening once the knee of the curve has been passed, much like some of the tensile coupons. This is probably due primarily

to the greater strength of the weld material and in some cases due to the properties of the material shown in the tensile tests (Fig. 7).

Another interesting result of the stub column tests is the occurrence of what might be called "cross bending" in the heavy column shapes composed of flame-cut plates. Figure 27 shows specimen C10 (flame-cut plates, A36 steel, fillet welds) after the completion of the test. Note the "wavy" appearance of the flanges. This was first noticed at a load of about 4.5 million pounds (53 ksi) and the values of flange deflection are shown at the bottom of the figure. As is evident, this is different from the local buckling phenomenon usually noted in stub column tests, where the flanges "rotate" about the web-flange joint.

### 3. THEORETICAL INVESTIGATION

#### 3.1 Tangent Modulus Curves

##### 1. Brief History

The buckling analysis used in this program was based on the tangent modulus concept. This was first proposed by Engesser in 1889 when he suggested that the column strength of an axially loaded specimen might be found if the "tangent modulus", or the slope of the stress-strain curve at a particular point, were substituted for the initial modulus in Euler's buckling equation. During the following years, under a number of influences, Engesser realized that upon buckling the fibers on the convex side of the column would begin unloading, and so he abandoned the tangent modulus theory, proposing in 1895 the reduced modulus theory. Again using the Euler equation, a substitution is made for the initial modulus, but in this case it is the "reduced" modulus which is dependent on both the tangent modulus (loading portion of curve) and the initial modulus (unloading portion) as well as on the cross-sectional properties of the column.

From the classical concept of instability, the reduced modulus theory was the correct one, but tests seemed to indicate that failure would occur at a load that more closely approximated the tangent modulus load. This paradox

was explained by Shanley in 1946 when he resurrected the tangent modulus theory as the true column buckling theory. He stated that the tangent modulus load was that load at which bifurcation could take place with no strain reversal occurring in the convex side of the column. Stated another way, this is "the lowest load at which bifurcation will occur whether or not an increase in axial load is required."<sup>3</sup>

## 2. Curve Construction

This "Shanley load" is the buckling load used in this analysis, and for a rectangular member it is given by:

$$\frac{P_t}{P_y} = \frac{\pi^2 E_t}{\sigma_y (L/r)^2}$$

where:  $P_t$  is the tangent modulus load

$P_y$  is the yield load

$\sigma_y$  is the yield stress

$L/r$  is the (effective) slenderness ratio of the column.

The tangent modulus,  $E_t$ , for steel can be found from the consideration that the residual stresses will cause uneven yielding over the cross-section and that the stiffness resulting can be expressed in two equivalent ways for the rectangular member: <sup>19</sup>

$$E_t I = E I_e$$

where:  $I$  is the moment of inertia  
 $E$  is Young's modulus  
 $I_e$  is the moment of inertia of the unyielded portion of the cross-section.

This is based on an assumption of an elastic-perfectly plastic stress-strain relationship, where the modulus of elasticity of the yielded portion is taken to be zero. Substituting this into the tangent modulus formula,

$$\frac{P_t}{P_y} = \frac{\pi^2 EI_e}{\sigma_y I (L/r)^2}$$

which is the form used for the column curve construction. Although it is shown here for a rectangular section, this equation is the one applicable to any section with a symmetrical residual stress pattern. 19

If an analytical expression can be derived to describe the residual stress distribution, and hence  $I_e$ , then the equation can be solved to give the curve. However, if the stress distribution is random or too complicated to describe analytically, then a numerical approach can be used. 17

In this approach, the flanges and web are divided into a number of elements, each with its own uniform value of residual stress. A uniform strain is imposed on the section and the yielded elements are found. The effect of these yielded elements is subtracted from the load causing the strain, and the net load on the column is found.

The effective moment of inertia is calculated from the unyielded elements. With these values, the corresponding length of a column at incipient buckling with this cross section can be found.

In the lighter shapes, these elements had thicknesses equal to the flange and web thicknesses, or in other words, the residual stress was assumed uniform across the plates. In the heavier sections, however, the plates were divided in both directions, through the thickness and across the width, to account for the variation of residual stress through the thickness of the thick plates.

All of the tangent modulus curves drawn were constructed using the actual residual stress distribution, including, in the heavy shapes, the variation through the plate thickness.

### 3.2 Ultimate Strength Analysis

The ultimate strength analysis is designed to determine the highest strength that can be attained by an initially straight, pinned-end, axially loaded column.

#### 1. Assumptions

The assumptions which were made for this analysis were: the column is initially straight; the load is axial, which includes a symmetrical residual stress distribution; the deflected shape of the column can be described by a sine series function <sup>2,20</sup>.

The analysis is based on the tangent modulus concept in that the column is assumed to bifurcate at the tangent modulus load. At the bifurcation point in a specimen free from residual stresses, the stress and strain distributions will be as shown in Fig. 28. A further increase in strain will cause unloading in the convex fibers, and the unloaded area of the section will progress across the section until enough material is either yielded or unloaded to cause a decrease in load. Figure 29 shows this action for a section containing a simplified distribution of residual stress.

## 2. Formulation

In formulating this analysis, only the strains occurring after those of the tangent modulus load are required, since all forces are in equilibrium until this time<sup>2</sup>. The method is nothing more than an equilibrium method, with the sum of forces, internal and external, and the sum of moments providing the basis. Examining the stress diagrams at the bottom of Fig. 28, it is seen that, in the deflected shape, if the column is to remain standing, the sum of the additional internal stresses must equal the increment in load. Also, the moment of the additional stresses about the column centerline must be balanced by the moment of the total force about the same point. Or:

$$\Sigma P = 0$$

$$\Sigma F_r + \Sigma F_l = \Delta P$$

$$\Sigma M = 0$$

$$\Sigma F_r \cdot X_r + \Sigma F_l \cdot X_l = (P_t + \Delta P) y$$

where:

$F_r$  and  $F_l$  are the stress resultants to the right and left of the column centerline,

$X_r$  and  $X_l$  are the moment arms of these resultants,

$P_t$  is the tangent modulus load,

$\Delta P$  is the increment in load above the tangent modulus load,

$y$  is the deflection of the point under consideration.

These relations, if they were to be formulated for the total length of the columns, would be quite complicated and virtually unsolvable<sup>2</sup>. A simplification is made, in that the problem is solved only for the mid-height of the member, which is the most highly stressed portion.

Since the residual stress pattern in the heavier section varies across the thickness of the plates, the mathematical expression describing it would be quite complicated, even if simplifications were introduced. Thus, a numerical



approach was adopted, which could be solved by use of a digital computer. The sectioning method lends itself easily to this computational process, since it produces a number of discrete elements, each with its own (assumed uniform) stress and usually equal in size to all others.

Taking each element, and applying the above equilibrium equations, for the summation of forces:

$$\delta F = tw E_t \phi (X_n + \beta b)$$

where:

$\delta F$  is the force contribution of a single element,

$t$  and  $w$  are the length and width of the element,

$E_t$  is the tangent modulus of the material in that element,

$\phi$ ,  $X_n$ ,  $\beta$ , and  $b$  are defined in Fig. 30 and together represent the strain on the element.

This leads to the increment of force on the total cross-section by summing over the area.

$$\Delta P = tw \phi \sum E_t (X_n + \beta b) \quad \text{---(a)}$$

where  $t$ ,  $w$ , and  $\phi$  are constant for all elements.

Now, formulating the sum of moments about the cross-section centerline, for a single element:

$$\delta M = t w E_t \phi (X_n + \beta b) X_n$$

where:

$\delta M$  is the contribution to moment from the element,

$X_n$  is the moment arm of the element about the centerline of the section.

Again, summing over the whole cross-section:

$$(P_t + \Delta P) e_c = t w \phi \sum E_t (X_n + \beta b) X_n \quad \text{---(b)}$$

where:

$(P_t + \Delta P)$  is the total axial load,

$e_c$  is the mid-height (maximum) deflection.

There are now two equations, but four unknowns:  $\Delta P$ ,  $e_c$ ,  $\beta$ ,  $\phi$ . One more relationship can be obtained between the deflection  $e_c$ , and the curvature,  $\phi$ .

One of the assumptions made earlier was that the deflected shape of the column could be expressed as a sine series function. A further assumption is needed, to use a

single term sine function to describe the deflection <sup>2</sup>.

In other words:

$$y = e_c \sin \frac{\pi z}{L}$$

where:

y is the deflection at any point,

z is the distance along the column,

L is the column length.

If this expression is differentiated twice,

$$\frac{d^2 y}{dz^2} = - \frac{L^2}{\pi^2} e_c \sin \frac{\pi z}{L}$$

and for the mid-height ( $z = L/2$ ):

$$\frac{d^2 y}{dz^2} = - \frac{L^2}{\pi^2} e_c \sin \frac{\pi}{2} = - \frac{L^2}{\pi^2} e_c$$

Recalling that, for small values of y,

$$\delta = - \frac{d^2 y}{dz^2},$$

gives:

$$\delta = \frac{L^2}{\pi^2} e_c$$

---(c)

There is still one more unknown than equations, but if a value is chosen for one parameter, for example,  $\beta$ , the equations can be solved for the others. However, as can be seen by examination of the equations, all of the relations are not explicit; that is, variables cannot be factored out with ease to aid in the summation process. Complicating this, upon yielding and unloading, the modulus of elasticity changes, so that a particular element may have a different modulus than the one next to it. (For this analysis, as in the tangent modulus analysis, it was assumed that the steel had an idealized elastic-perfectly plastic stress-strain curve.)

Since the desired terms could not be factored out of the expressions, a trial-and-error solution was employed. A value of  $\beta$  was chosen, and a nondimensionalized value of  $e_c$  was assumed.  $\phi$  was found from equation (c), and substituted into equation (a). With the resulting value of  $\Delta P$ , all the knowns were inserted into (b), and a new value of  $e_c$  calculated. This calculated  $e_c$  was checked with the initially assumed one, and if the difference was greater than 2% of the initial, the calculated value was taken as the initial and the cycle repeated. When the difference had been reduced sufficiently, a second value of  $\beta$  was chosen and the whole process repeated.

Each element was assumed elastic at first, and after each calculation, this assumption was checked. If the

stress had turned out to be greater than its elastic capacity, its known stress value at yield (tension or compression) was inserted instead.

### 3. Limitations

There were some limitations placed on the computations:

1. The unloading of the fibers was not taken into account once yield had occurred. In other words, the material was assumed to follow the stress-strain curve from all locations, whether loading or unloading. This was due to time restrictions on the use of the computer.
2. The residual stress (or strain) values were averaged to give one representative half-flange, and one half-web, which were subsequently used for the strength calculations.
3. All elements were assumed the same size. This was not strictly true, since in the heavy shapes the elements near the weld had various sizes, but since it was weak axis bending, their effect would be rather small.

## 4. DISCUSSION OF RESULTS

### 4.1 Tangent Modulus Column Curves

Shown in Fig. 31 are the tangent-modulus curves for the light shapes composed of UM plates. The reason for the concern over strength loss in the welded shapes can be seen, with the results of the column tests and the column curves falling well below the average curve for the rolled wide-flange shapes. In Fig. 32 are the tangent modulus curves for the heavy shape composed of UM plates. In the low slenderness ratios, all the curves are grouped, but at a lower strength than the rolled shapes. As the slenderness ratios increase, the strength of the A36 columns is reduced and approaches that of the lighter shapes. The A441 columns maintain a somewhat greater carrying capacity, consistent with earlier work on rolled shapes<sup>6</sup>, but they do not approach the curve for rolled wide-flange shapes of high-strength steel.

Figures 33 and 34 show the tangent modulus curves for the shapes composed of flame-cut plates. The lighter shapes, although they show improvement over those with UM plates, are still weaker than the comparable rolled shapes over most of the slenderness ratios. The heavy shape, however, is nearly as strong as the rolled shapes for most values of slenderness ratios, for both the A36 and A441 steels.

Figure 35 is a comparison of the tangent modulus curves for the mild steel, fillet welded specimens. Only the heavy shape composed of flame-cut plates compares in a satisfactory way with the rolled tangent modulus curve.

The tangent modulus curve can be obtained from the stub column test results by determining the tangent to the stress-strain curve at a number of points and solving the tangent modulus buckling equation. This curve should coincide with that obtained directly from the residual stress distribution. However, particularly in the heavy shape, this was not so (see Fig. 36). This is explained by the fact that the shape of the stress-strain curve for the stub column showed a continual strain hardening, while in the numerical solution the modulus after yielding is taken to be zero, and no strain hardening is taken into account.

The curve obtained from the stub column test is expected to be the correct one, since it considers the complete cross-section as a whole and not a number of small elements; also it considers the actual stress-strain relationship. The "reinforcing" provided by the weld metal and its neighboring heat-affected zone could alter the curve in a fashion not taken into account by the residual stress method. However, the latter method was used here to check the stub column test results, since there was a difficulty in alignment. This difficulty arose from the low proportional limit that reduced the alignment loads.

#### 4.2 Ultimate Strength Curves

Examples of the computer output from the ultimate strength program are shown in Fig. 37. The output is in the form of load versus mid-height deflection curves, and consideration of a number of column lengths will give an ultimate strength curve. From previous work <sup>2</sup>, it would be expected that the deflection curves obtained will not agree very well with the experimental curves, but the ultimate strength values should be fairly close. This is because of the simplifying assumptions made.

The indications from these deflection curves are that the columns with the higher slenderness ratios will have lower post-buckling strengths but will maintain this strength for a greater deflection, or analogous to the plastic behavior of beams, the "rotation capacity" of the longer column is greater than that for the short.

The ultimate strength curves for the heavy shape are shown in Figs. 38 through 41. In all cases, the largest increase in strength over the tangent modulus curve is no greater than about 10%, this being in the lower slenderness ratios. If the effect of initial eccentricities and the resulting decrease in strength are taken into account, it may be concluded that the tangent modulus approach represents a good upper bound to the strength of these heavy columns.



### 4.3 Strength Comparisons

#### 1. Plate Edge Preparation

For all the columns involved in this study, the flame-cutting of the component plates resulted in an increase in strength over those sections made up of UM plates. This increase was most significant for the light sections (Figs. 31 and 33), and for the heavy shape of A36 steel in the higher slenderness ratios (Figs. 32 and 34). The heavy shape of A441 steel showed some increase due to flame-cutting, but it was relatively small for most values of slenderness ratio.

#### 2. Grade of Steel

In the heavy sections of UM plates, the A441 steel columns showed a greater strength than those of A36 steel for the higher slenderness ratios, and were approximately equal to the A36 specimens in the low slenderness ratios (Fig. 32). This confirms the work done earlier on rolled wide-flange shapes<sup>6</sup>. However, for the sections composed of flame-cut plates, both steels showed approximately equivalent strengths (Fig. 34).

The lower magnitude of residual stress relative to the yield stress of the material would indicate that the high strength steel should have a greater carrying capacity than the mild steel, but the pattern of residual stress

caused by the flame-cutting operation seems to reduce the effect of the grade of steel on column strength of heavy sections.

### 3. Weld Type

A comparison of the fillet welded specimens with the full penetration groove welded columns shows that there is little effect of weld type on heavy column strength (Fig. 32 and 34). This would be in line with the earlier statement on the small effect of welding on the residual stress pattern in the heavy section. Since the residual stress distribution is used for the column curve construction, and it reflects little of the welding process, the curve would also contain very little welding effects.

### 4. Plate Thickness

In Figs. 35 and 42 are shown the tangent modulus and ultimate strength curves, respectively, of the mild steel (A7 and A36), fillet welded specimens. It is evident that the heavy column section of UM plates displays a higher strength than the light shape of UM plates in the low values of slenderness ratio in both analyses, and the two curves approach each other as the length increases. For the flame-cut sections, however, while the tangent modulus curves show that the heavy column is again stronger, the ultimate strength curves show that both the light and

heavy shape have comparable strengths over the lower slenderness ratios, the heavy section being the stronger for the greater lengths.

## 5. SUMMARY AND CONCLUSIONS

The purpose of this investigation on welded H columns was to determine the effect on the strength characteristics of these members of using component plates of A7, A36, and A441 steels which varied in thickness from 1/2" to 2 1/2". The study was a preliminary one, and the conclusions are tentative; more work being needed in all aspects of heavy column shapes.

Some of the conclusions obtained from this program are:

1. The general shape of the residual stress distributions in heavy column sections is similar to that found in rolled shapes, and in light welded shapes. (Section 2.2)
2. The magnitudes of residual stress found in the UM heavy sections are much higher than would be expected from the welding process, and are due, apparently, mainly to the cooling stresses in the plates prior to welding. (Section 2.2)
3. There is a significant variation of residual stress through the component plate thickness of heavy welded columns. (Section 2.2)
4. The variation of residual stress across the thickness of the component plates of the heavy

sections is either a straight line or else slightly parabolic in nature. This allows the prediction of the interior stress values, knowing the surface measurements and making straight line interpolations. This could lead to nondestructive measuring. (Section 2.2)

5. The ultimate strength analysis can be easily extended to take into account stress variation across the thickness of component plates by using an elemental approach, and utilizing a digital computer. (Section 3.2)
6. From the tangent modulus analysis, all of the welded shapes display strengths lower than the rolled wide-flange shapes, the heavier shapes of flame-cut plates most closely approximating the rolled curve. (Section 4.1, Figs. 31 through 35)
7. The tangent modulus analysis represents a good upper bound to the strength of heavy welded columns. (Section 4.2)
8. Flame-cutting of the component plates of a welded column results in an increase in column strength, particularly for light shapes, and mild steel heavy shapes. (Section 4.3, Figs. 31 through 34)

9. The use of high strength steel for the heavy column sections composed of UM plates, results in an increase in column strength over mild steel specimens. The sections composed of flame-cut plates do not show this increase, due to the altered residual stress pattern. (Section 4.3)
10. The type of weld used to fabricate the heavy column section (partial penetration vs. full penetration) has little effect on the column strength. (Section 4.3)
11. The use of heavy UM plates in column fabrication results in an increase in strength over the comparable light welded shape in the low slenderness ratios. The use of heavy flame-cut plates gives a modest increase in strength in comparison with similar light shapes for higher slenderness ratios. (Section 4.3, Fig. 42)

## 6. ACKNOWLEDGEMENTS

This thesis presents the results of an investigation into the influence of component plate thickness on the strength of welded built-up columns. The program was conducted at Fritz Engineering Laboratory, Department of Civil Engineering, Lehigh University. Dr. Lynn S. Beedle is Director of the Laboratory and Acting Chairman of the Department.

This was part of a study of the strength of welded built-up columns sponsored by the Pennsylvania Department of Highways, the Bureau of Public Roads of the U. S. Department of Commerce, the Column Research Council, and the American Institute of Steel Construction. The guidance of Task Group 1 of the Column Research Council, under the chairmanship of Mr. John A. Gilligan, is gratefully acknowledged.

The advice and critical review of this work given by Dr. Lambert Tall, professor in charge, is especially appreciated, as is the assistance provided by the author's colleagues, particularly Messrs. Richard McFalls, Koichiro Okuto, and Ching Yu.

Finally, the author wishes to express his thanks to Mr. Kenneth Harpel, laboratory foreman, and his staff for their aid in the test program, Mr. Richard Sopko and his staff for the preparation of photographs and drawings, and Mrs. Diane Kroohs for her care in typing the manuscript.

7. NOMENCLATURE AND DEFINITIONS

A	cross sectional area
b	flange width
E	Young's modulus of elasticity
$E_t$	tangent modulus
$e_c$	deflection at column mid-height
F	force
$\delta F$	force in small element
I	moment of inertia
$I_e$	effective moment of inertia
K	effective length factor
L	column length
M	moment
$\delta M$	moment due to force in a small element
P	column load
$P_{max}, P_u$	maximum column load
$P_t$	tangent modulus load
$P_y$	yield load
$\Delta P$	load above the tangent modulus load
r	radius of gyration
t	thickness of plate or small element
w	width of small element
X	distance from an axis
$X_n$	location of a small element
y	deflection of any point along the column



$z$	distance along column
$\beta$	parameter locating distance of instantaneous neutral axis from column centerline
$\epsilon$	strain
$\lambda$	nondimensionalized slenderness ratio
$\sigma$	stress
$\sigma_t$	tangent modulus stress
$\sigma_y$	yield stress
$\sigma_{yf}$	yield stress in flange
$\sigma_{yw}$	yield stress in web
$\phi$	curvature

**Buckling** Process by which a structure or any part of a structure passes from one deflected pattern to another with no change in load.

**Rotation Capacity** The angular rotation which a shape can accept in the plastic state without prior local failure.

**Ultimate Load** The largest load a structure will support.

**Yield Stress** The stress at which a material exhibits a specified deviation from the proportionality of stress to strain.

**Yield Stress Level** The average stress during yielding in the plastic range.

8. TABLES AND FIGURES

TABLE 1

EXPERIMENTAL COLUMN SECTIONS

Shape	Web	Flange	Plate Edge Preparation	Steel	Weld	1	2
7H28	6 x $\frac{3}{8}$	6 x $\frac{1}{2}$	UM	A7	3/16" Fillet	-	-
			FC	A7	3/16" Fillet	-	-
10H62	9 x $\frac{1}{2}$	9 x $\frac{3}{4}$	UM	A7	1/4" Fillet	-	-
			FC	A7	1/4" Fillet	-	-
15H290	10 x $1\frac{1}{2}$	14 x $2\frac{1}{2}$	UM	A36	1/2" Fillet	C1	C2
			UM	A36	60° Groove	C3	C4
			UM	A441	1/2" Groove	C5	C6
			UM	A441	60° Groove	C7	C8
			FC	A36	1/2" Fillet	C9	C10
			FC	A36	60° Groove	C11	C12
			FC	A441	1/2" Fillet	C13	C14
			FC	A441	60° Groove	C16	C15

Notes: 1 - Specimen designations of sections used for residual stress measurements and tensile coupon tests.

2 - Specimen designations of sections used for stub column tests; also used for column curve identification.

UM - Universal Mill; FC - Flame-cut; H - Symbol for welded H shape

TABLE 2

TENSILE COUPON TEST RESULTS  
(given in ksi)

Light Shapes:

Shape	Plate Edge Preparation	$\sigma_{yw}$	$\sigma_{yf}$	$\sigma_y^*$
7H28	UM	46.8	48.3	47.9
10H62	UM	32.8	33.3	33.2
7H28	FC	36.8	36.9	36.9
10H62	FC	34.3	30.9	31.8

Heavy Shapes:

Specimen	$\sigma_{yw}$	$\sigma_{yf}$	$\sigma_y^*$
C1	36.2	33.2	33.7
C3	-	-	36.0
C5	48.2	46.4	46.7
C7	45.6	45.1	45.2
C9	46.4	33.6	35.9
C11	37.2	35.6	35.9
C13	45.5	44.4	44.6
<del>C16</del>	36.1	42.8	42.0

\* Weighted Average

TABLE 3COLUMN TEST RESULTS

Shape	Plates	L/r	P <sub>max</sub> (kips)	p/P <sub>y</sub>
7H28	UM	53	298	.754
		32	353	.894
10H62	UM	103	302	.505
		78	375	.628
		59	389	.651
7H28	FC	53	261	.856
10H62	FC	59	444	.776

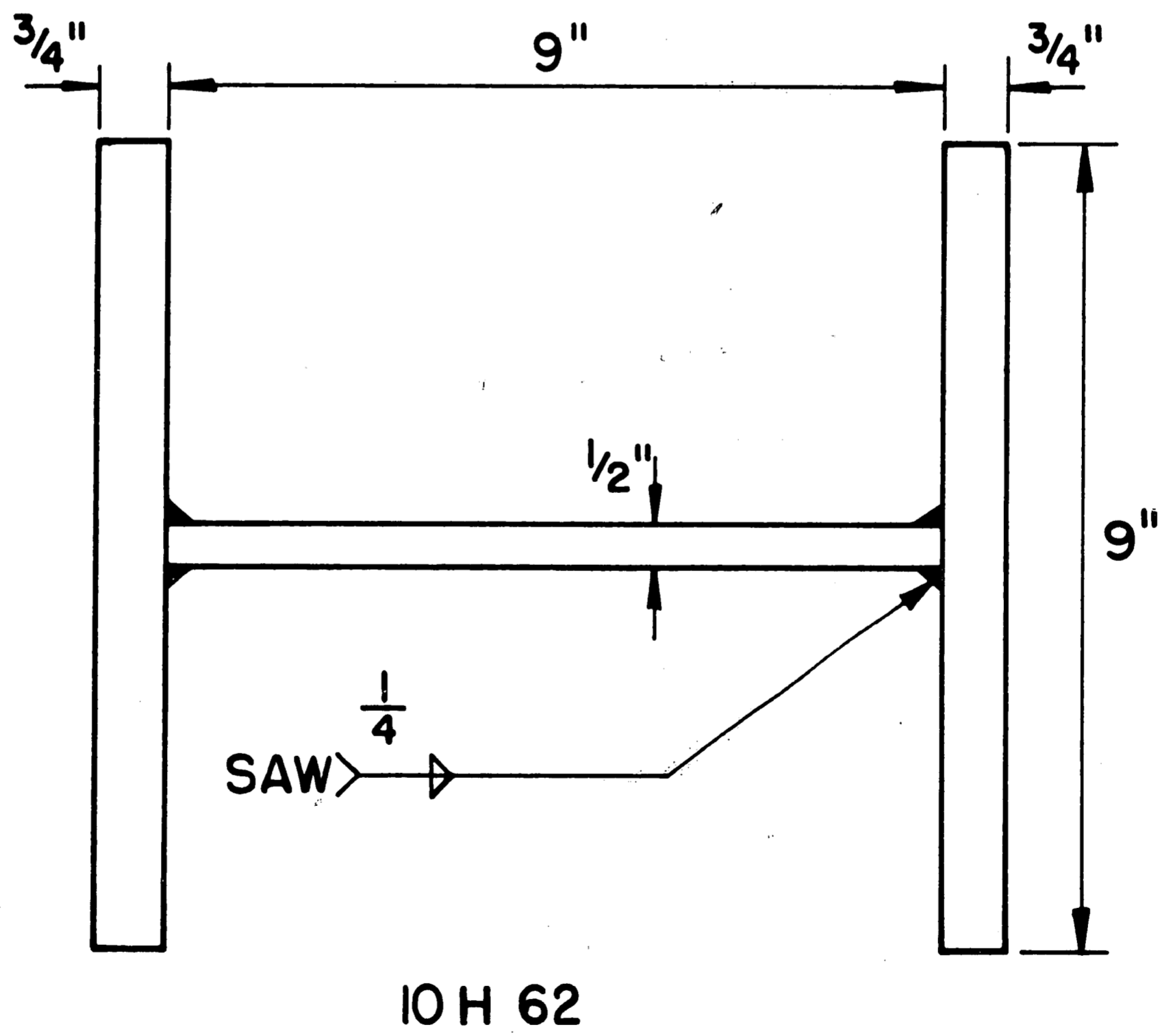
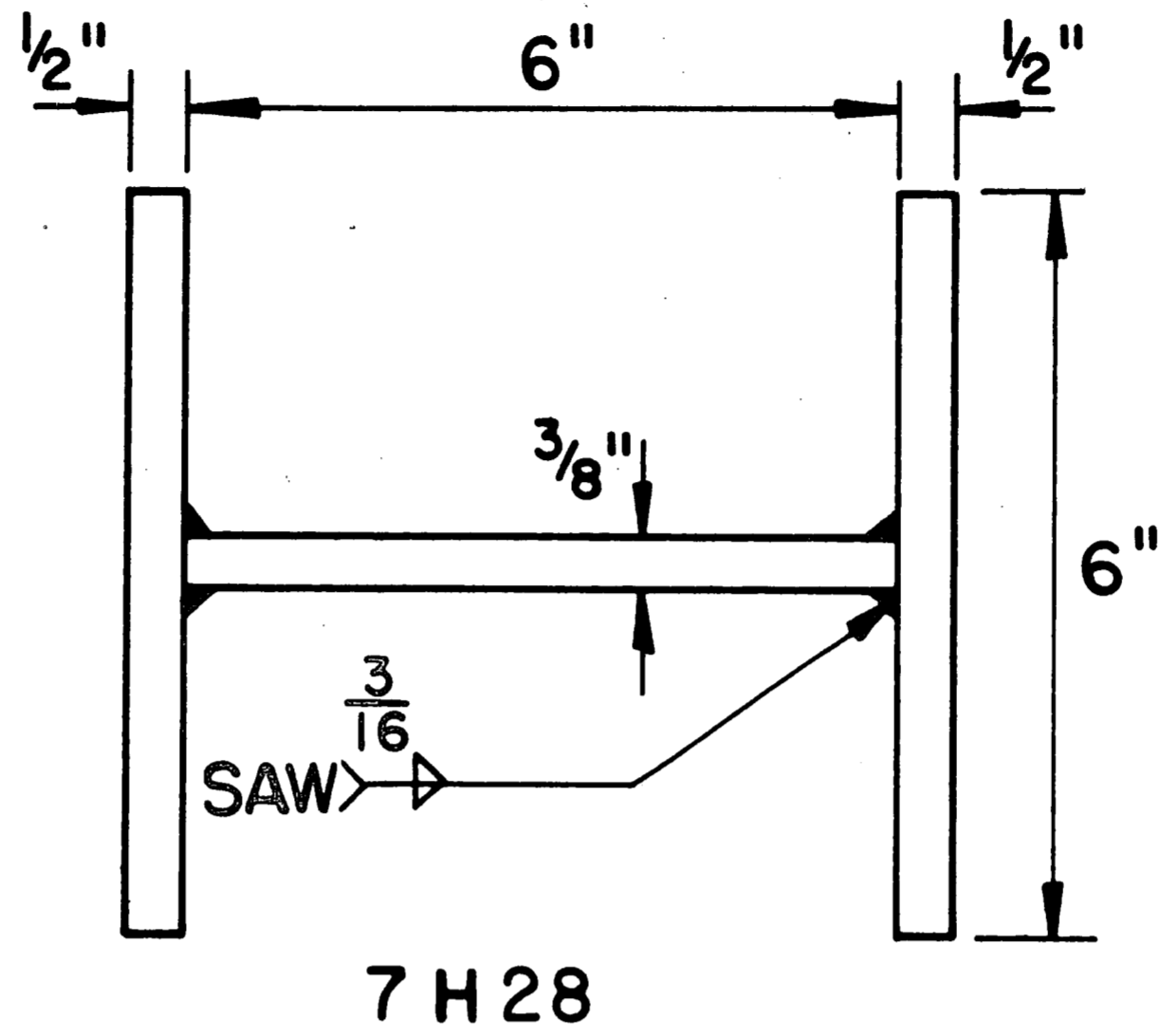
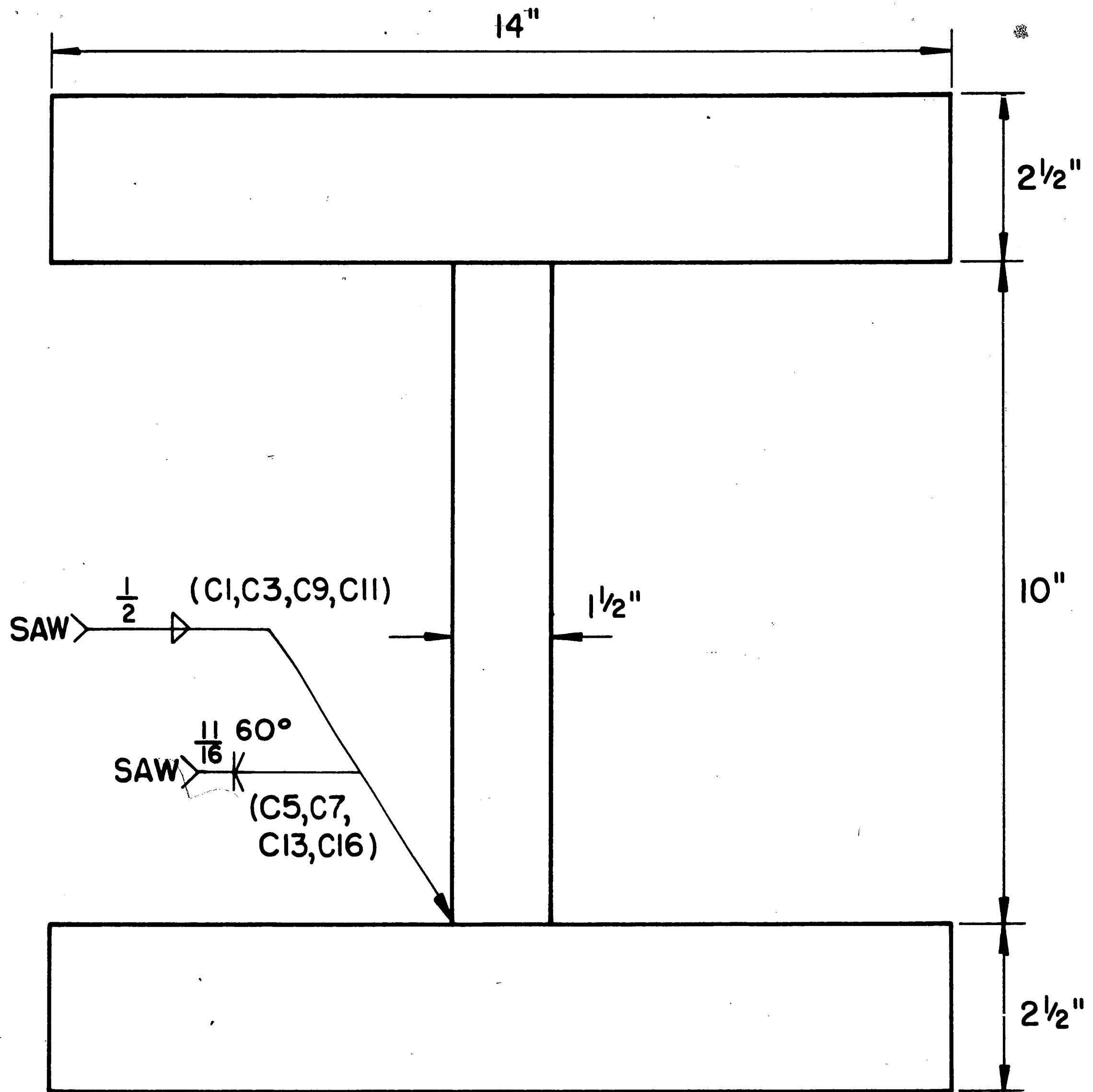


Fig. 1 Dimensions Of Light Welded Shapes



15 H 290

Fig. 2 Dimensions Of Heavy Welded Shapes

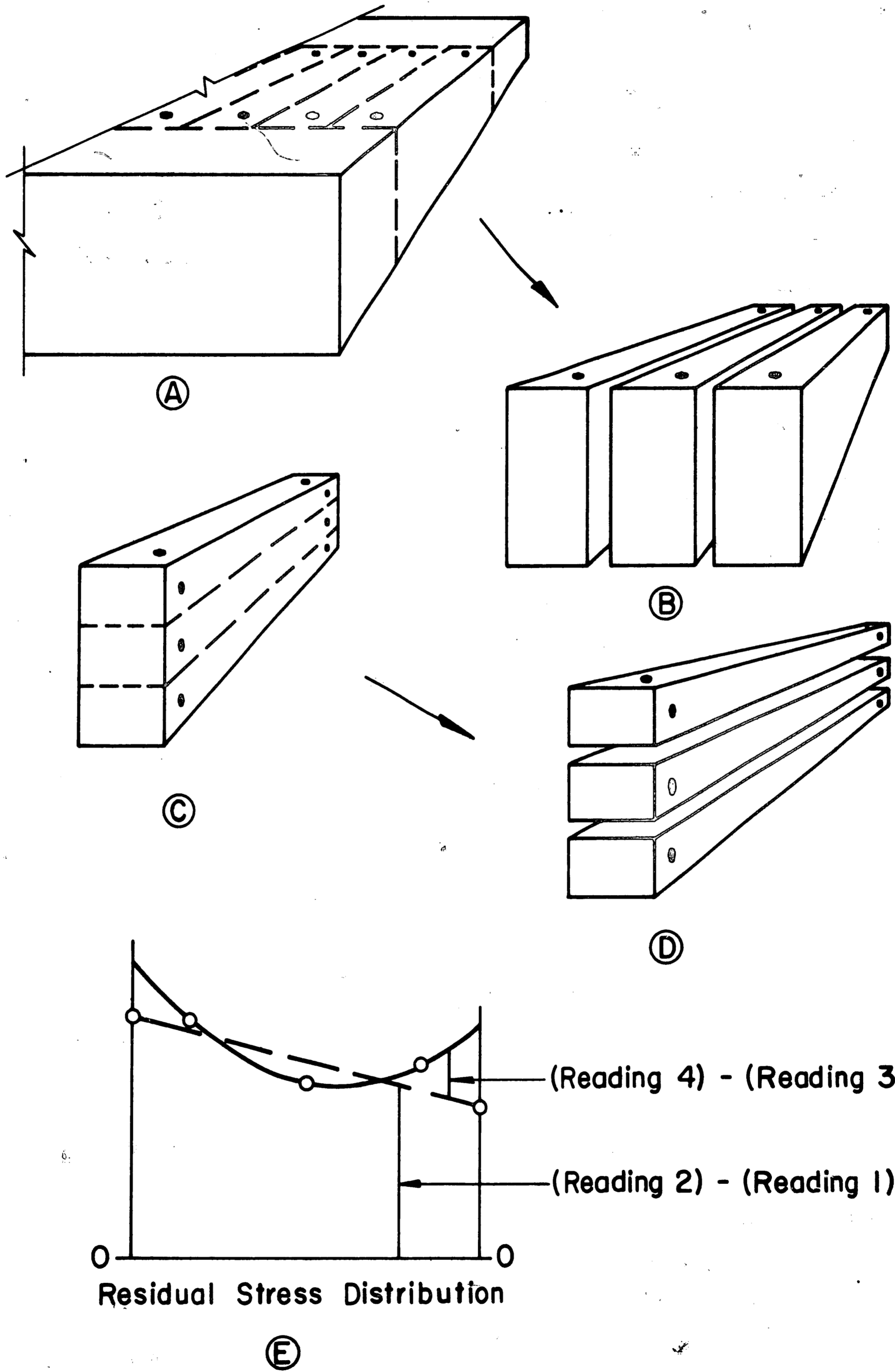


Fig. 3 Residual Stress Measurement By Sectioning



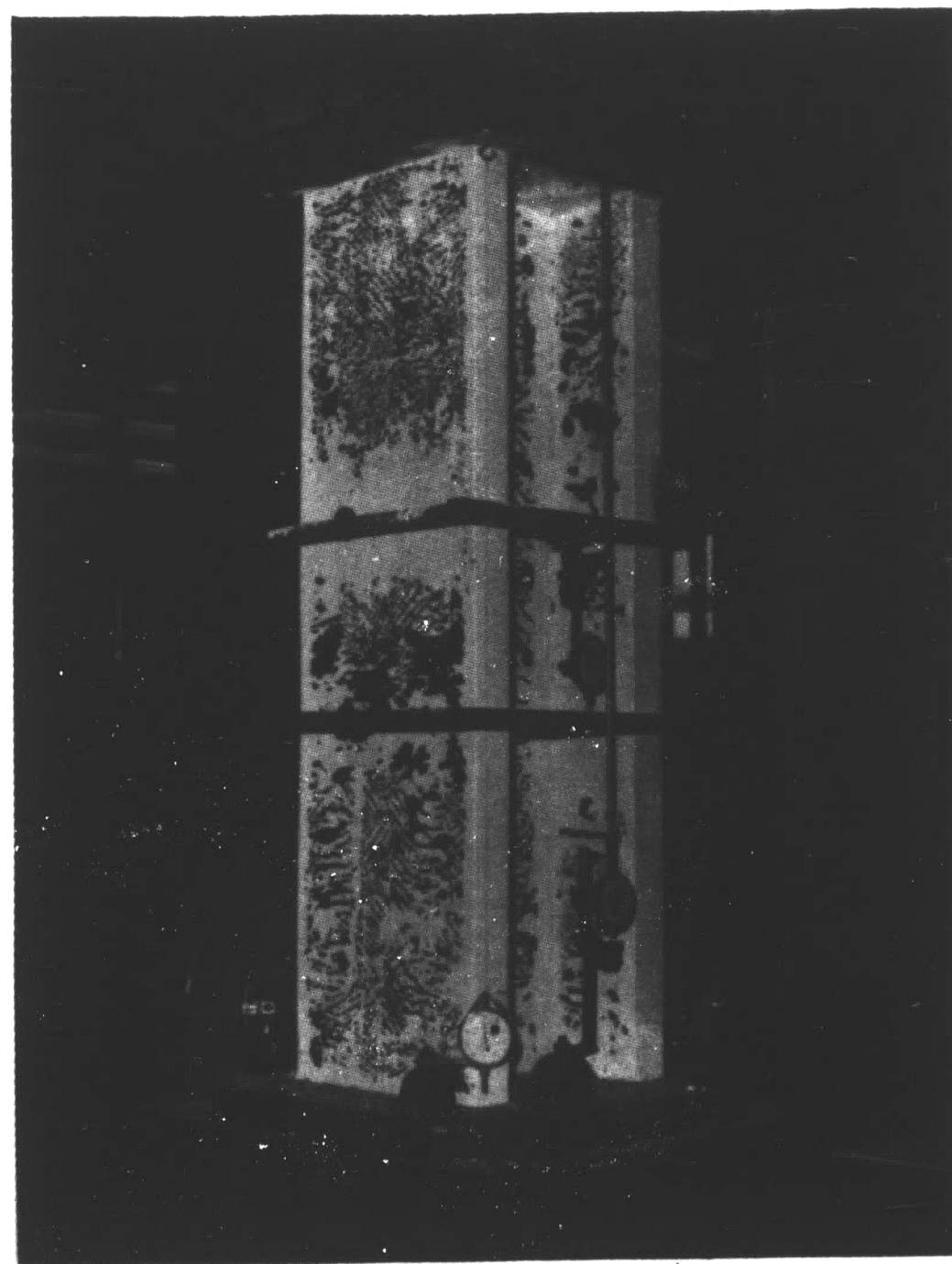
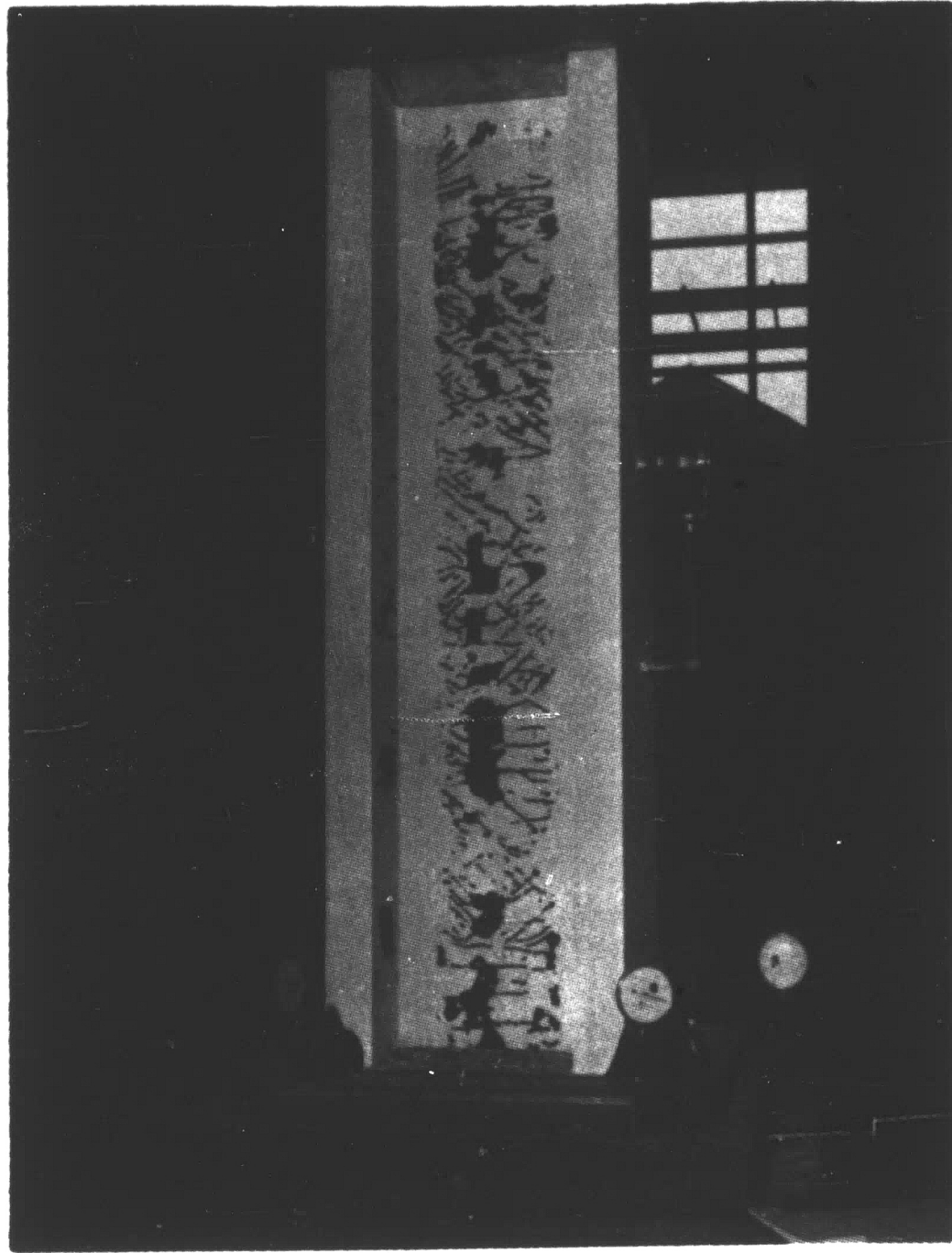


Fig. 4 Arrangements Of Dial Gages On Stub Columns

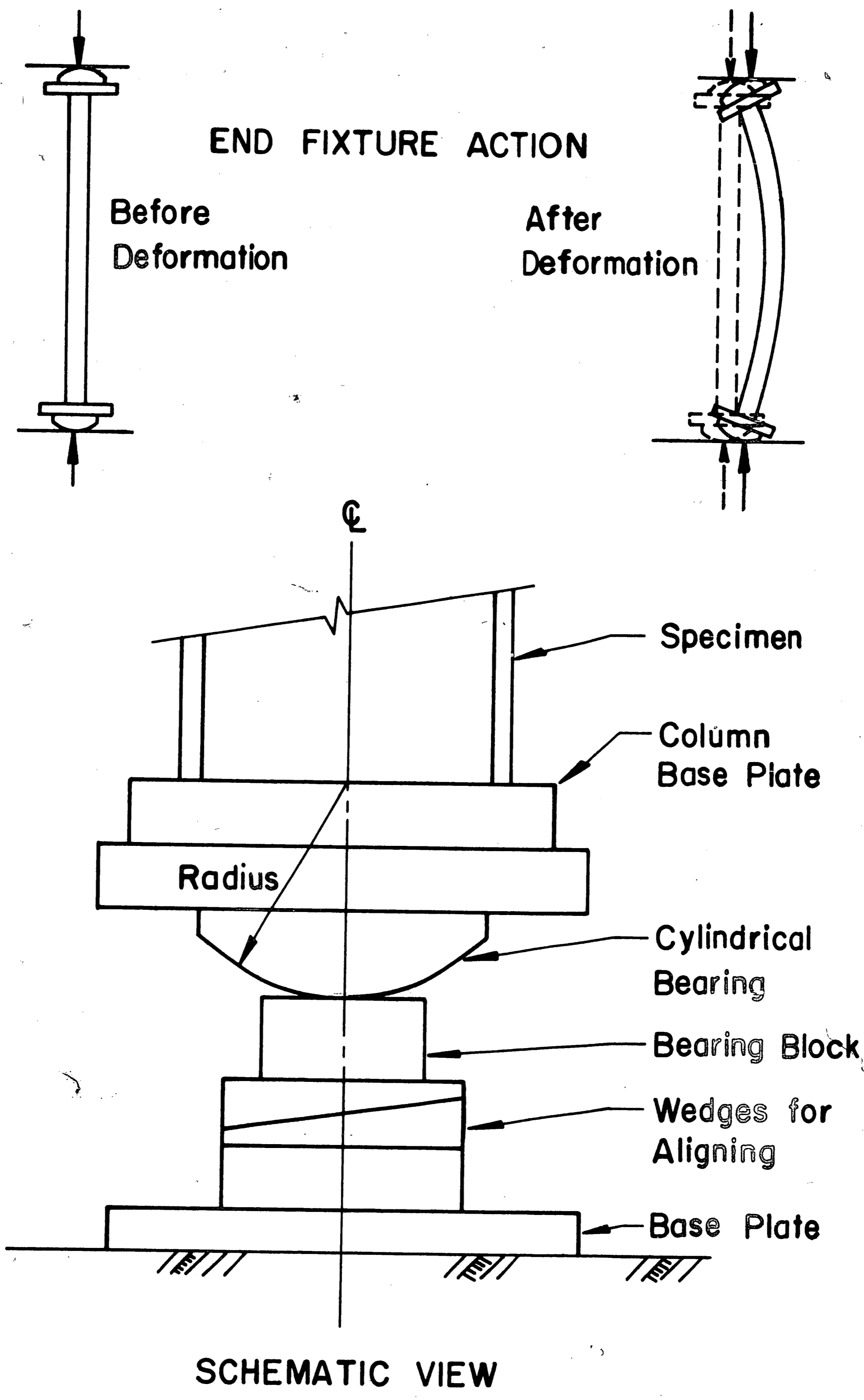


Fig. 5 Column End Fixtures

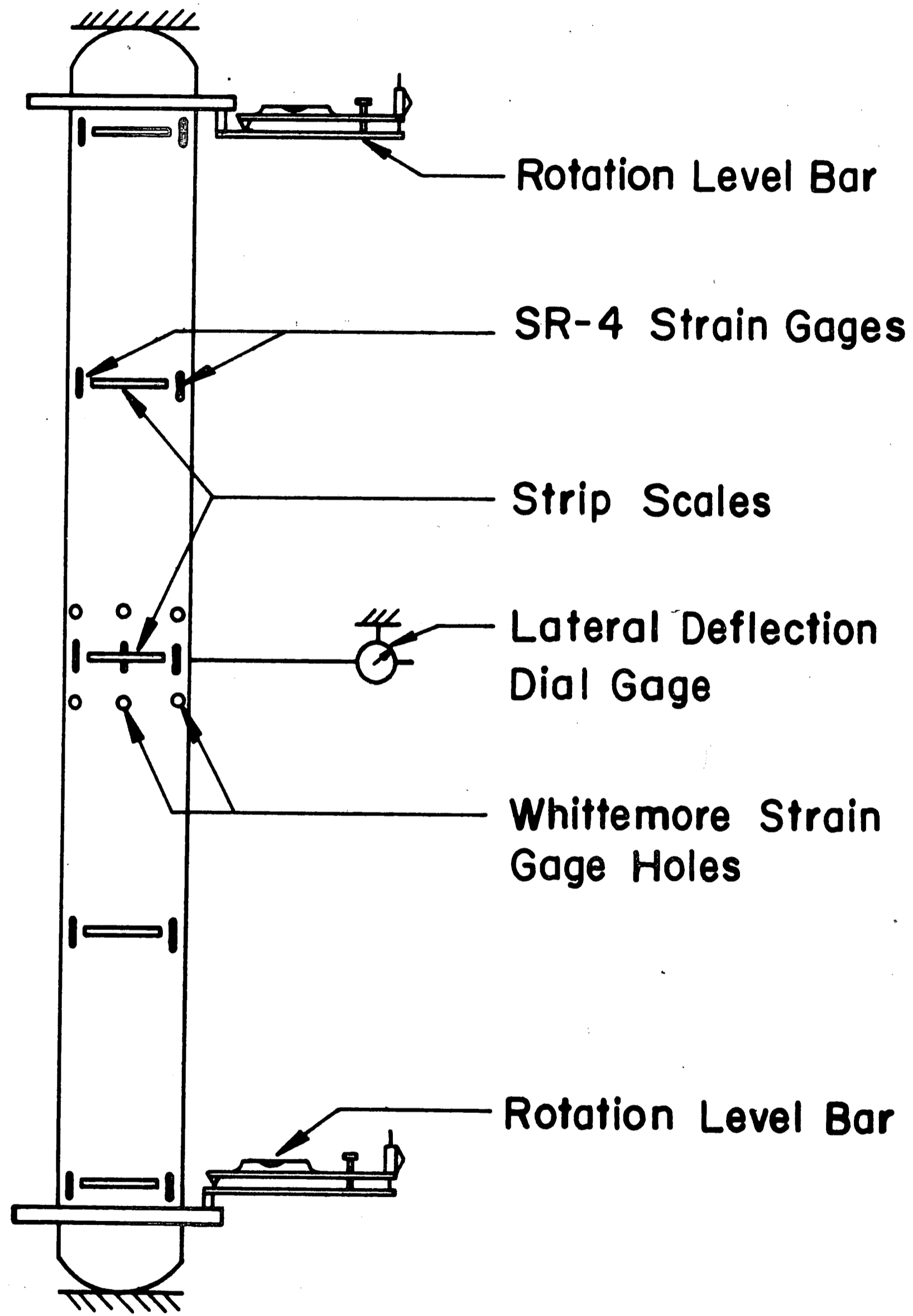


Fig. 6 Column Instrumentation

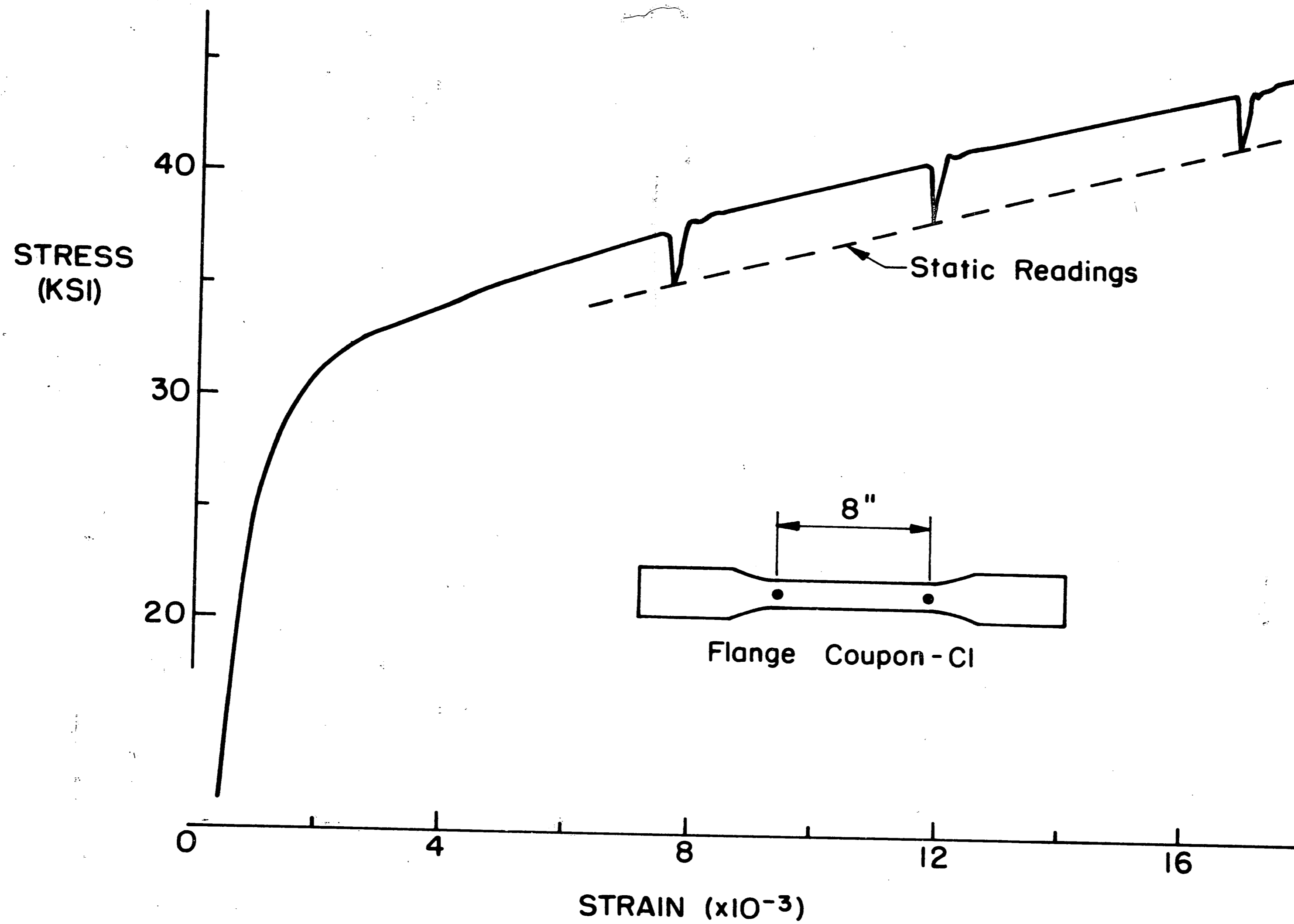


Fig. 7 Stress-Strain Curve From Heavy Shape Coupon

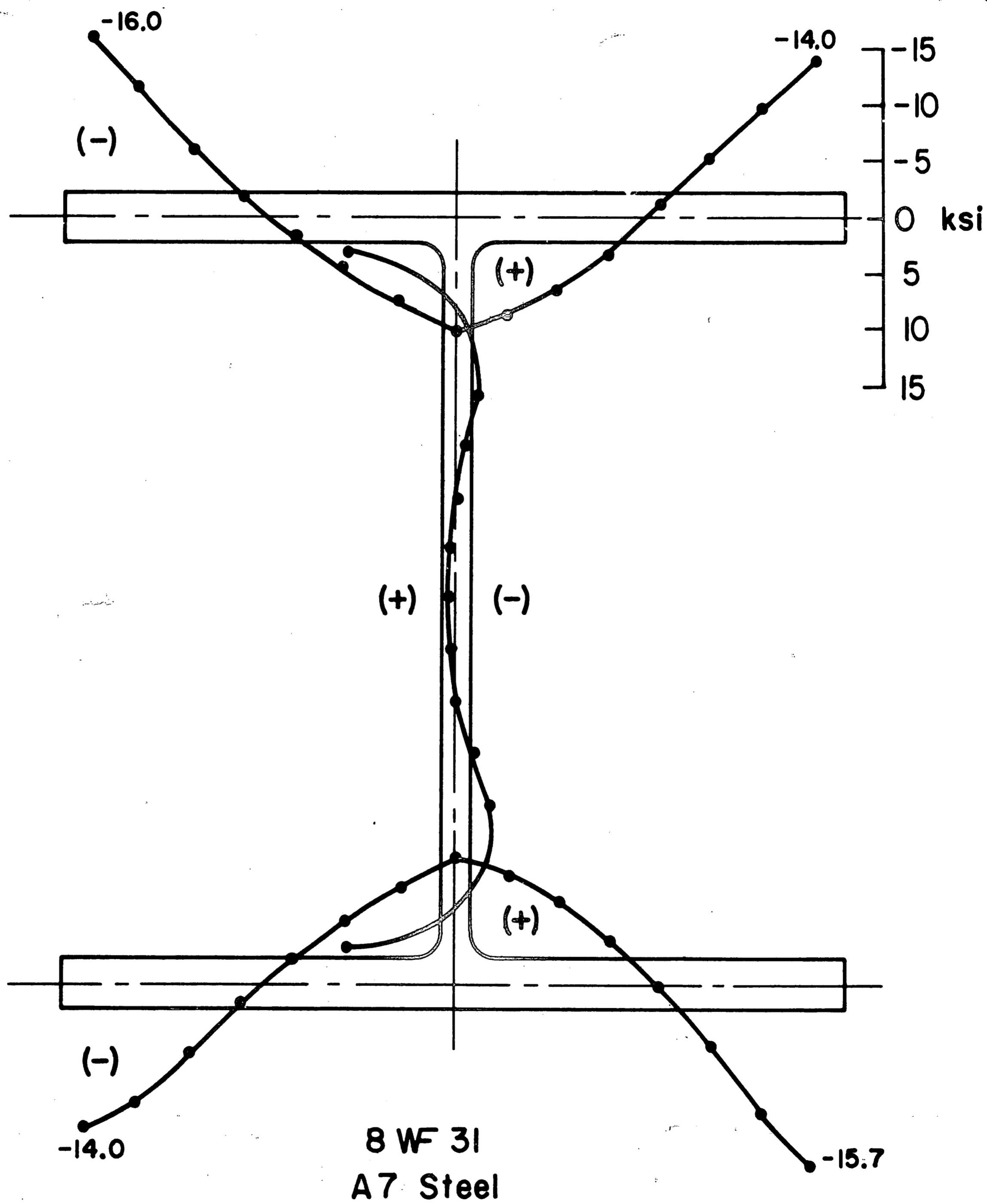


Fig. 8 Residual Stress Distribution In Rolled Shape

LIGHT WELDED SHAPES  
A7 STEEL, U.M. PLATES

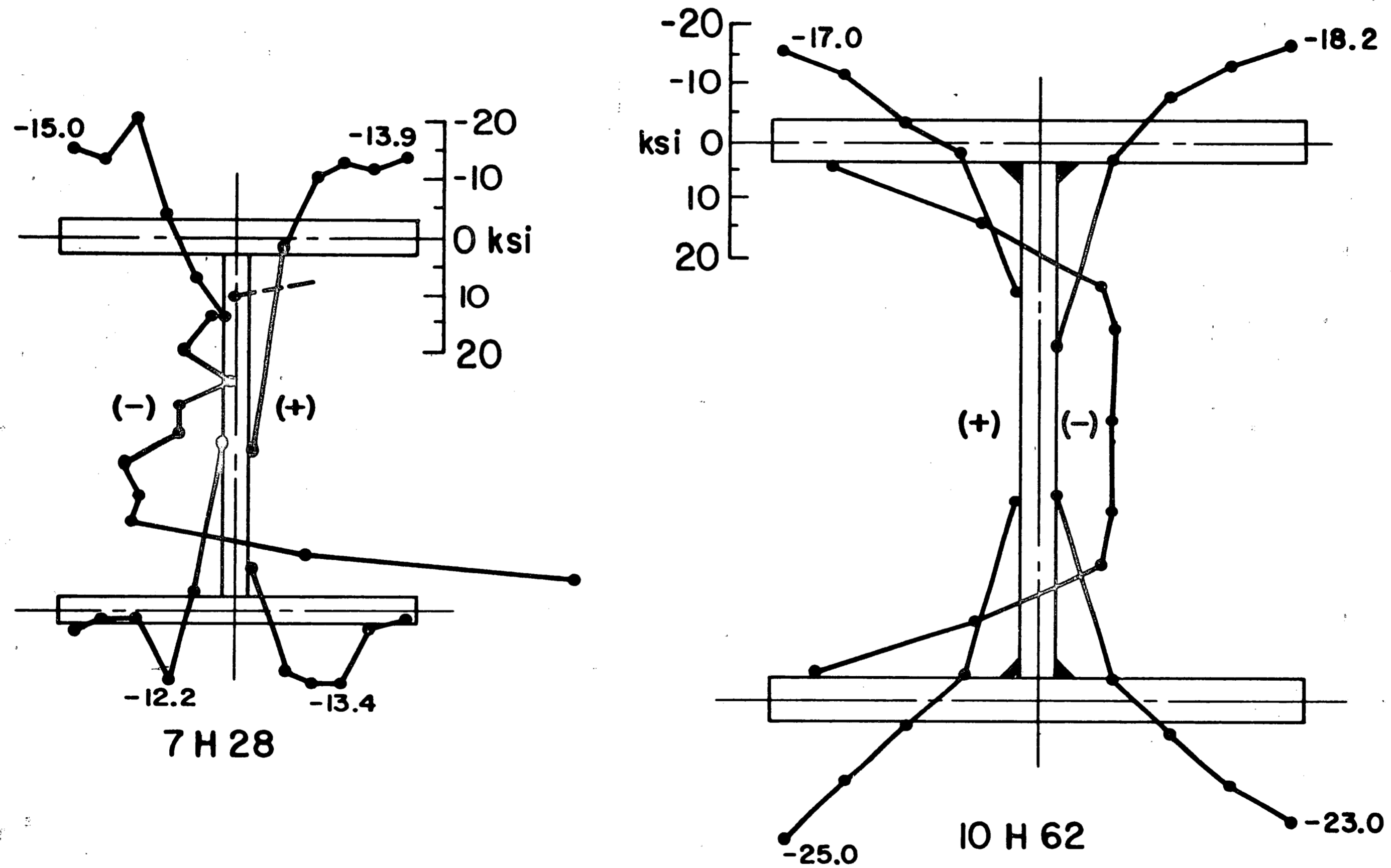


Fig. 9 Residual Stress Distributions In Light Welded Shapes  
Of UM Plates

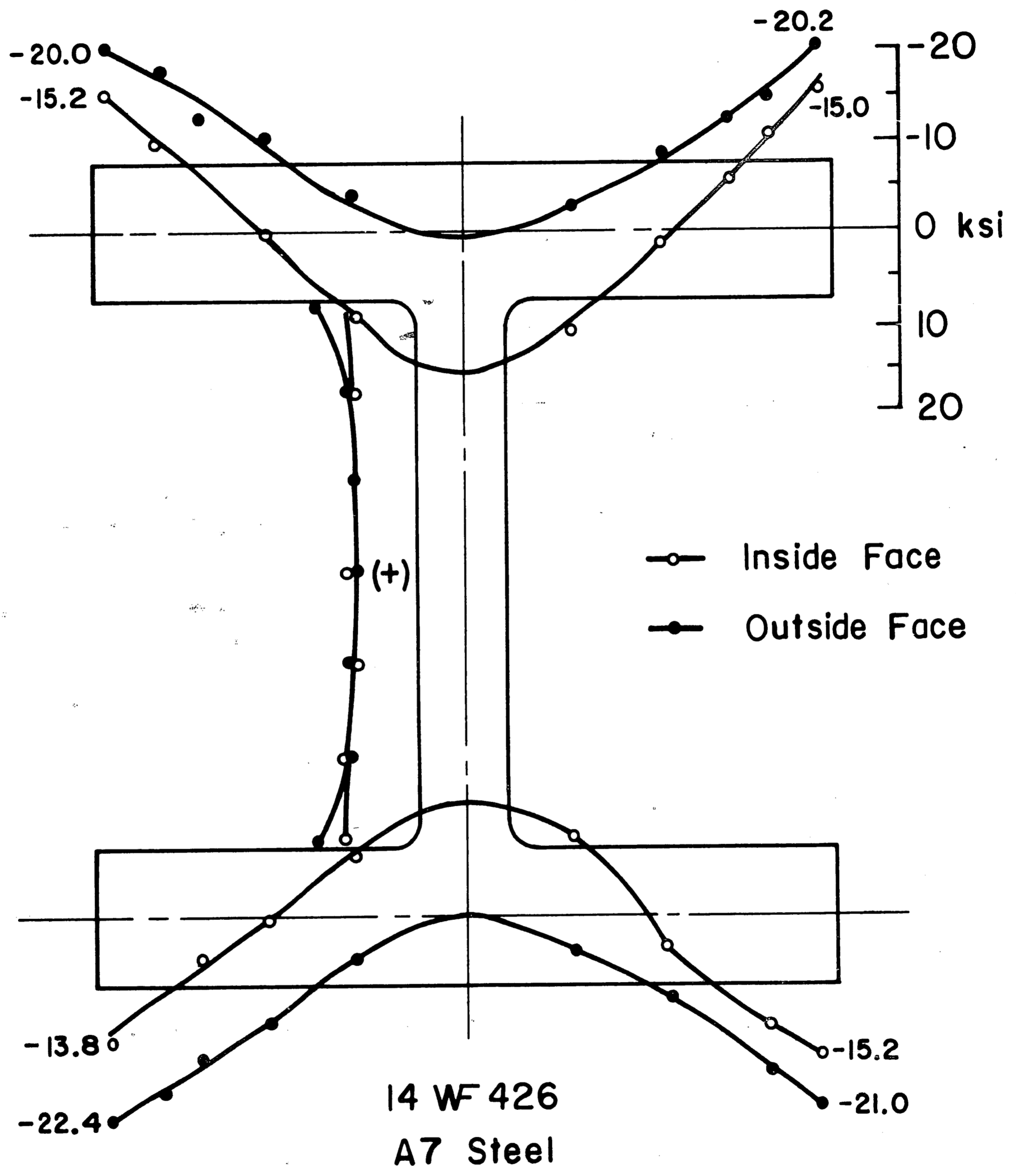


Fig. 10 Residual Stress Distribution In Heavy Rolled Shape

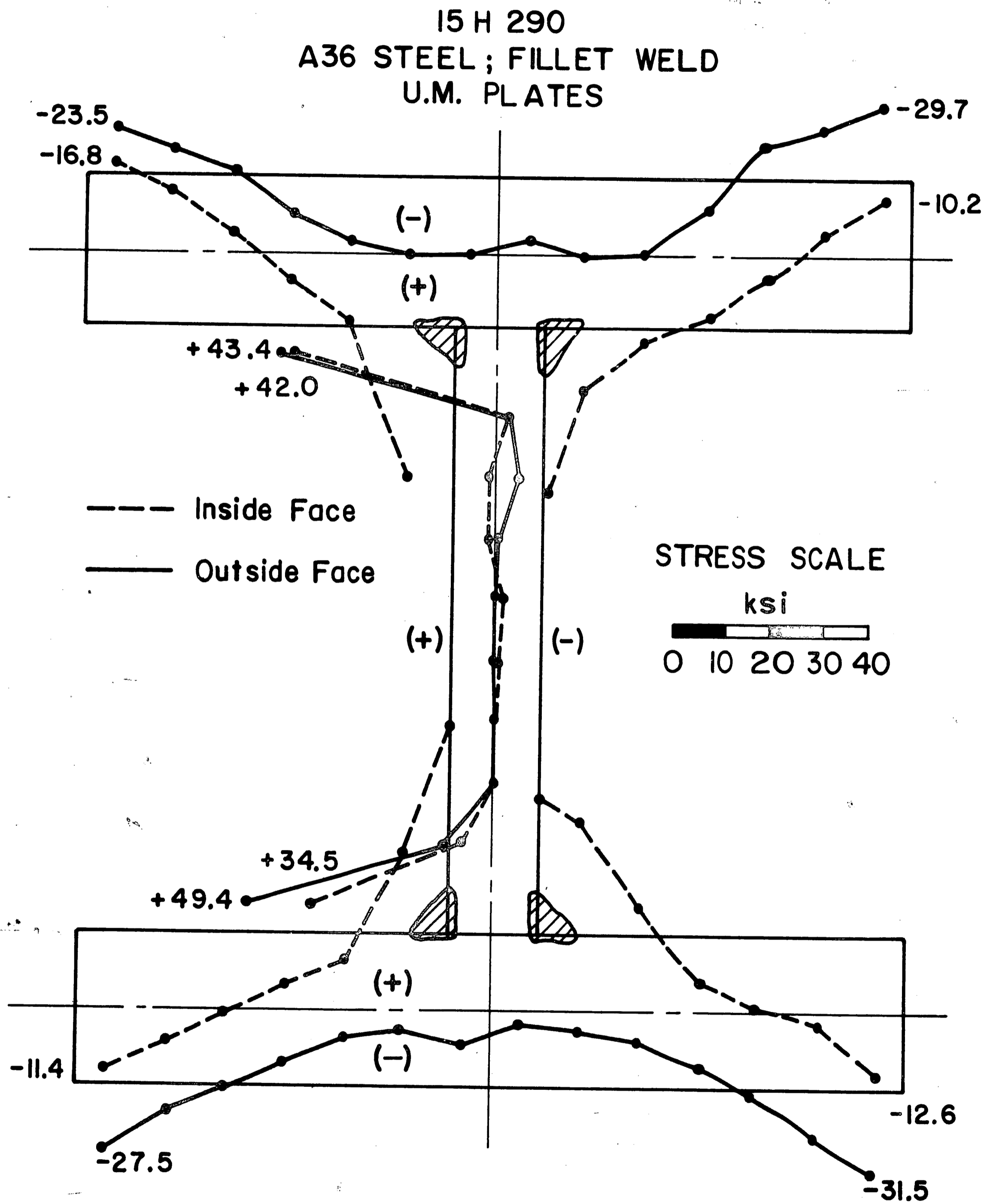


Fig. 11 Residual Stress Distribution In Column C1



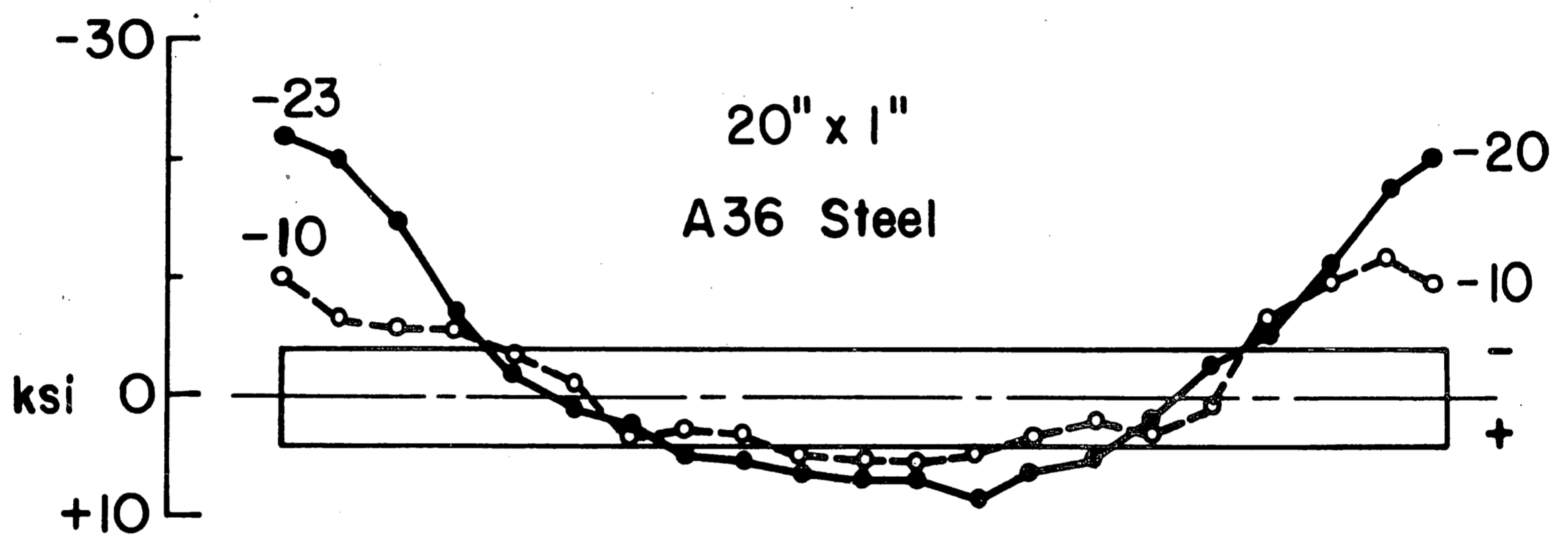


Fig. 12 Cooling Residual Stress Distribution In 20" x 1"  
Plate Of A36 Steel

15 H 290  
A36 STEEL ; FILLET WELD  
U.M. PLATES

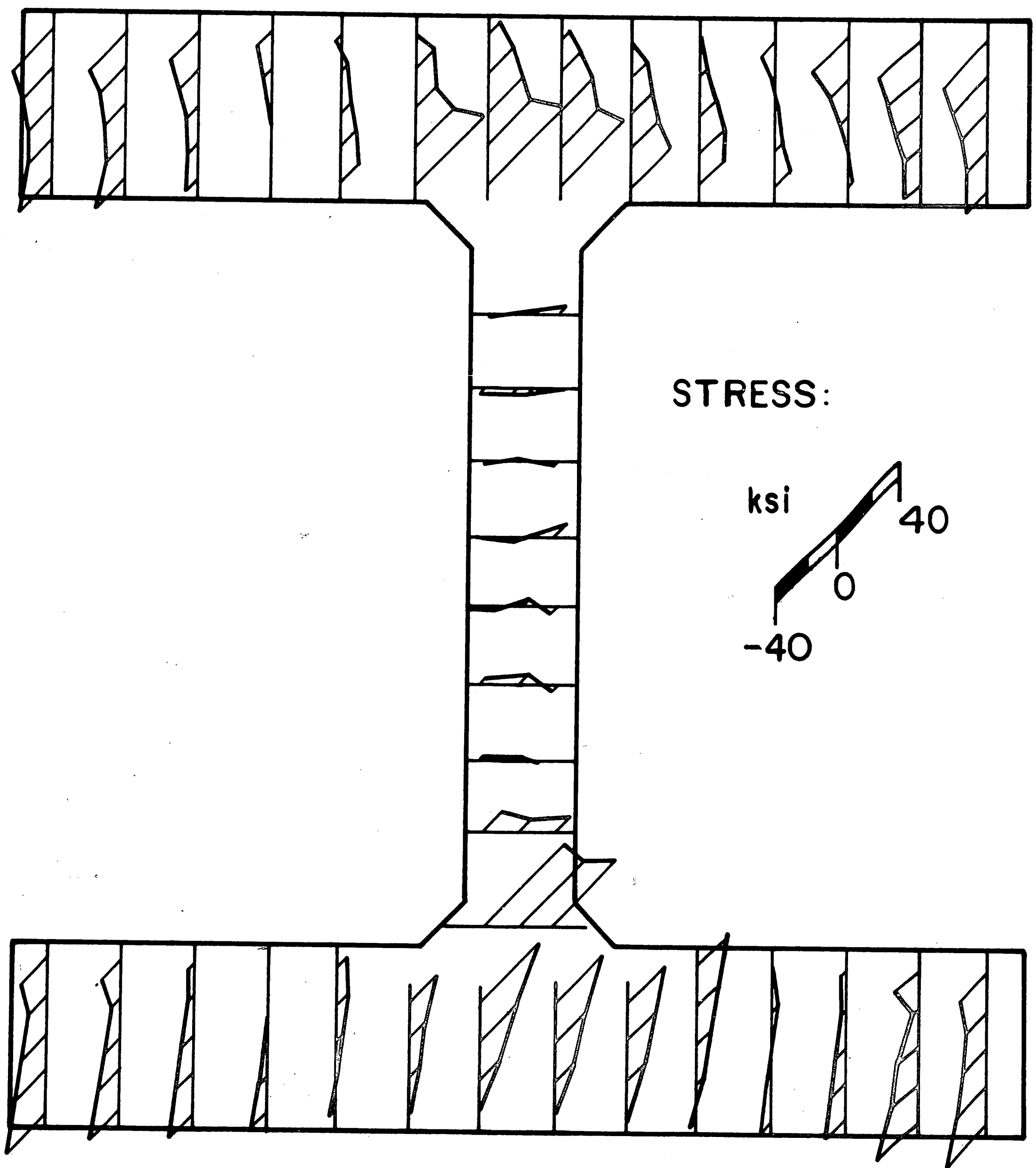


Fig. 13 Residual Stress Variation Through The Thickness  
Of Plates Of Column C1

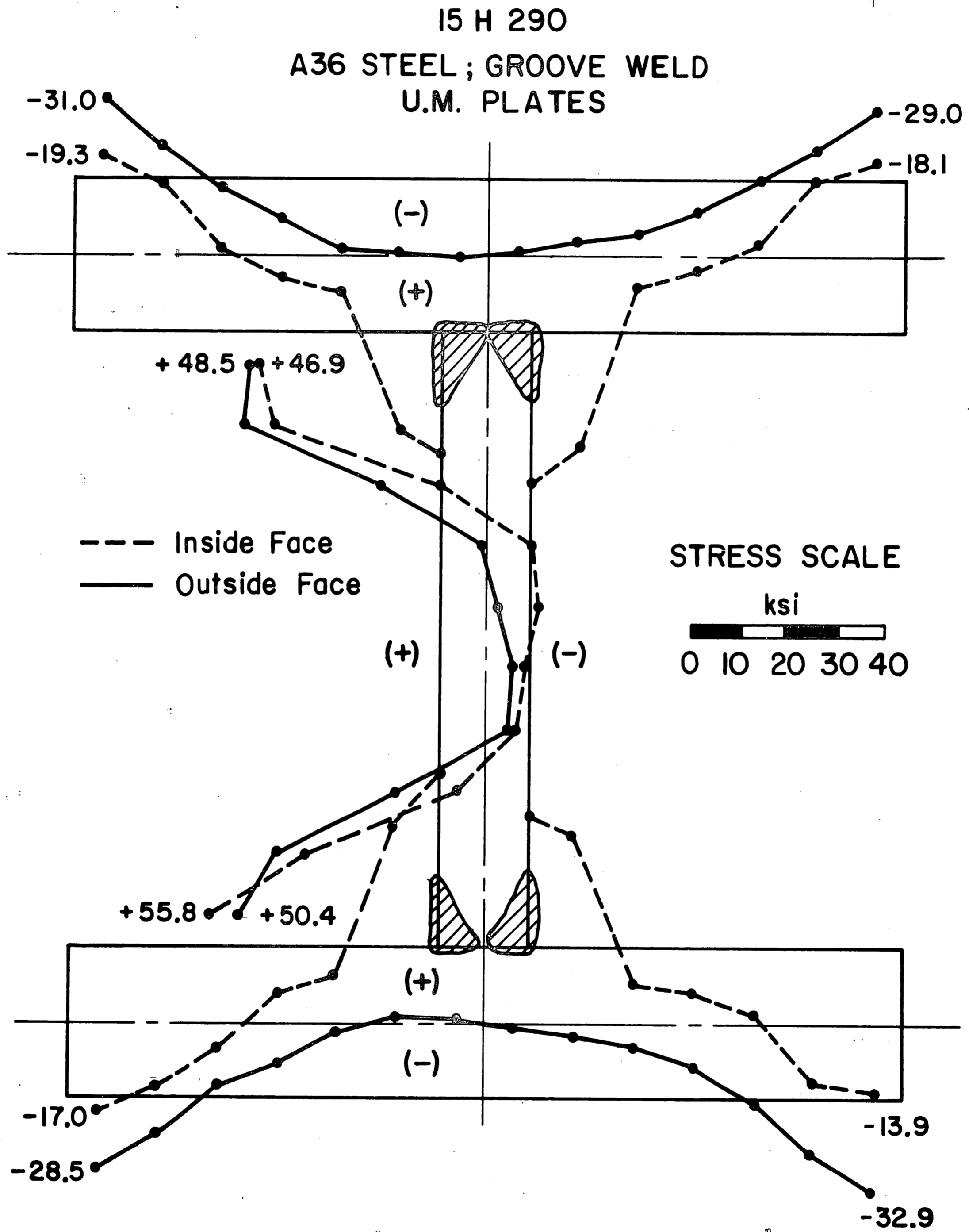


Fig. 14 Residual Stress Distribution In Column C3

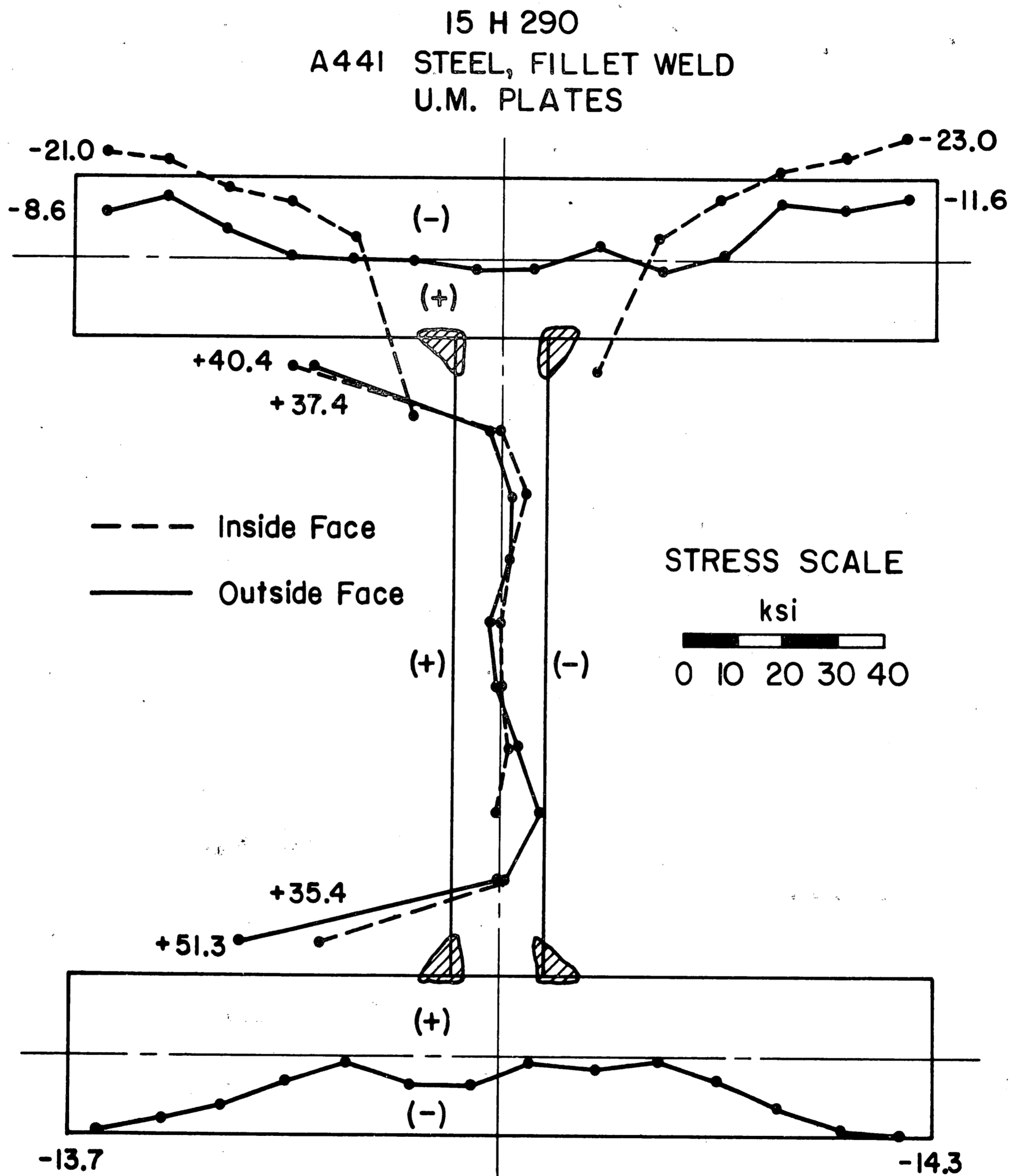


Fig. 15 Residual Stress Distribution In Column C5

15 H 290  
A441 STEEL ; GROOVE WELD  
U.M. PLATES

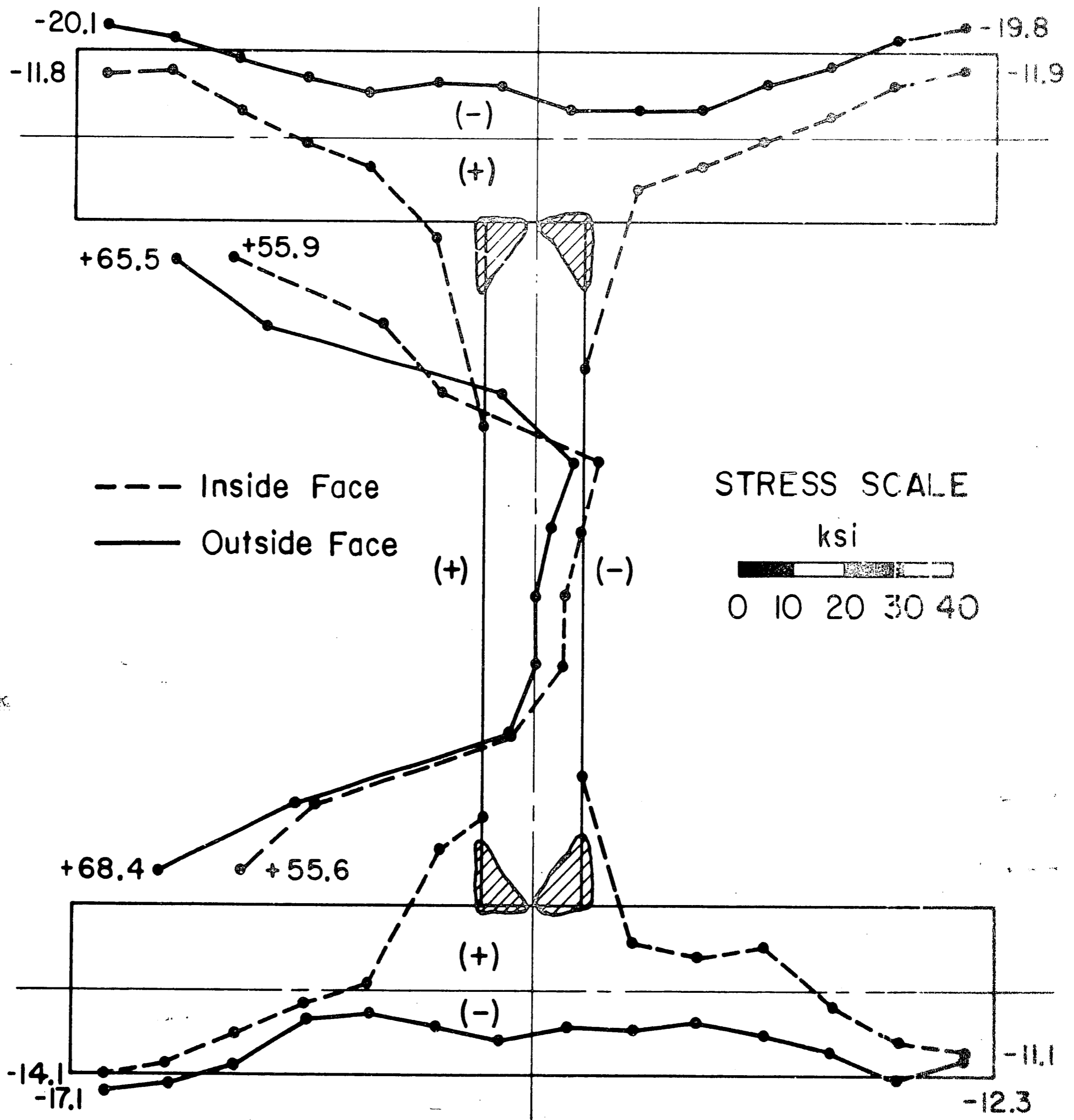


Fig. 16 Residual Stress Distribution In Column C7

LIGHT WELDED SHAPES  
A7 STEEL, F.C. PLATES

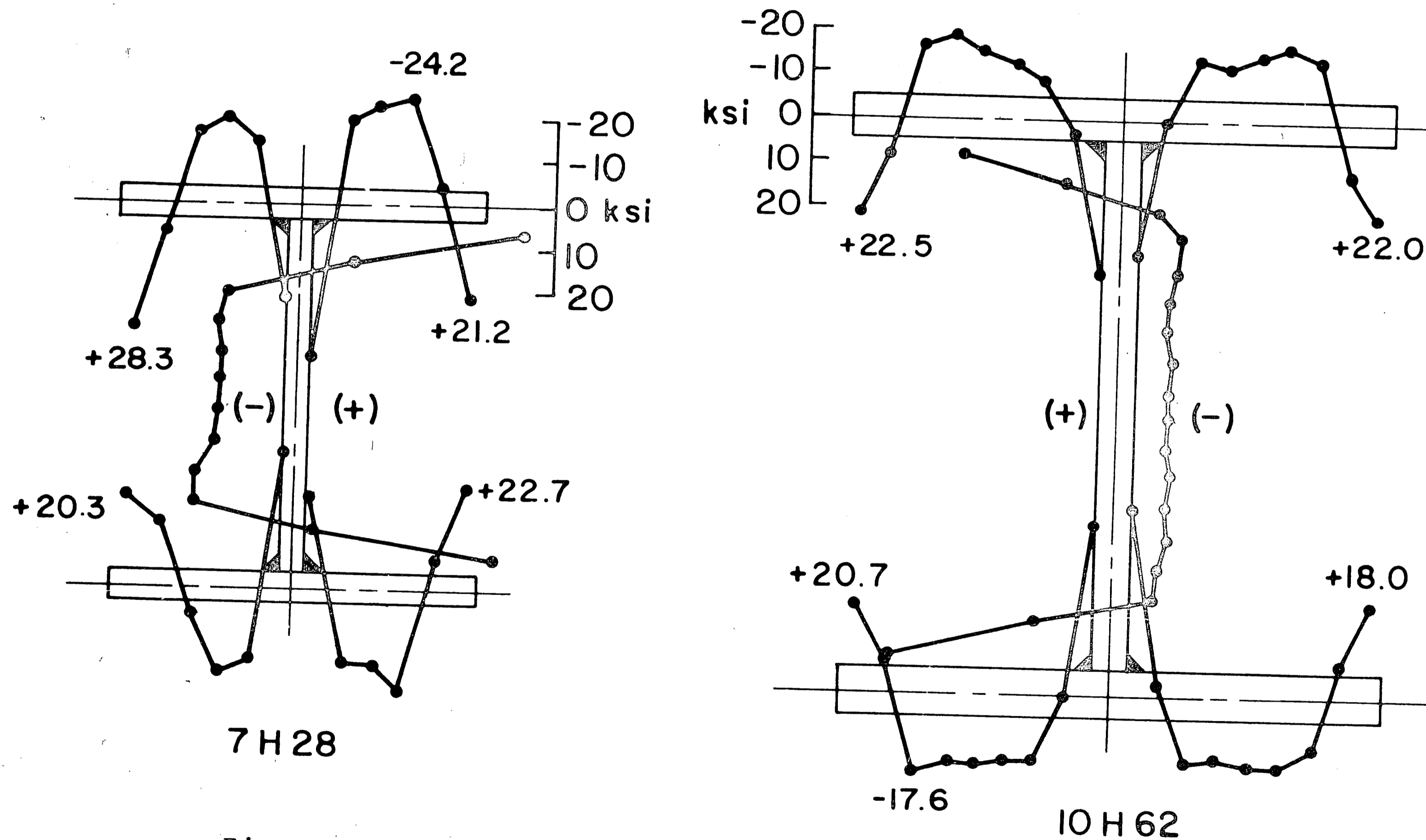


Fig. 17 Residual Stress Distributions In Light Welded  
Shapes Of Flame-Cut Plates

15 H 290  
A36 STEEL, FILLET WELD  
FLAME-CUT PLATES

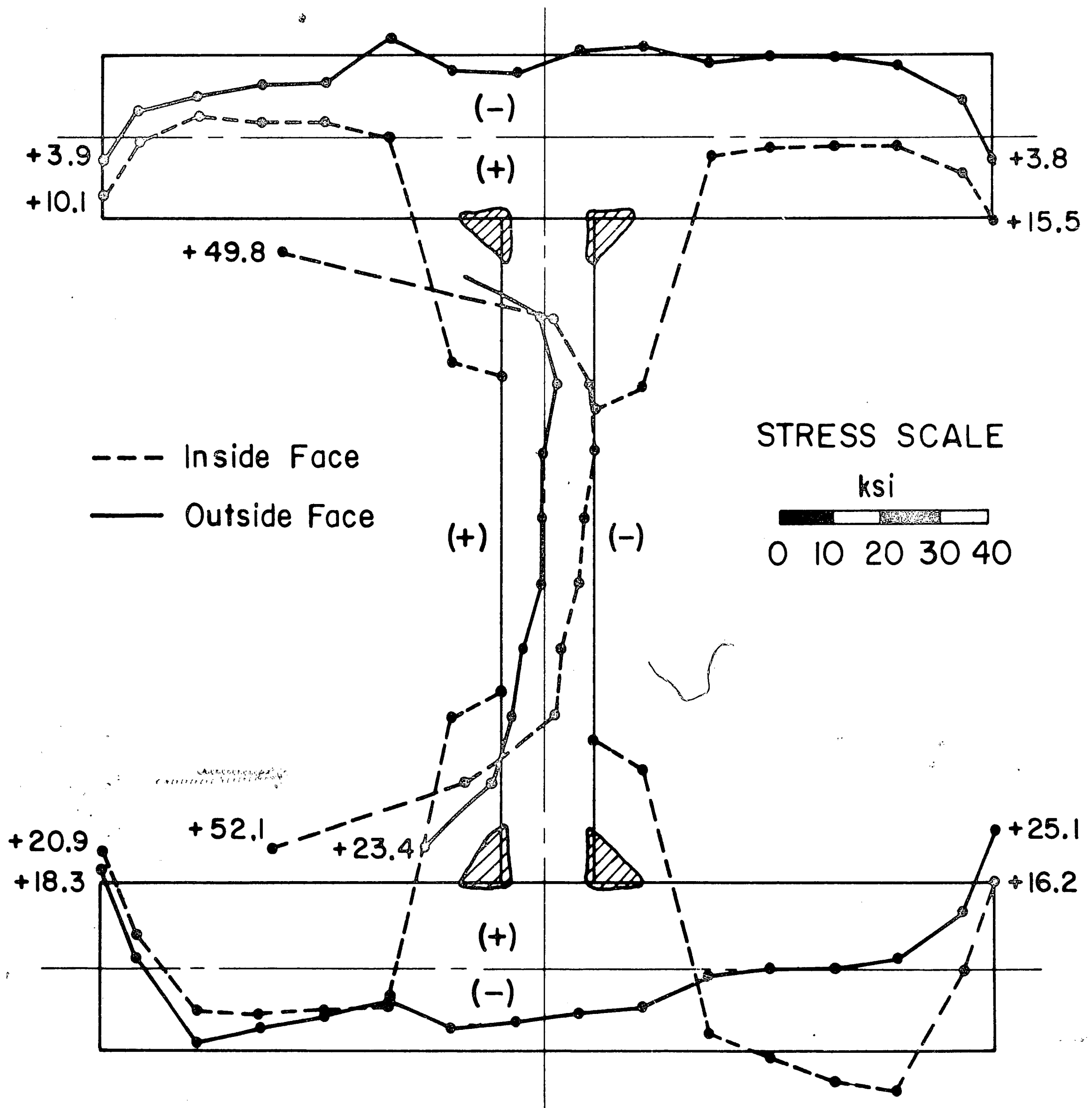


Fig. 18 Residual Stress Distribution In Column C9

15 H 290  
A36 STEEL; FILLET WELD  
FLAME-CUT PLATES

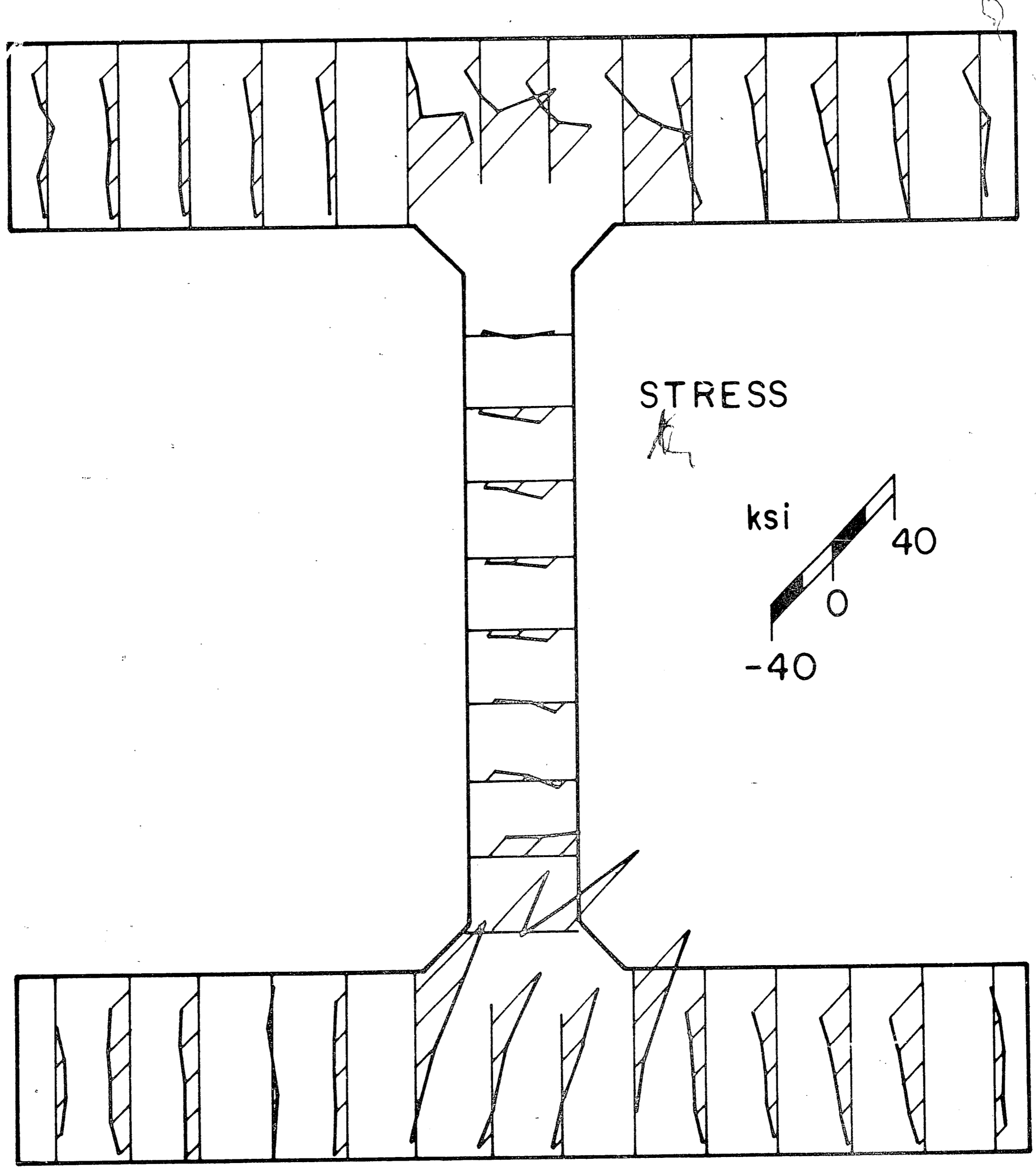


Fig. 19 Residual Stress Variation Through The Thickness  
Of Plates Of Column C9



15 H 290  
A 36 STEEL, GROOVE WELD  
FLAME-CUT PLATES

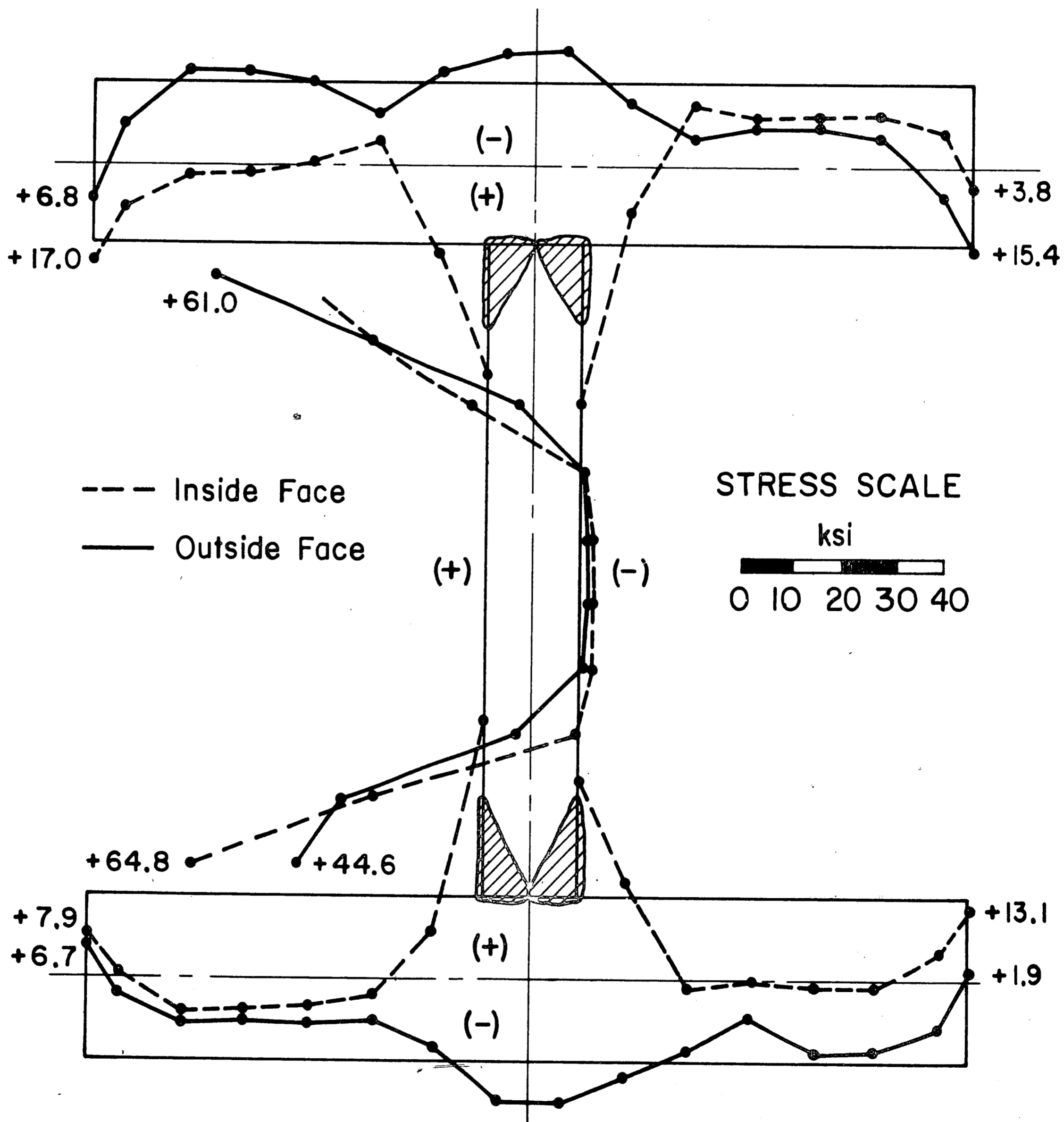


Fig. 20 Residual Stress Distribution In Column C11

15 H 290  
A441 STEEL, FILLET WELD  
FLAME-CUT PLATES

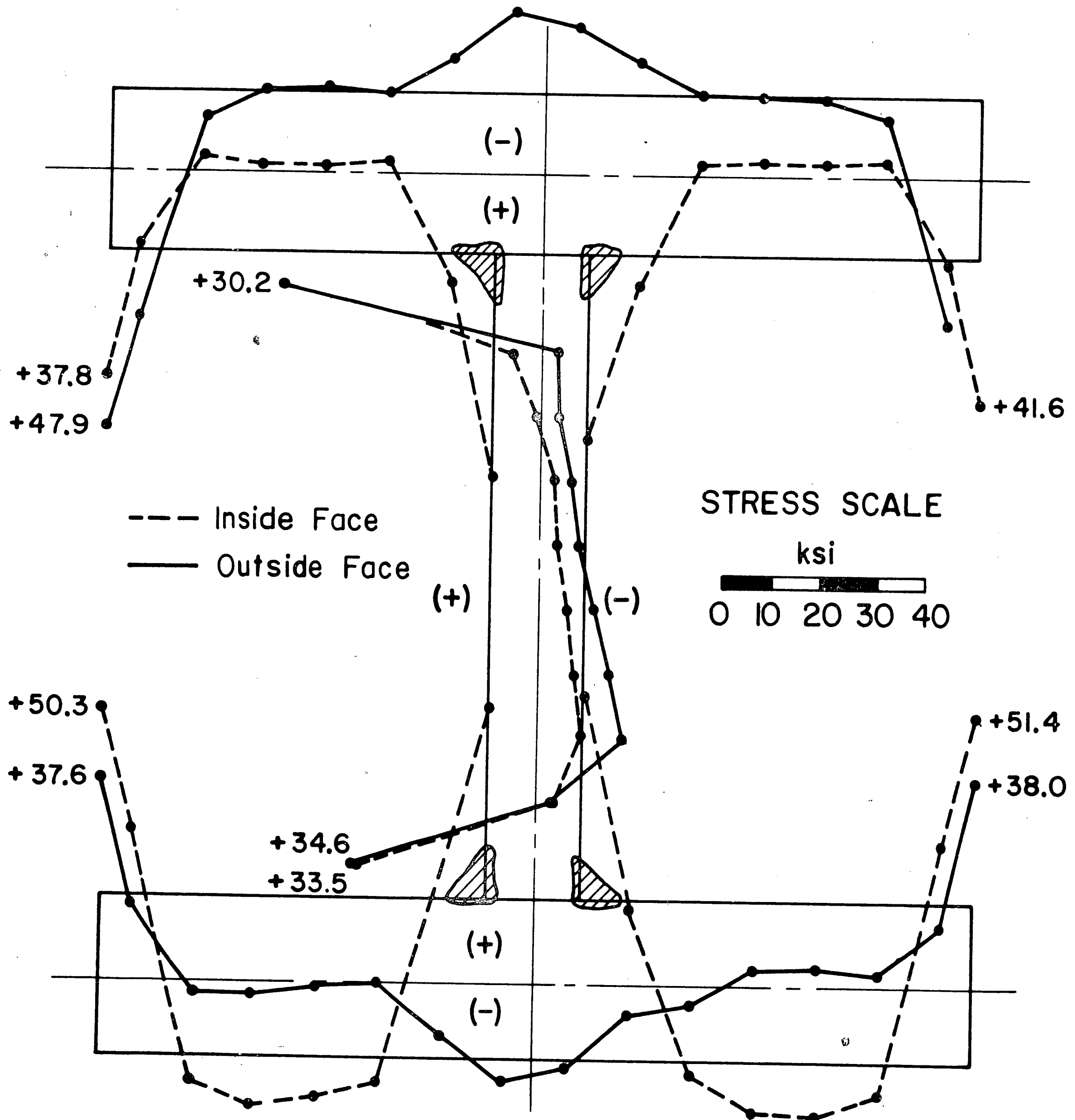


Fig. 21 Residual Stress Distribution In Column C13

15 H 290  
A441 STEEL, GROOVE WELD  
FLAME-CUT PLATES

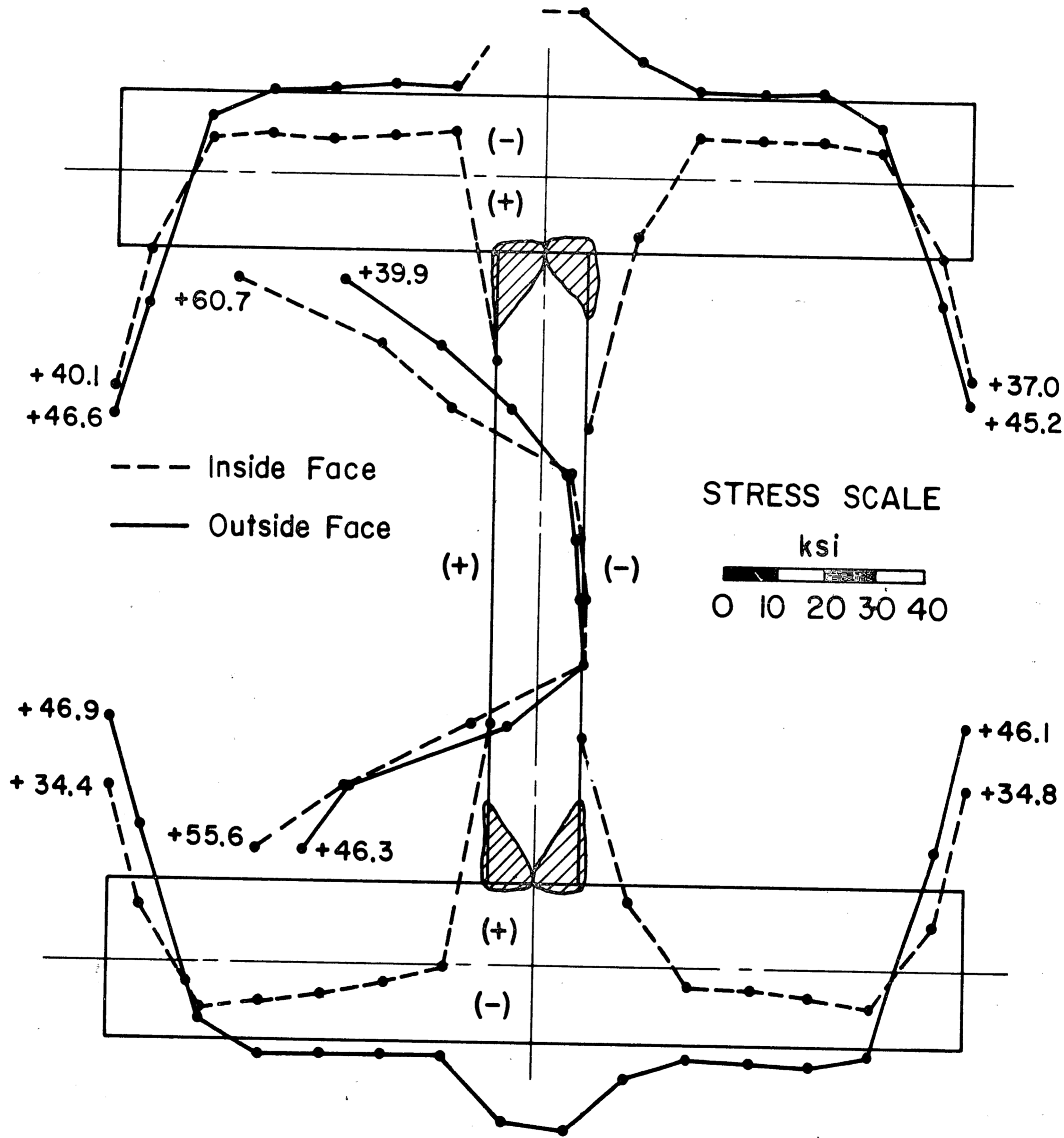


Fig. 22 Residual Stress Distribution In Column C16

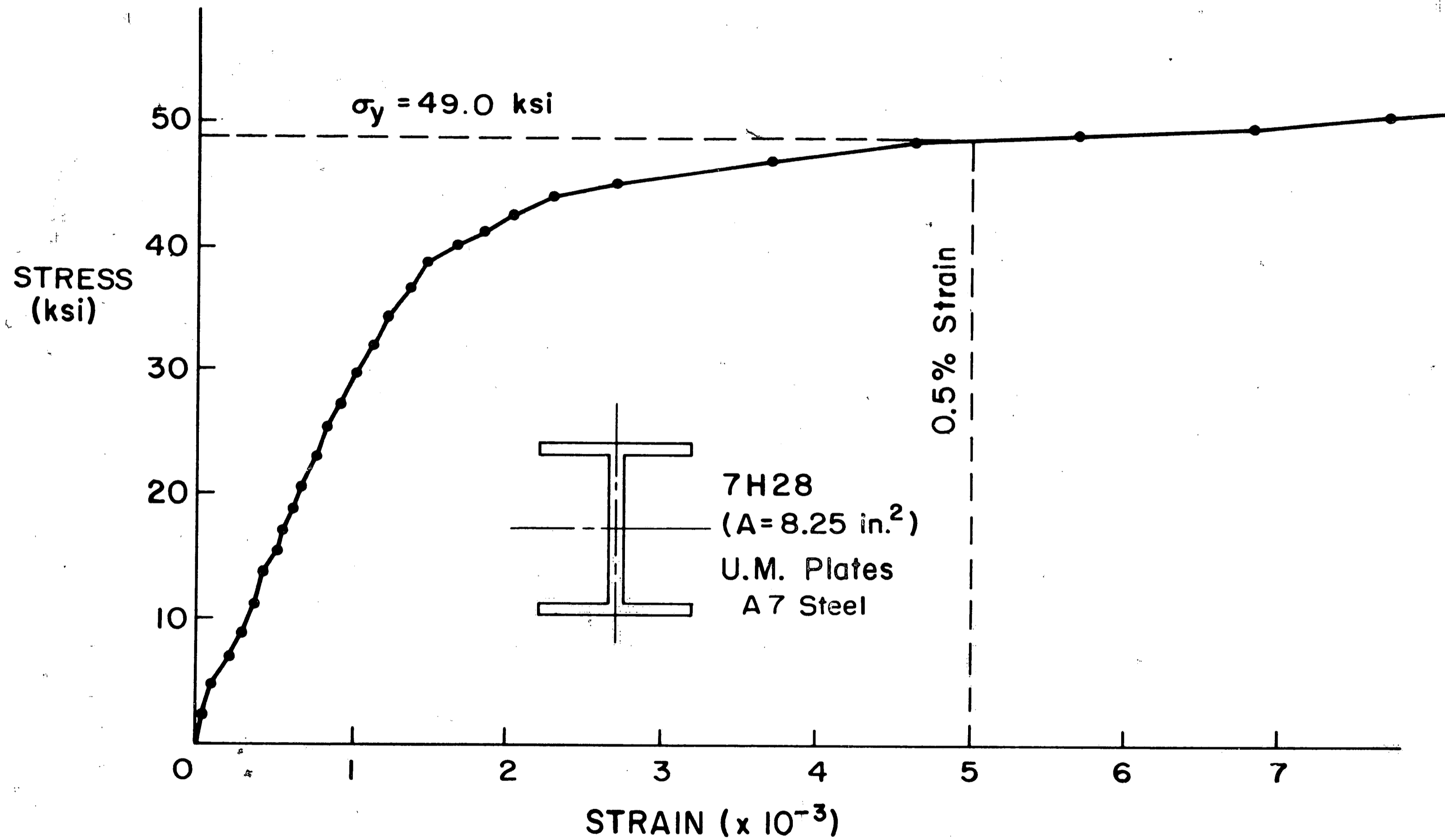


Fig. 23 Stub Column Test Results For 7H28 Shape  
With UM Plates

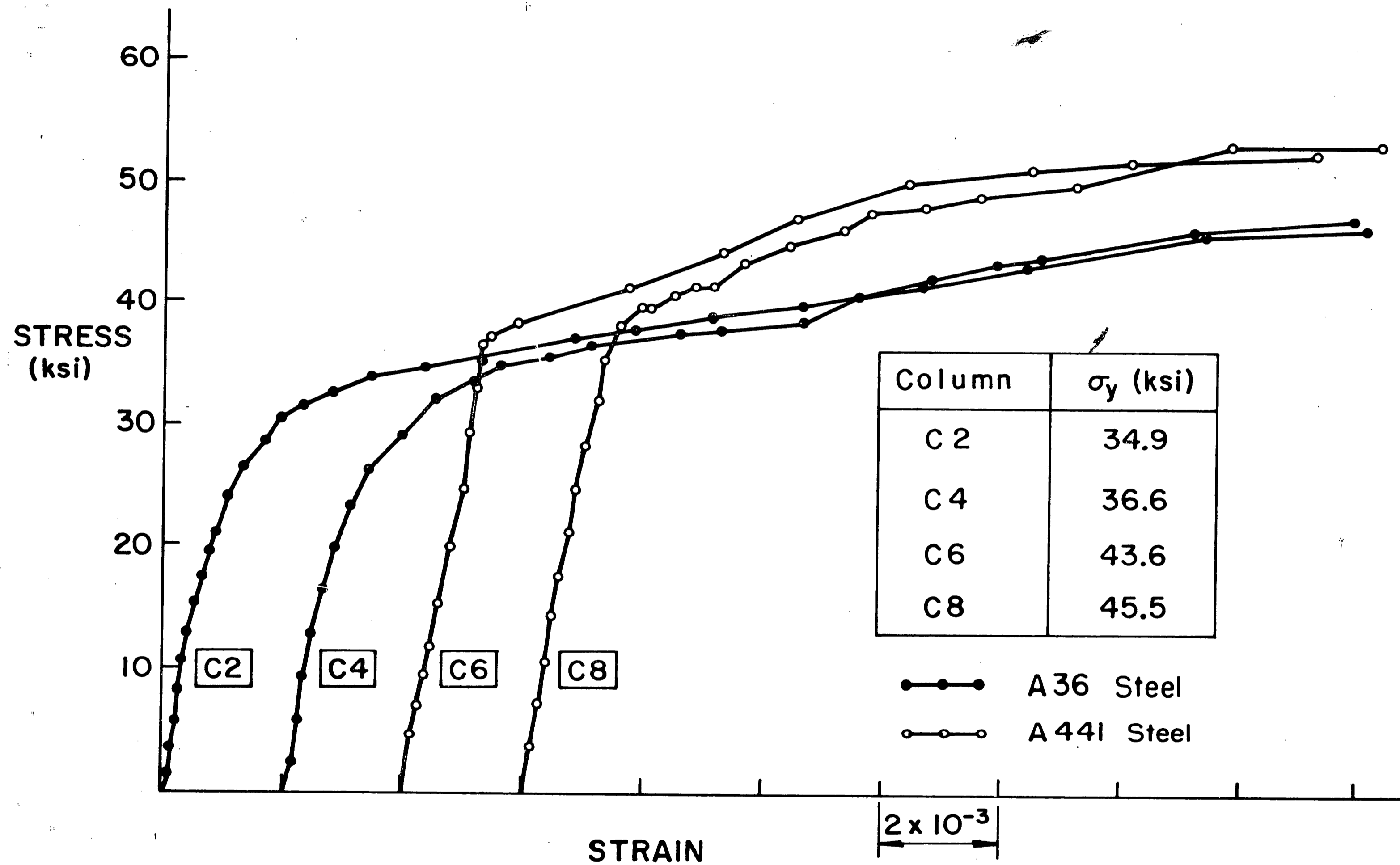


Fig. 24. Stub Column Test Results For Heavy Shapes  
With UM Plates

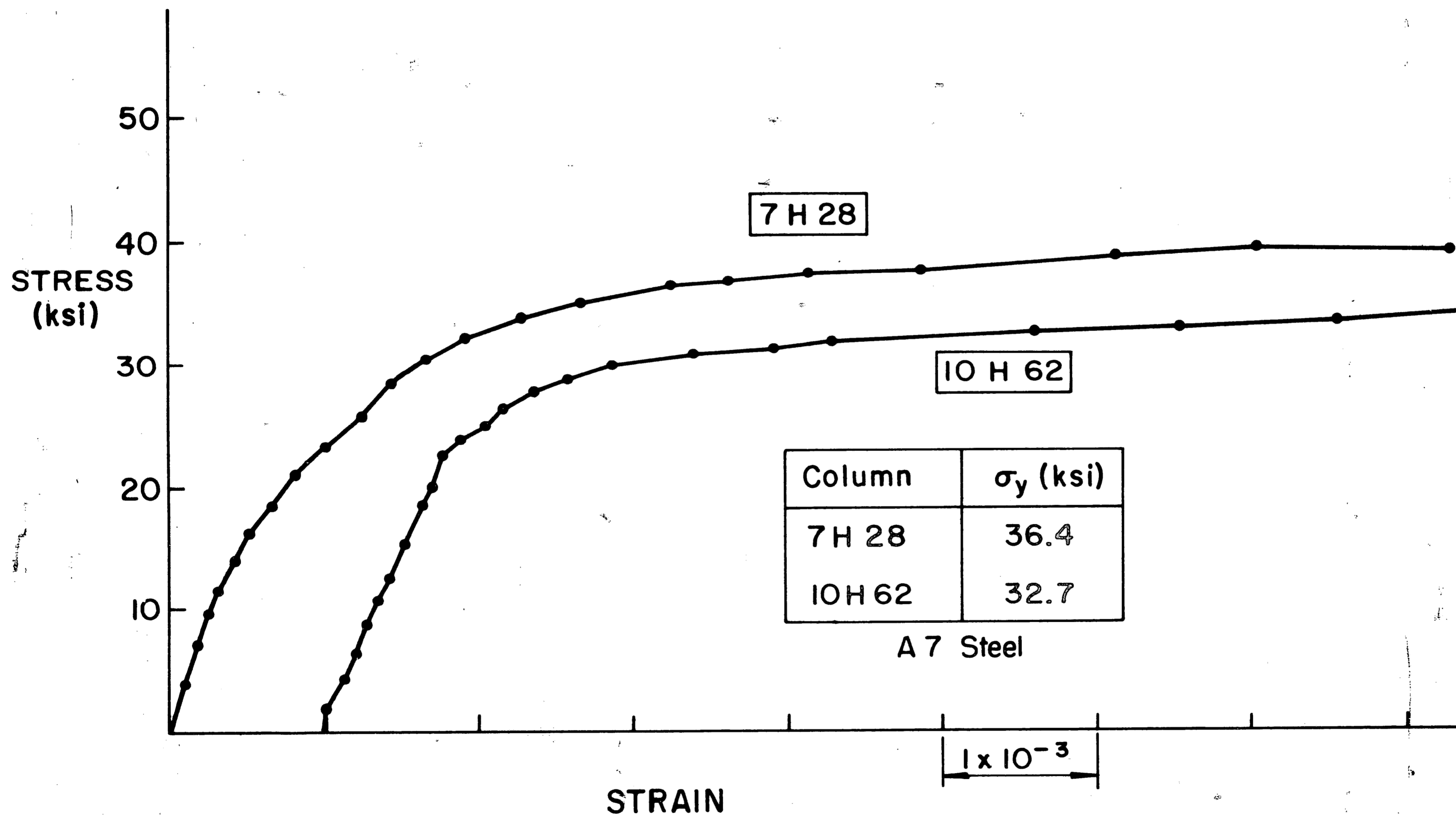


Fig. 25 Stub Column Test Results For Light Shapes  
With Flame-Cut Plates

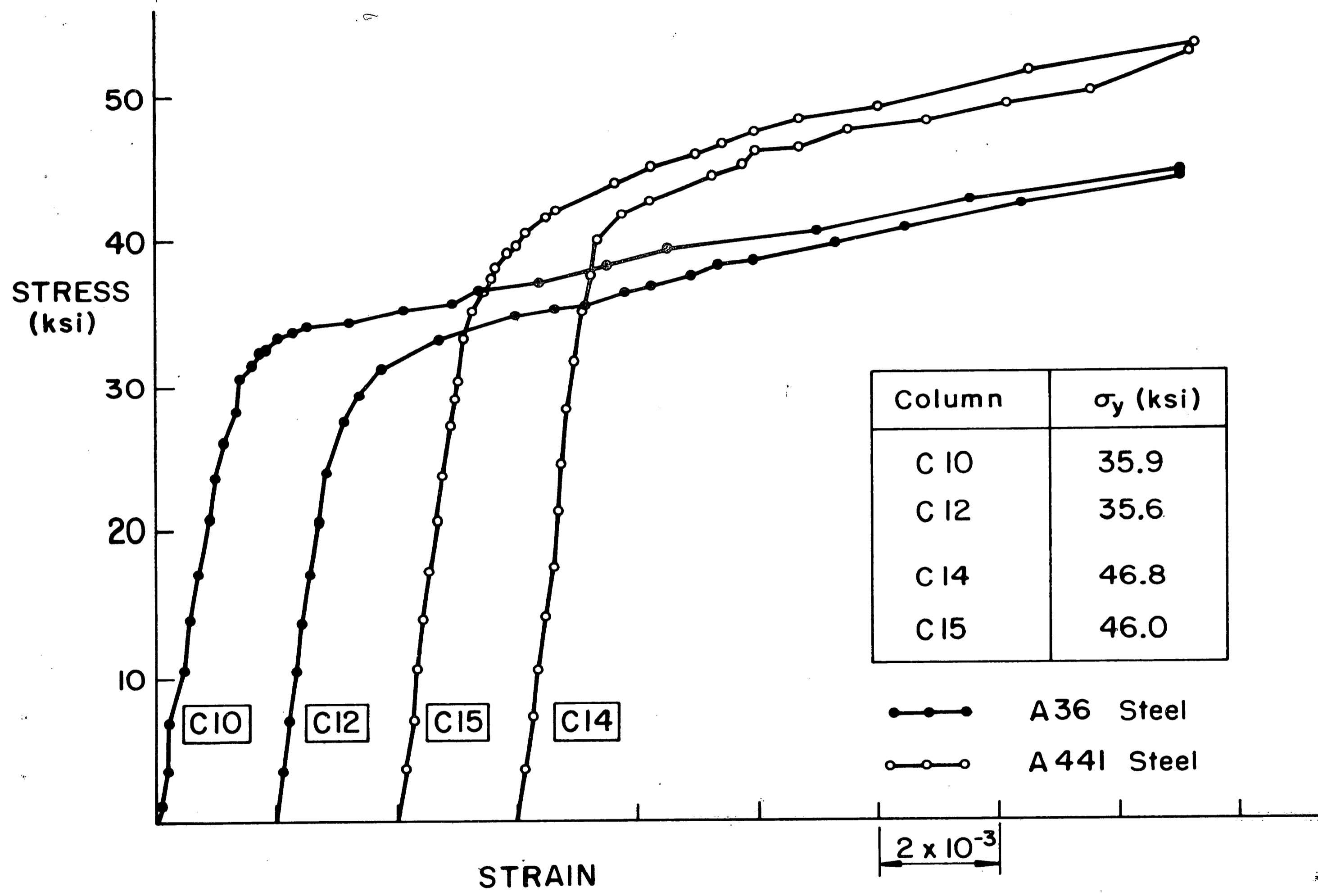


Fig. 26 Stub Column Test Results For Heavy Shapes  
With Flame-Cut Plates

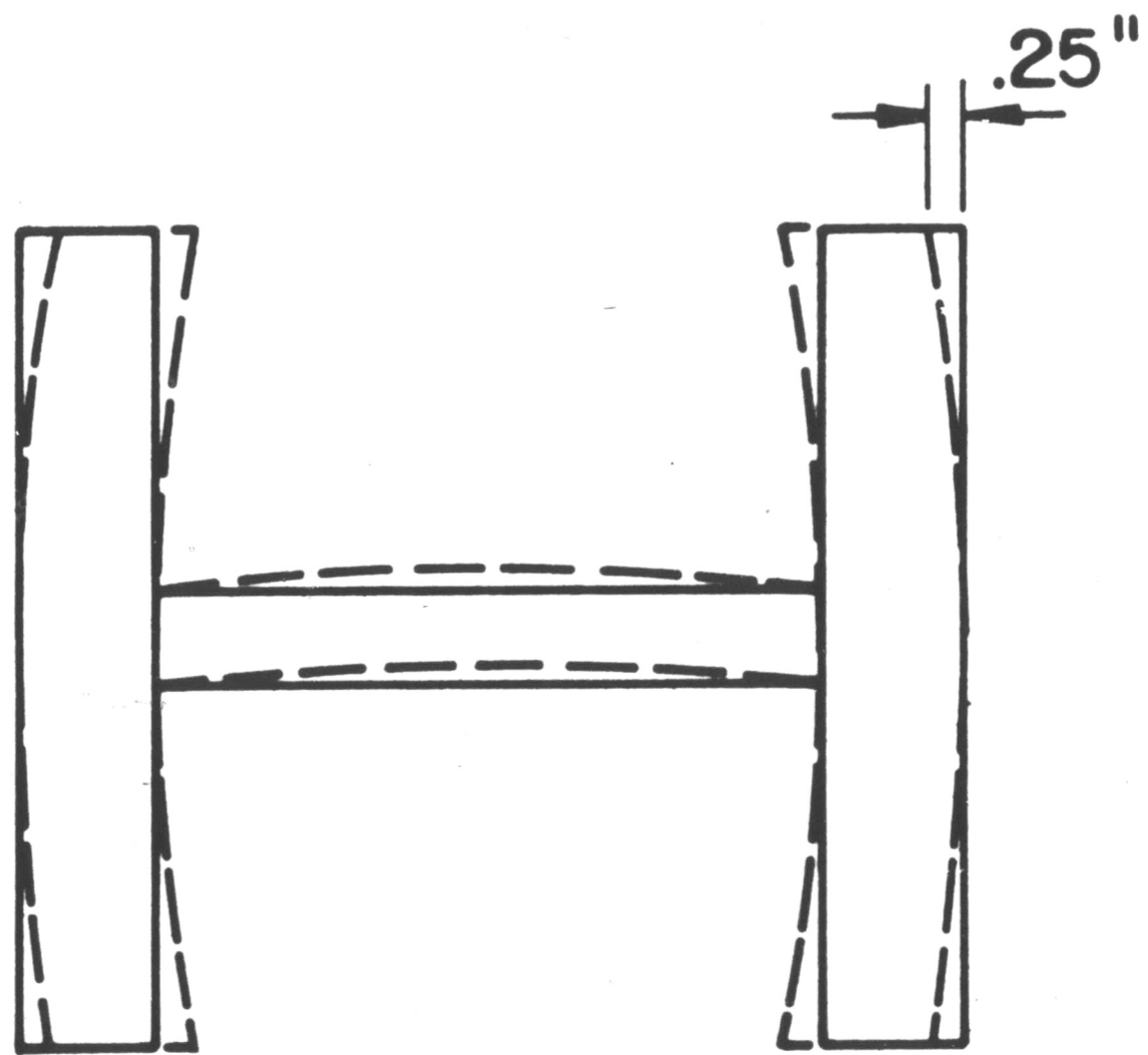
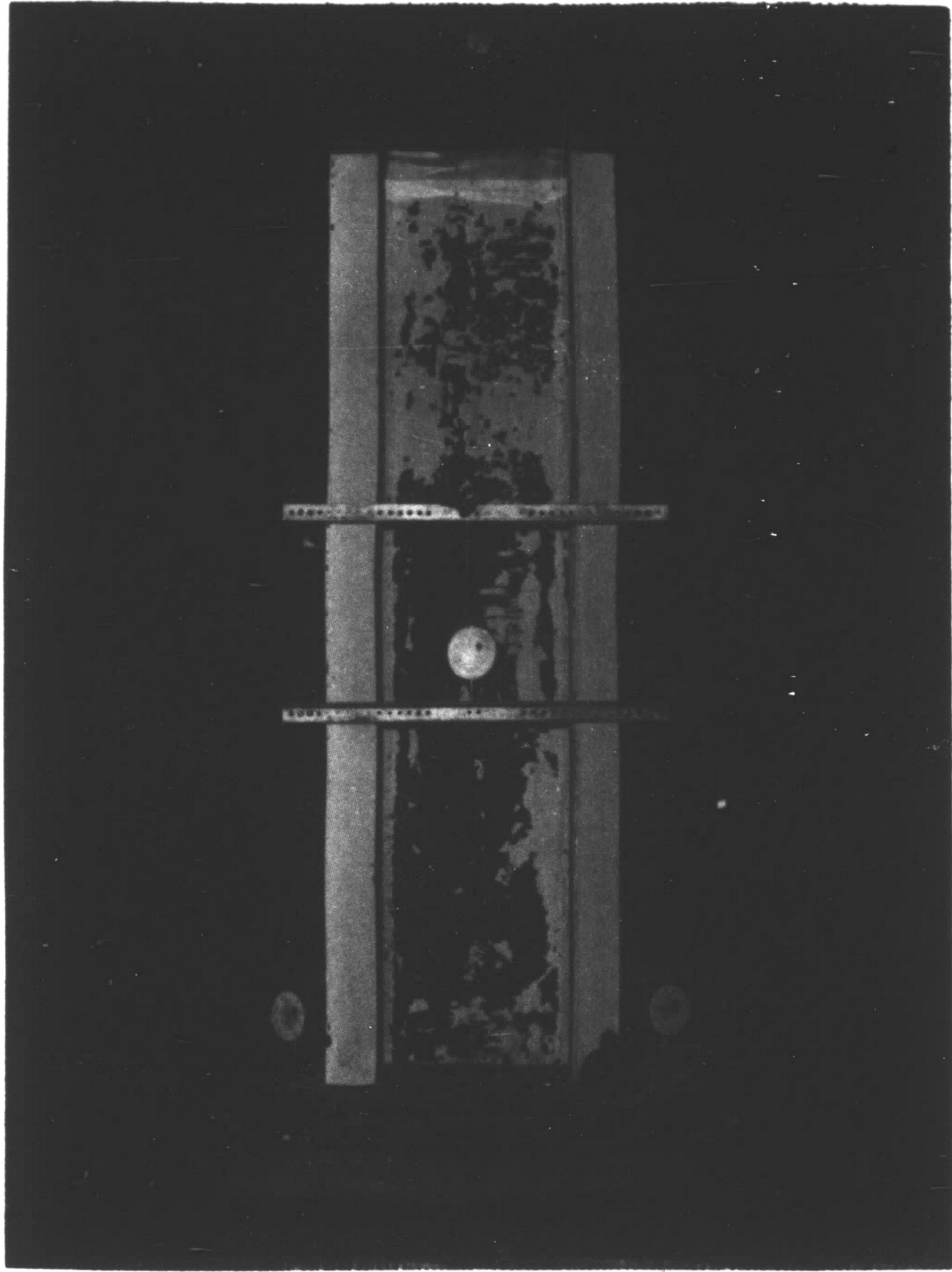


Fig. 27 "Cross Bending" In Stub Column C10



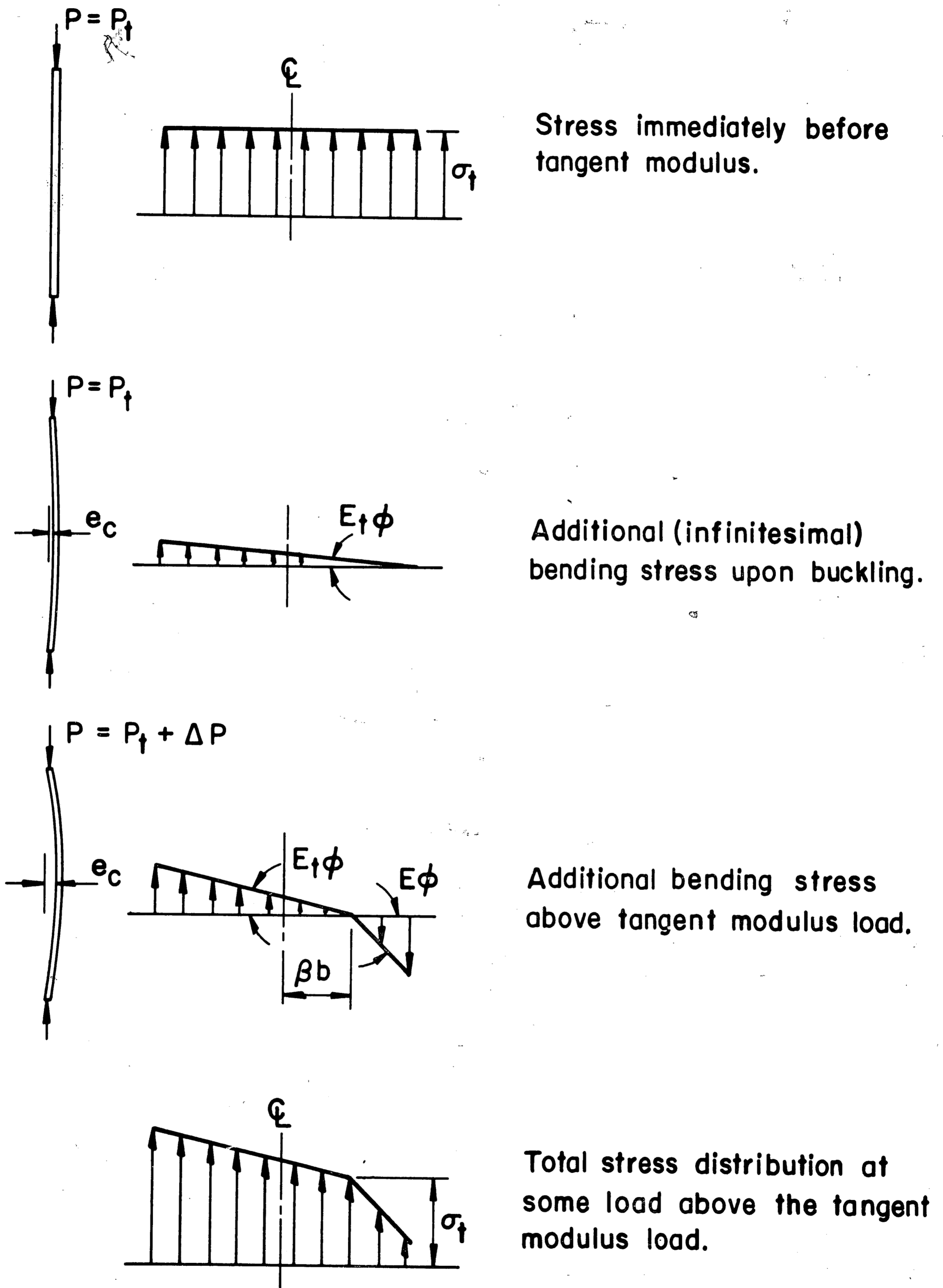


Fig. 28 Stress Distribution In Column At Bifurcation

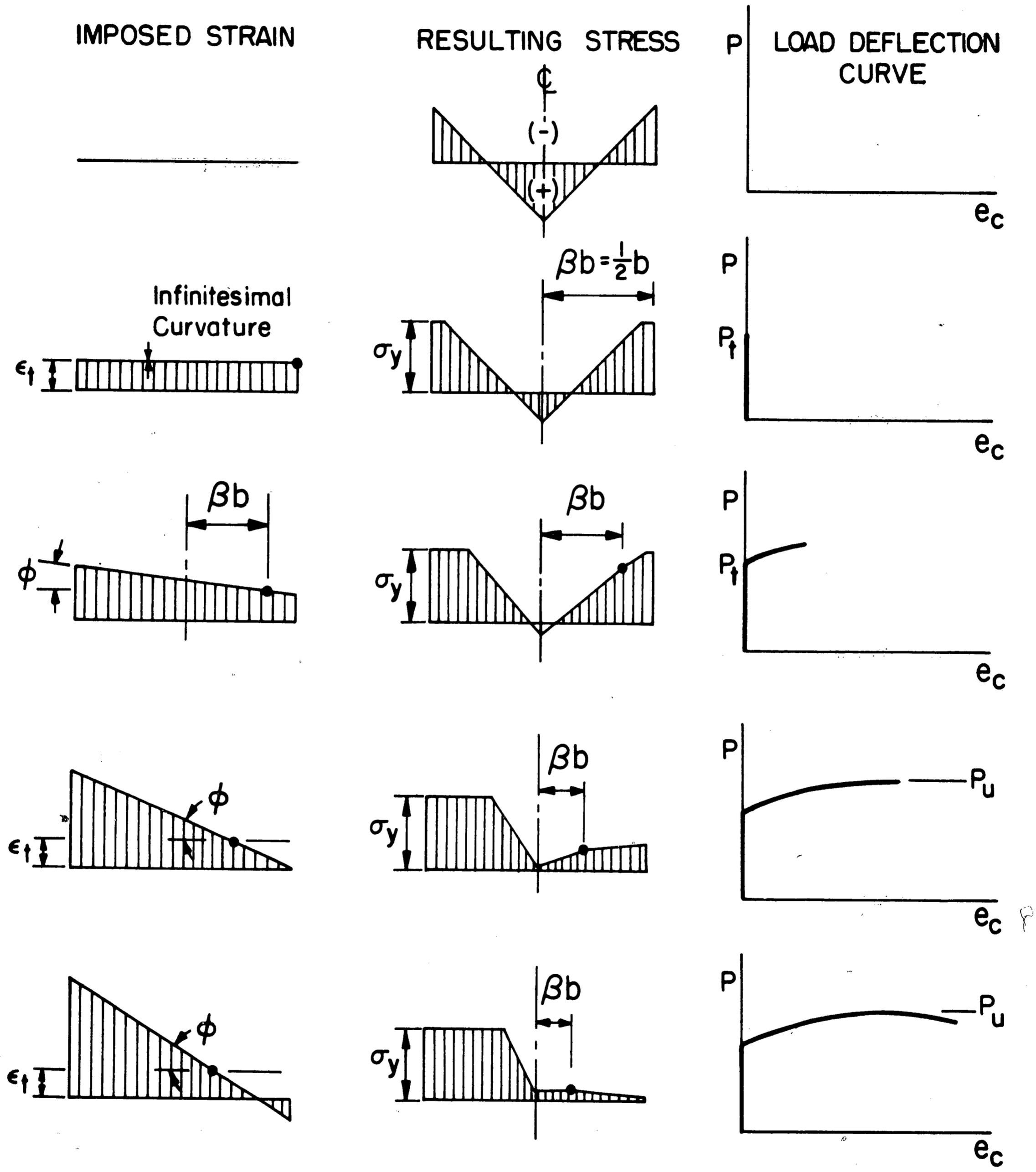
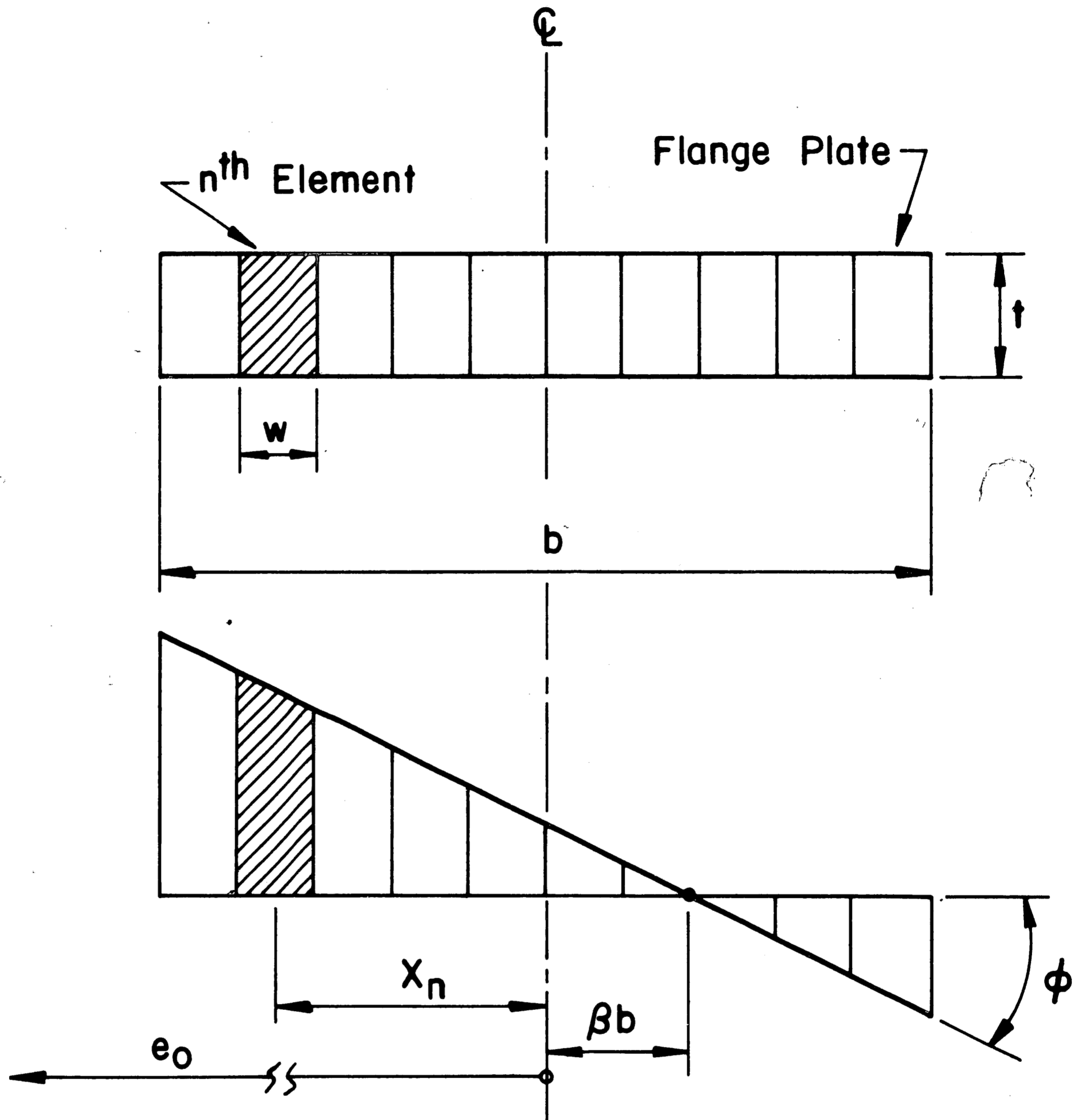
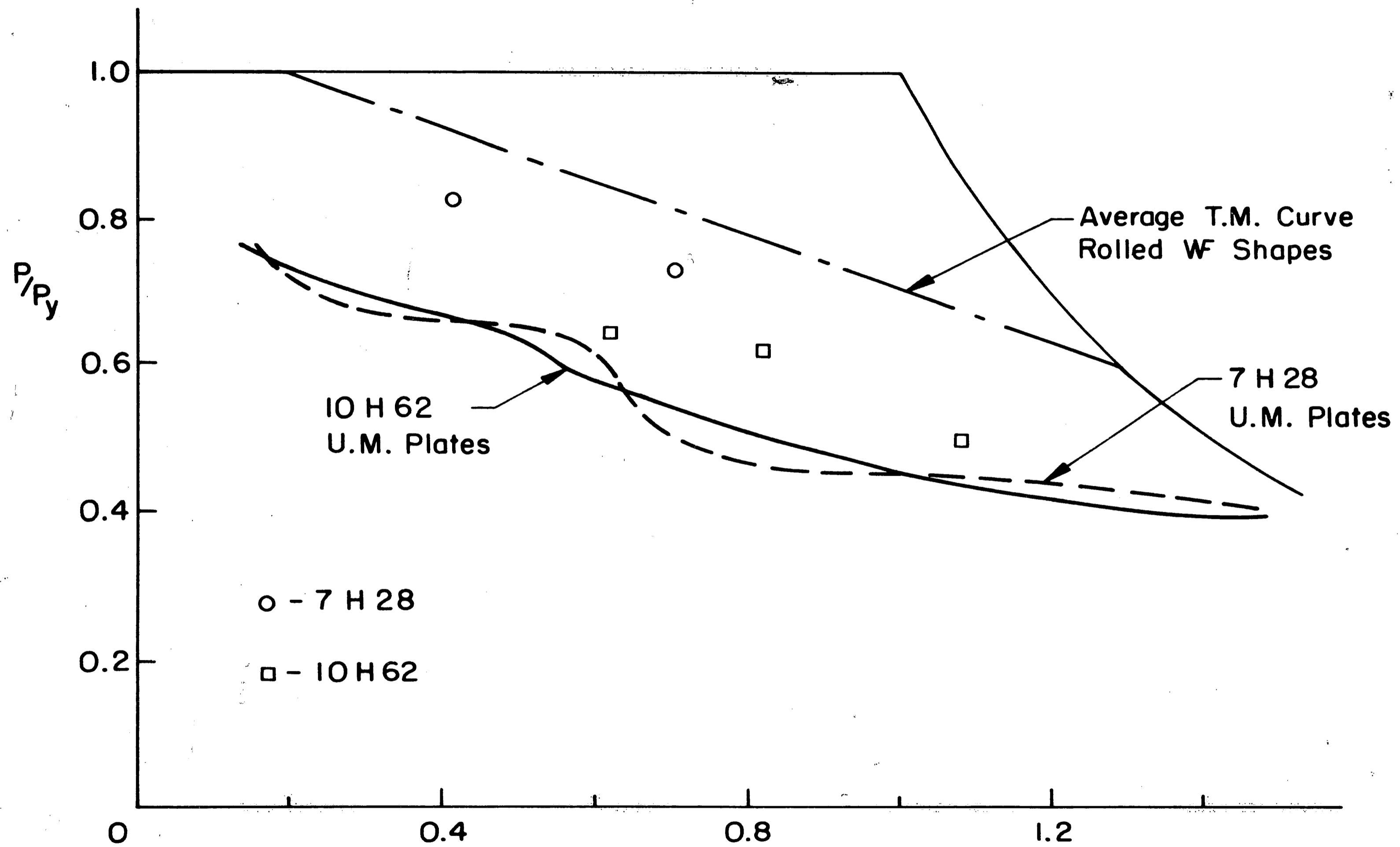


Fig. 29 Post-Buckling Behavior Of Columns Containing Residual Stress



**Additional Strain Above  
Tangent Modulus Load**

Fig. 30 Bending Strain In Deflected Column



$$\lambda = \sqrt{\frac{\sigma_y}{\pi^2 E}} \cdot \frac{KL}{r}$$

Fig. 31 Tangent Modulus Curves For Light Shapes With U.M. Plates (Weak Axis)

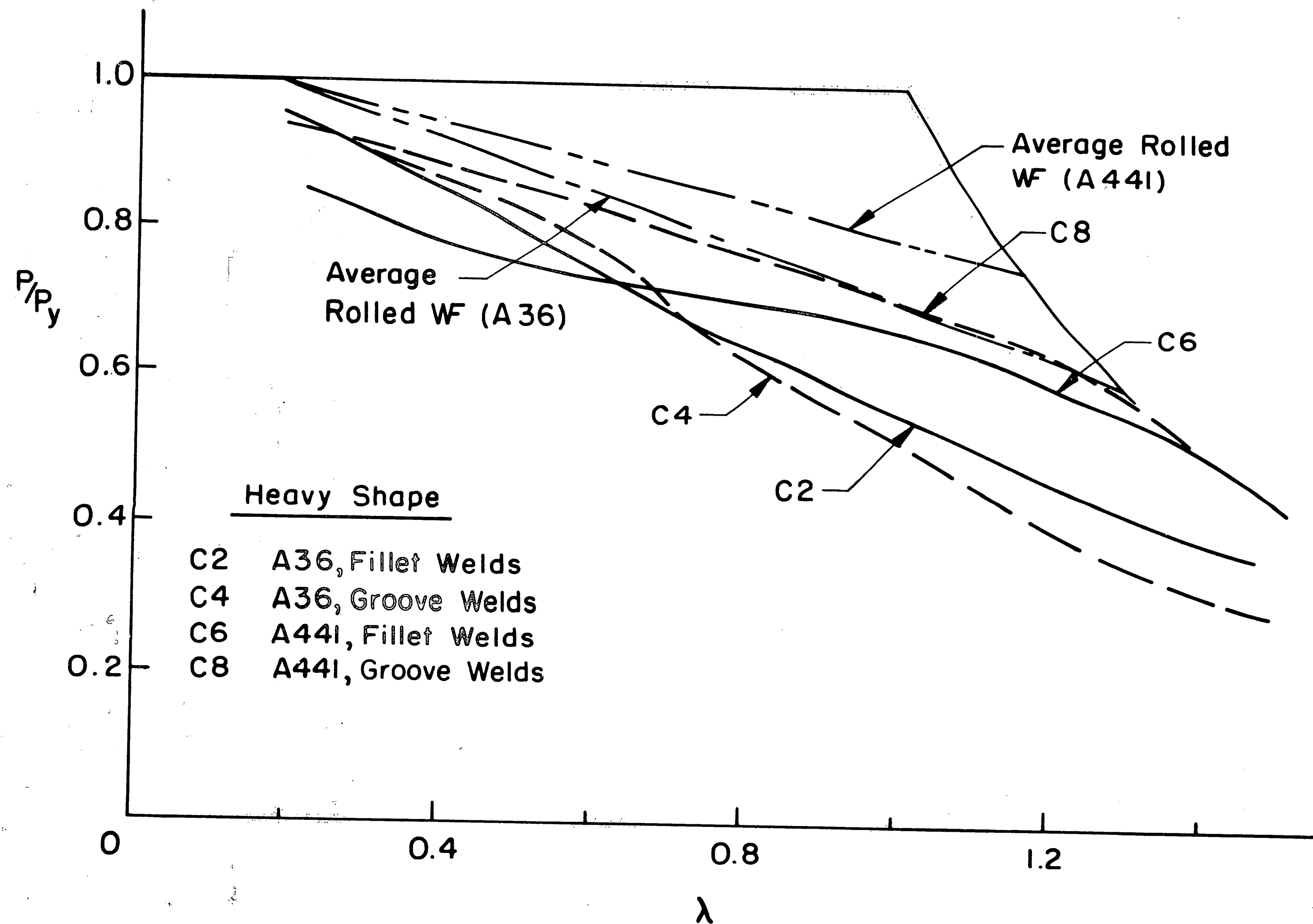


Fig. 32 Tangent Modulus Curves For Heavy Shapes With UM Plates (Weak Axis)

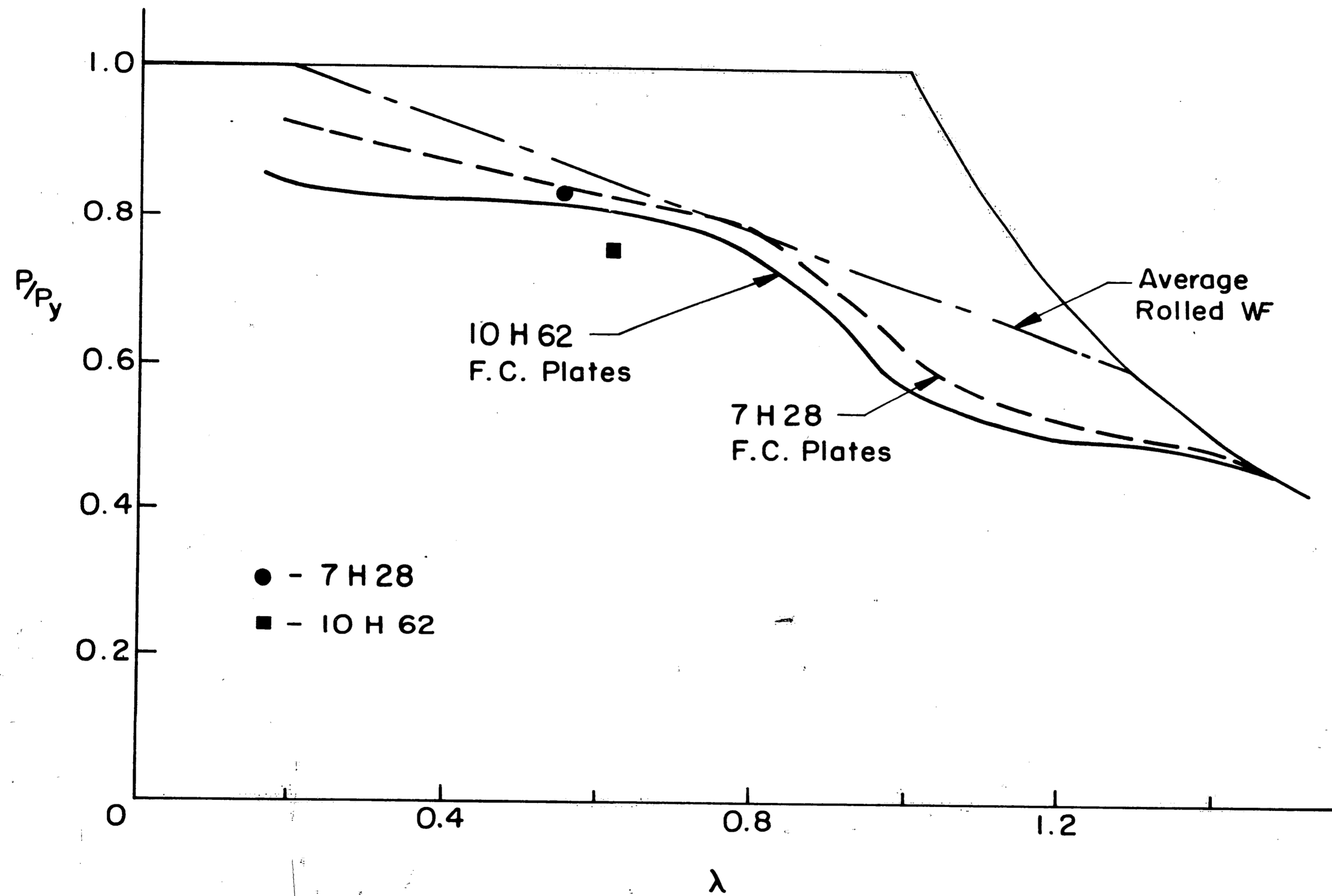


Fig. 33 Tangent Modulus Curves For Light Shapes With  
Flame-Cut Plates (Weak Axis)

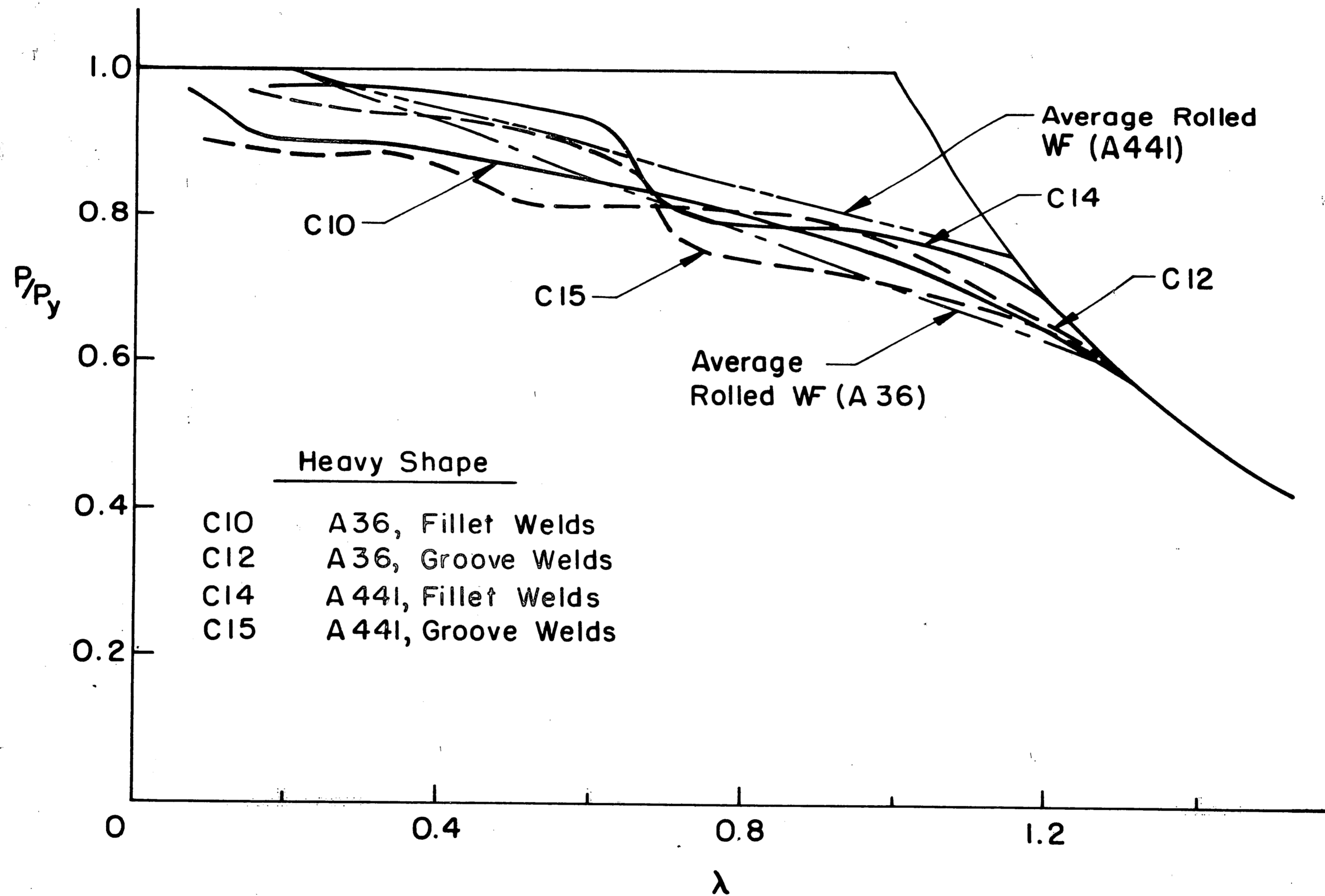


Fig. 34 Tangent Modulus Curves For Heavy Shapes With Flame-Cut Plates (Weak Axis)

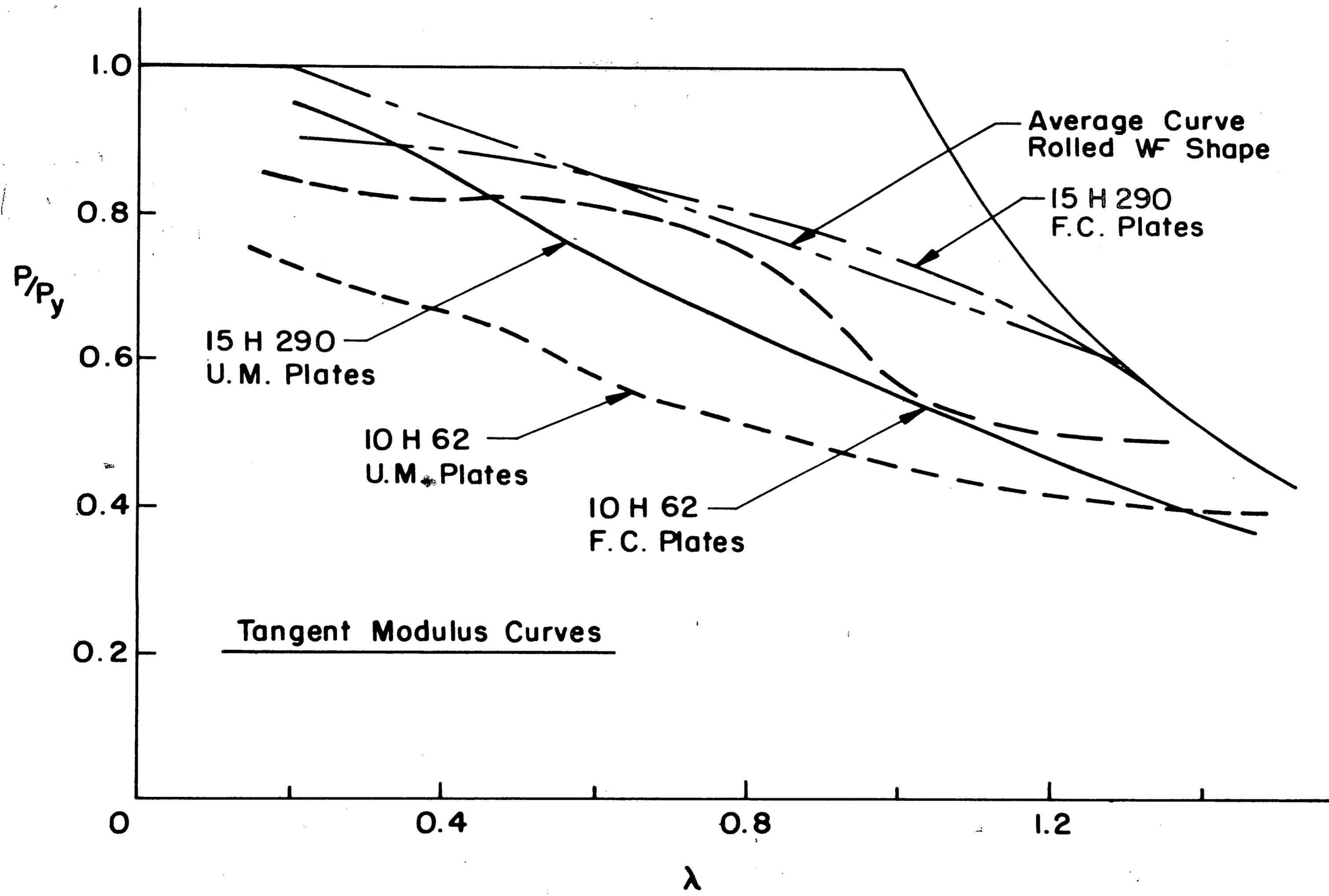


Fig. 35 Tangent Modulus Curves For Fillet Welded Specimens of Mild Steel



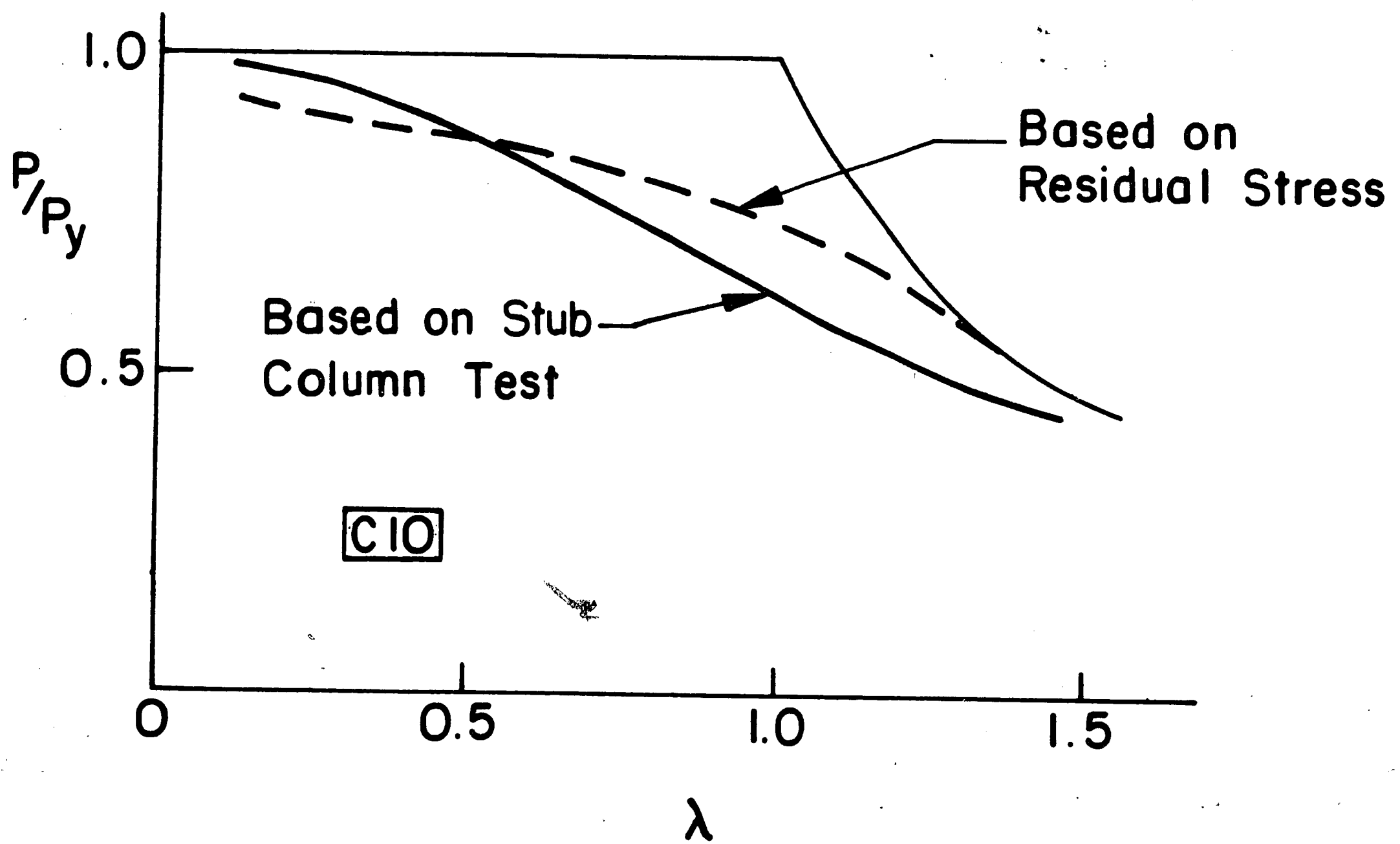
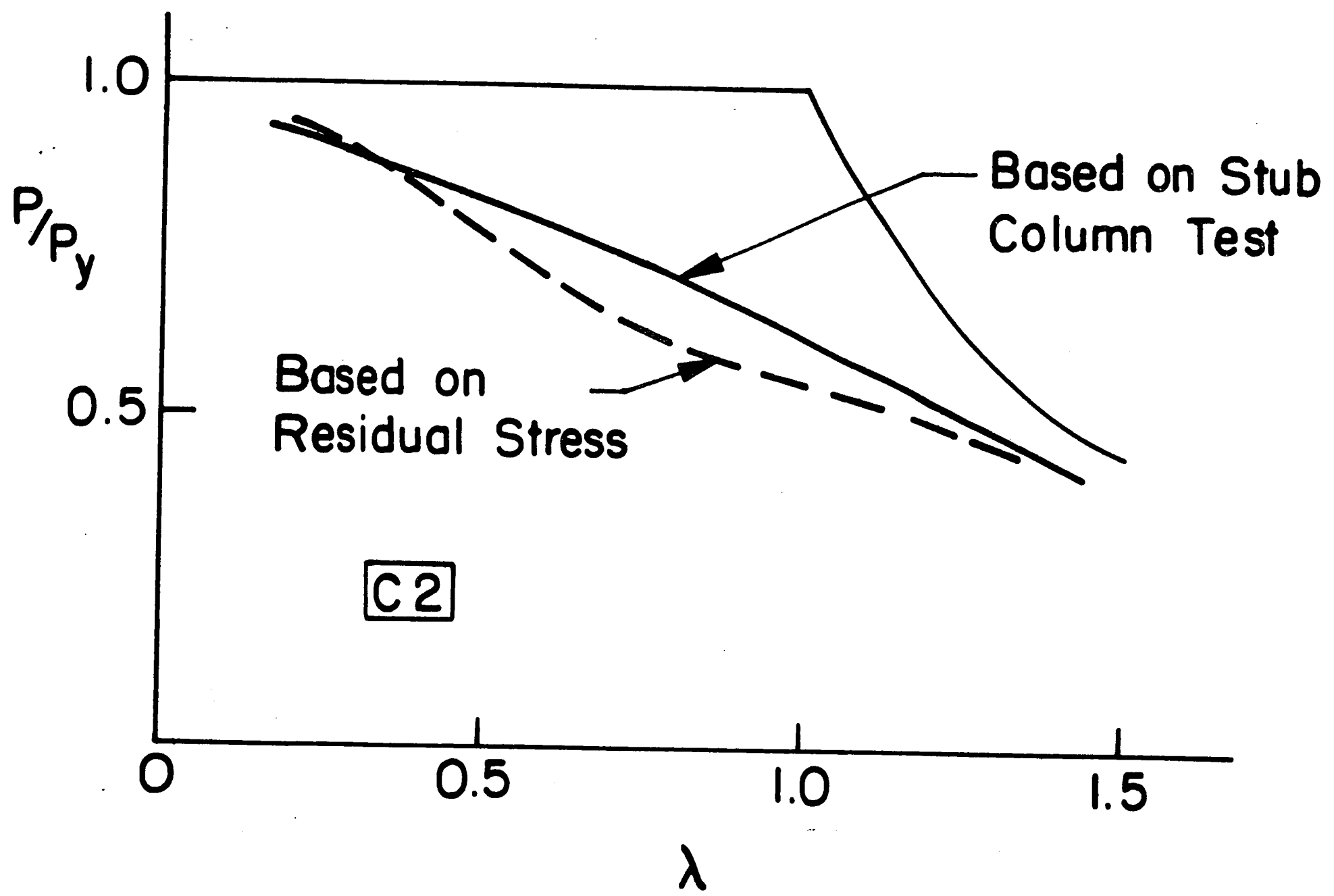


Fig. 36 Comparison Of Tangent Modulus Curves From Stub Column Tests With Those From Residual Stress Distributions

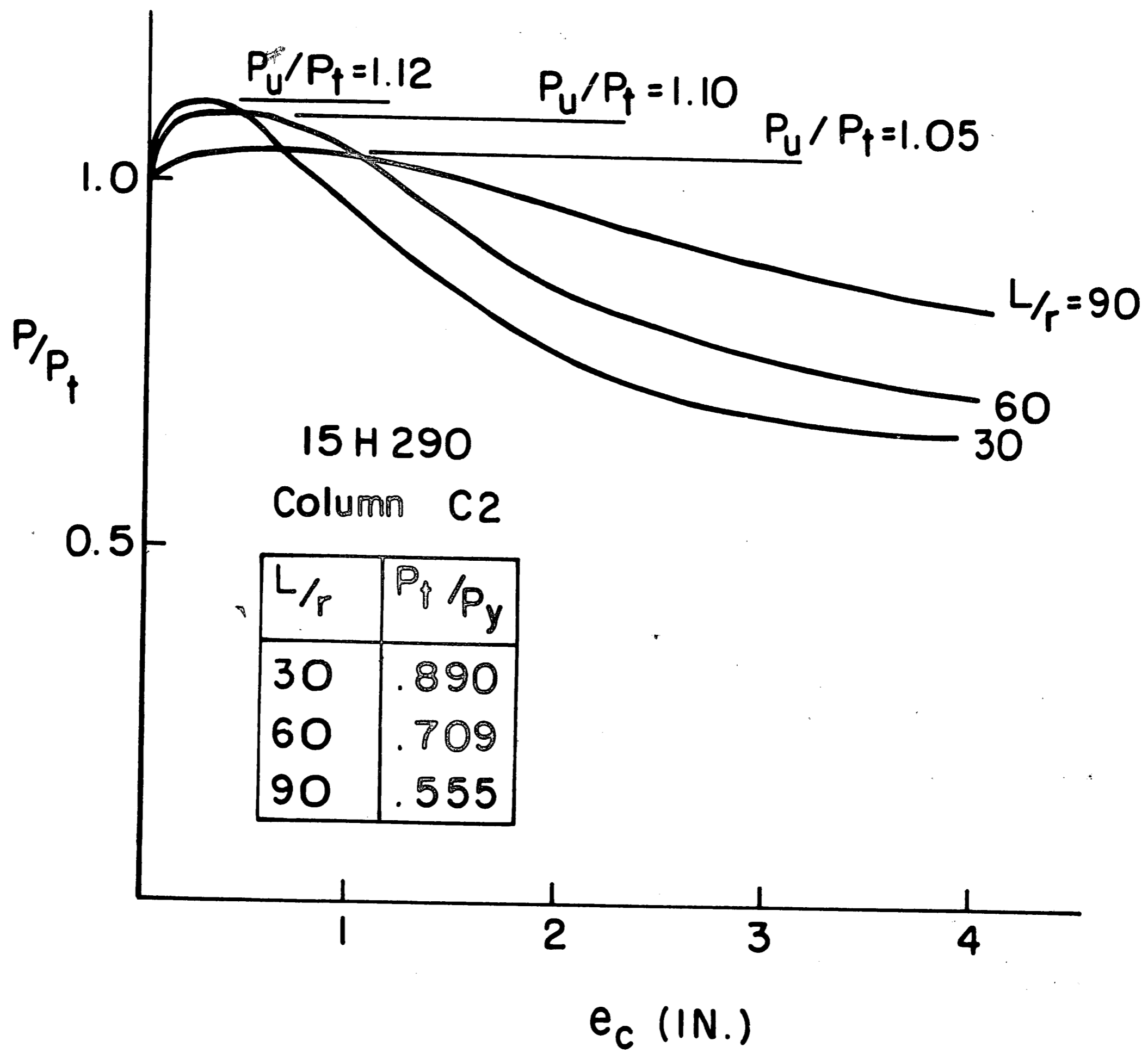


Fig. 37 Examples Of Load Versus Mid-Height Deflection  
Curves From Computer Program For Ultimate Strength

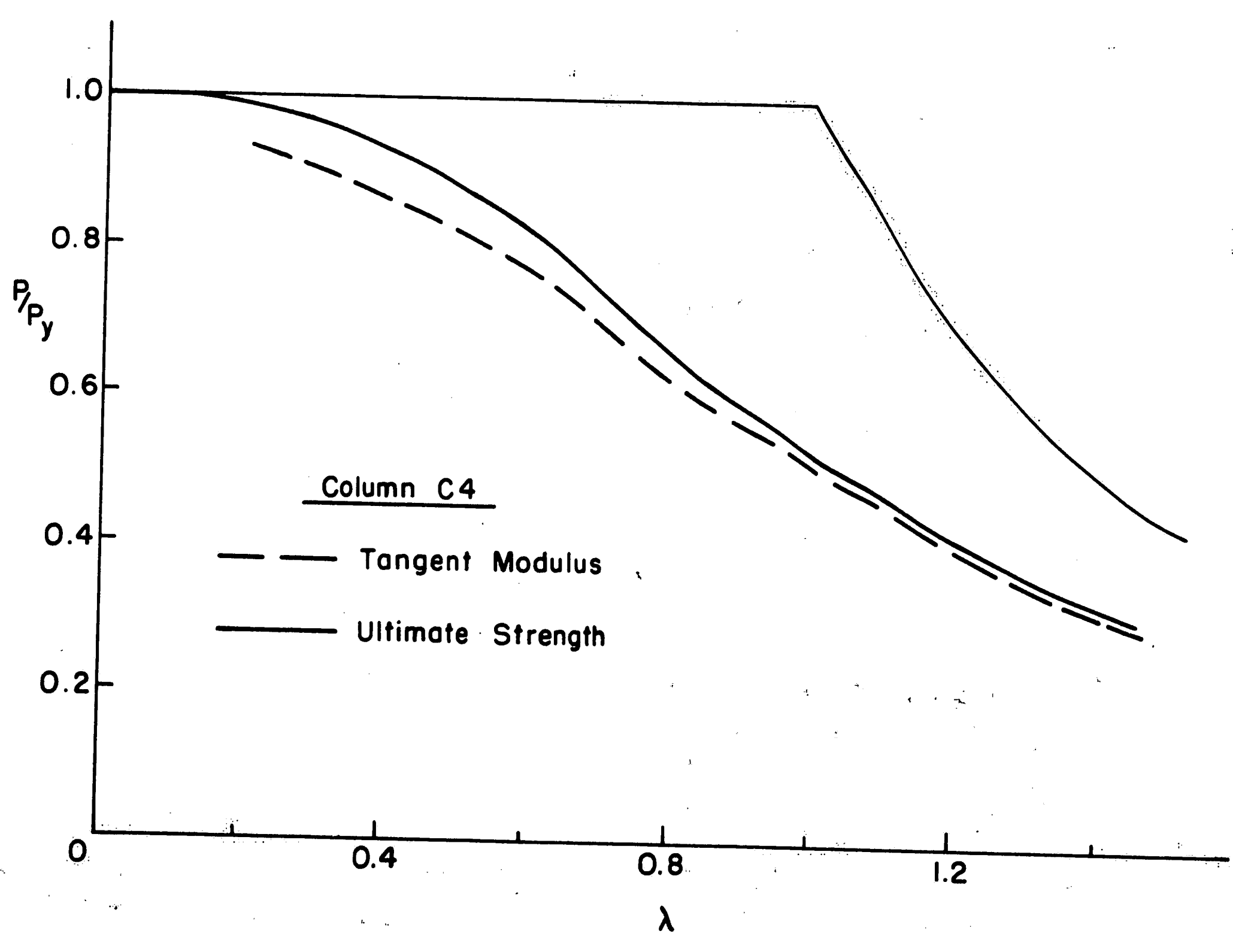
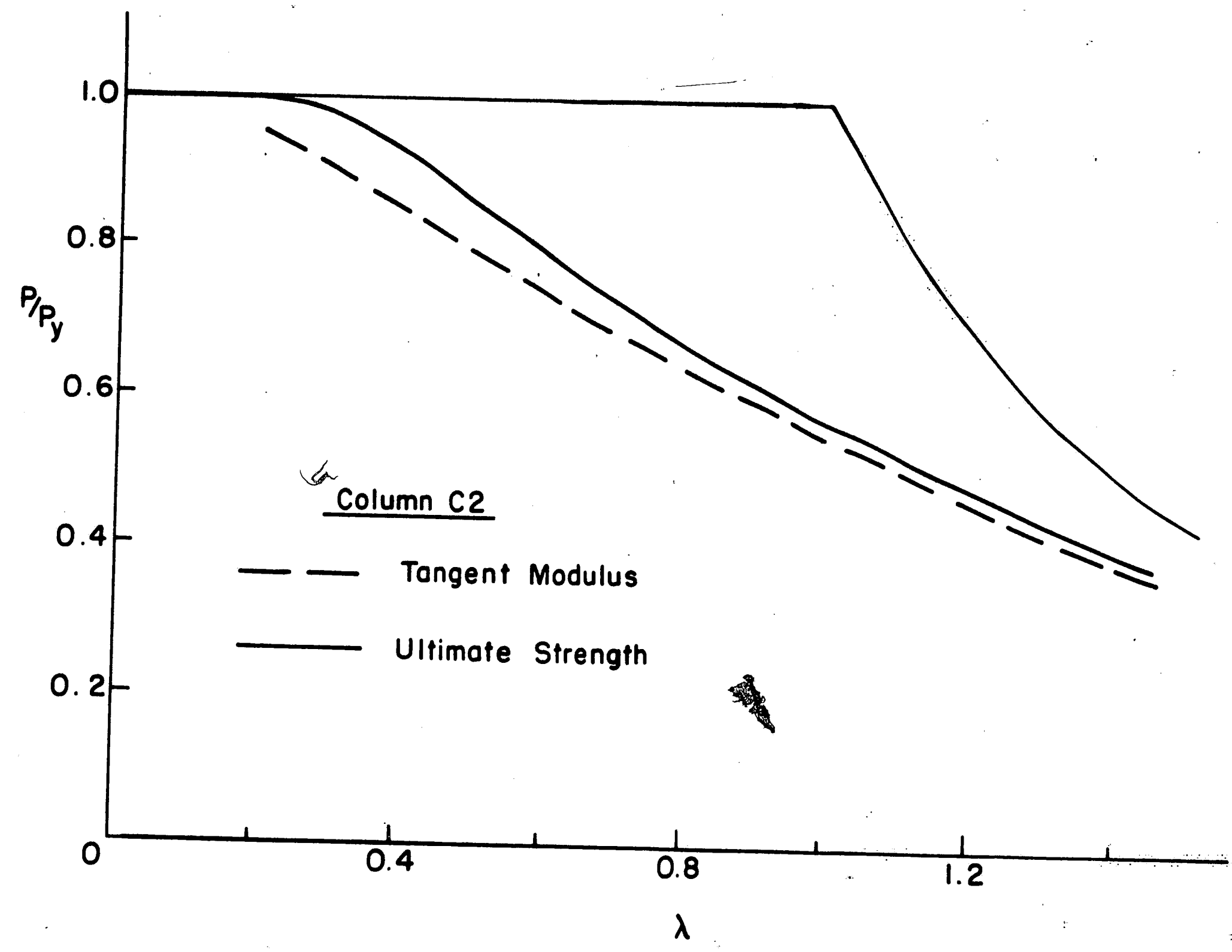


Fig. 38 Ultimate Strength Curves For Columns C2 and C4

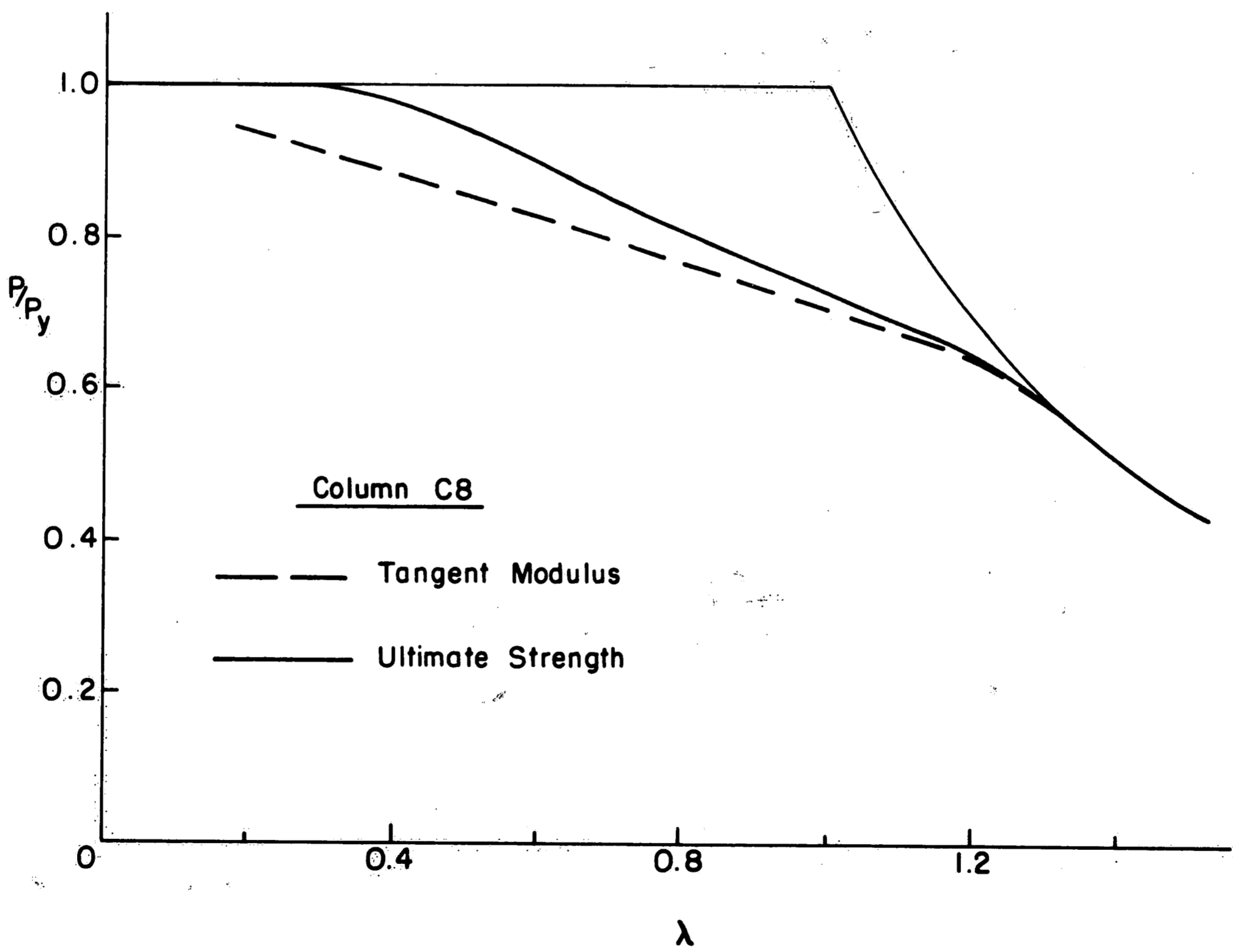
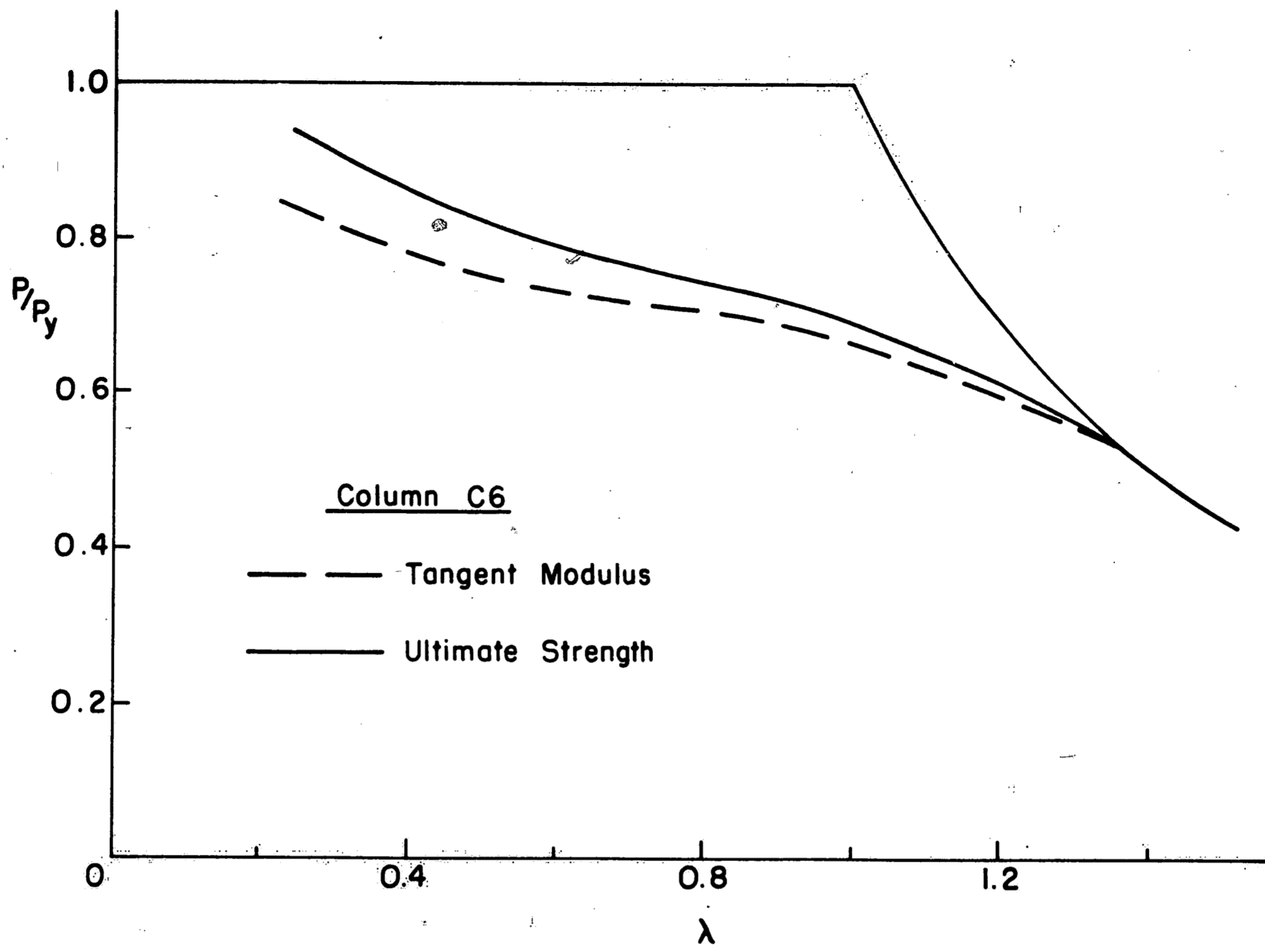


Fig. 39 Ultimate Strength Curves For Columns C6 and C8

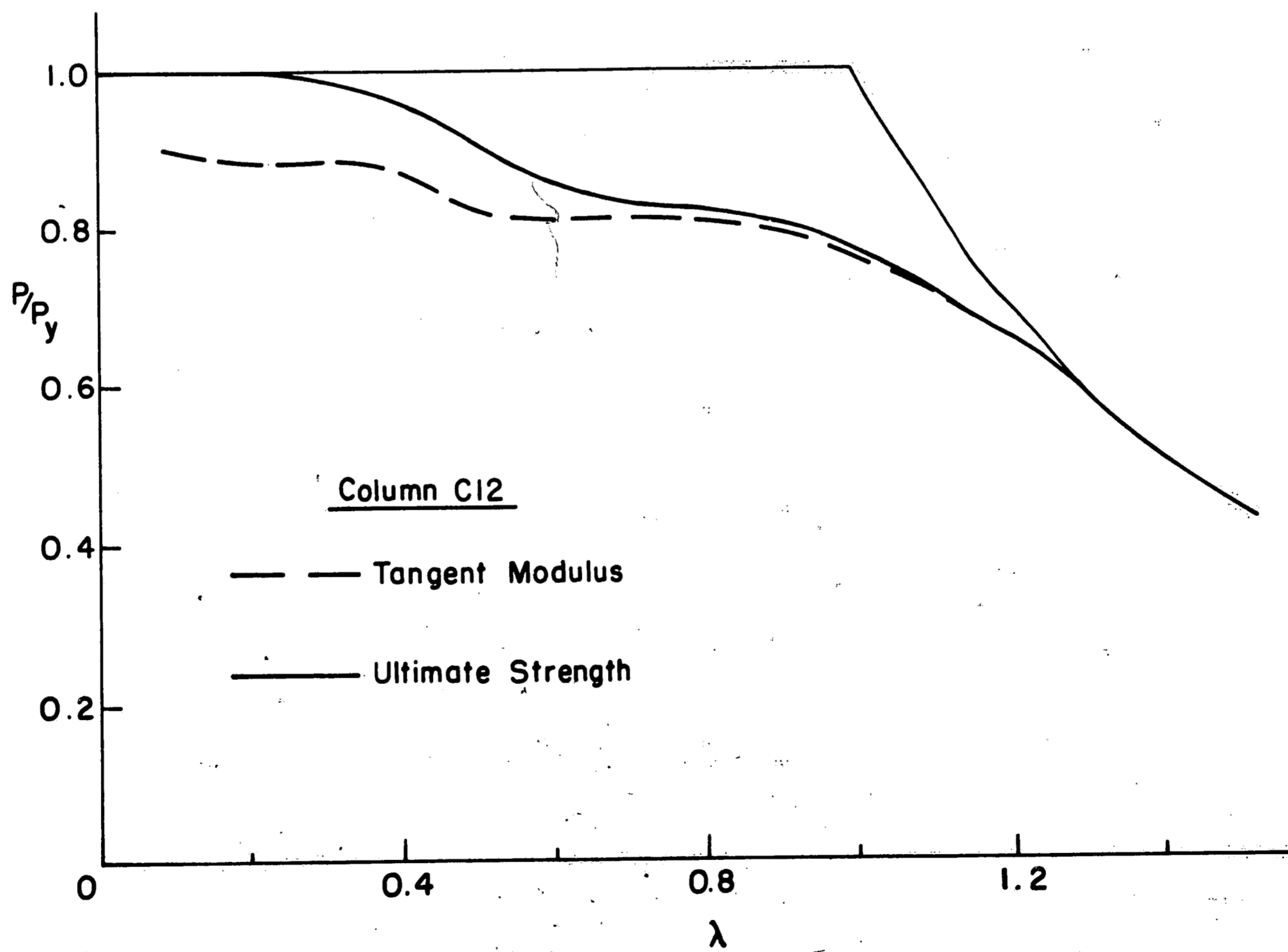
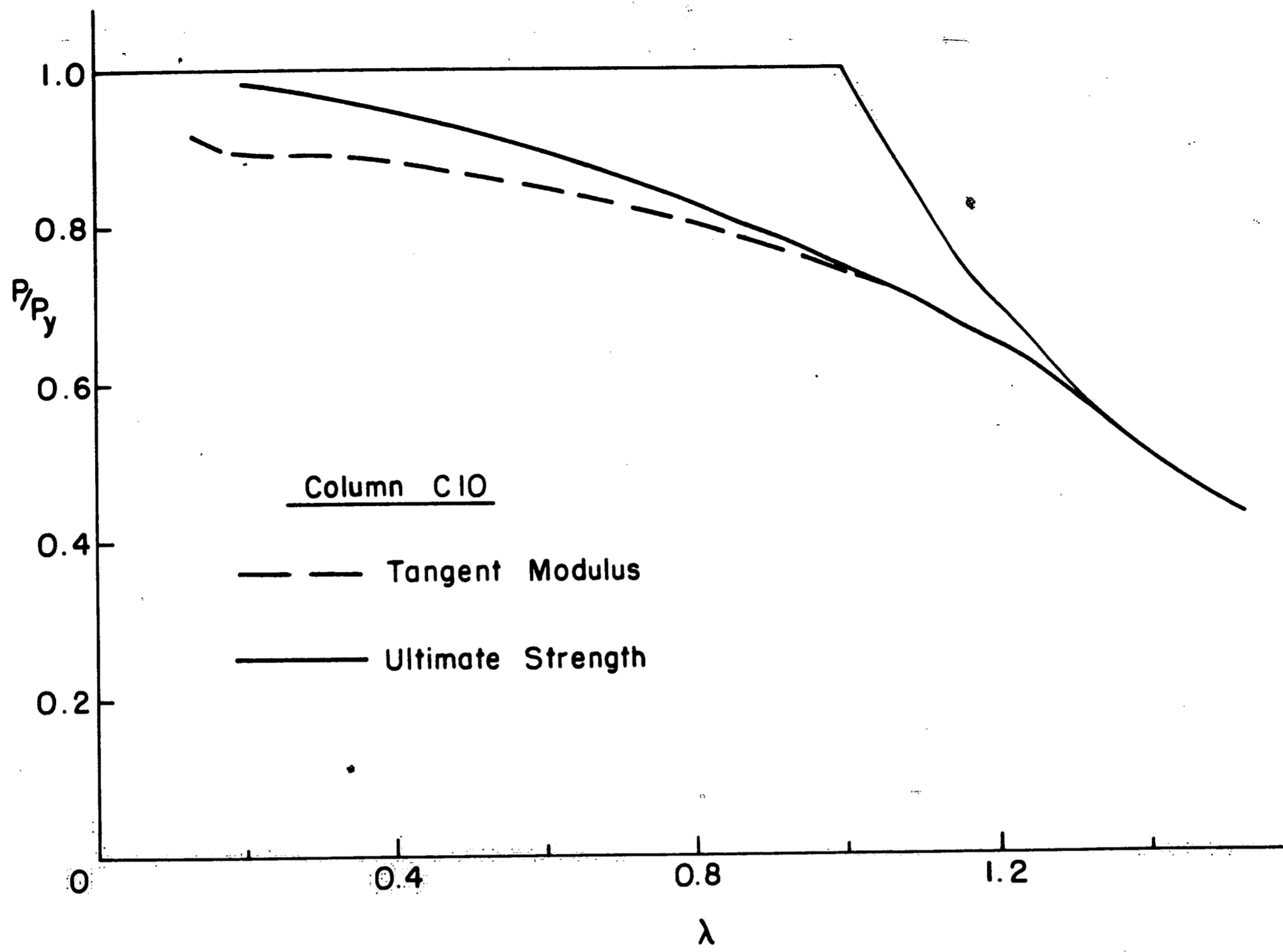


Fig. 40 Ultimate Strength Curves For Columns C10 and C12

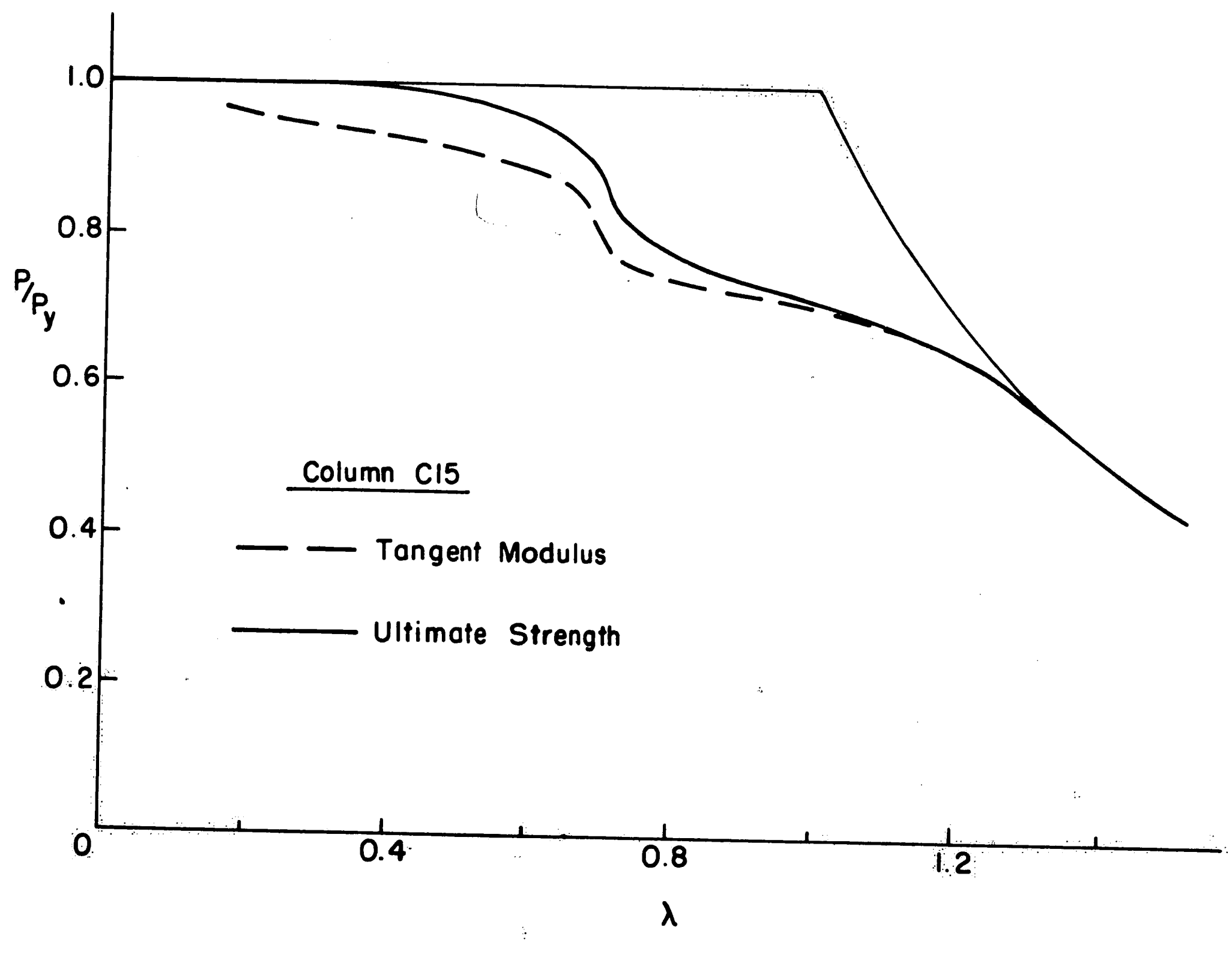
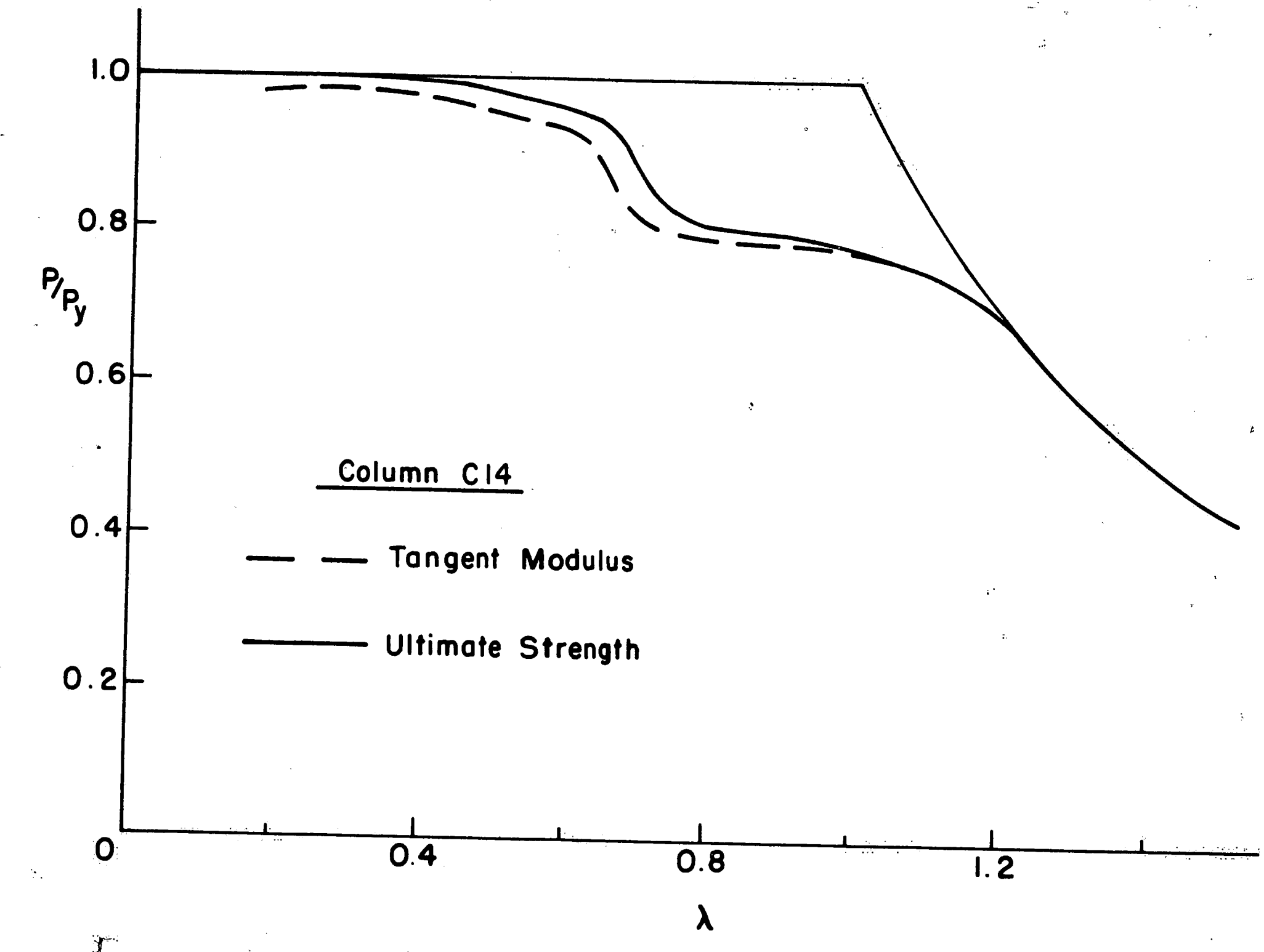


Fig. 41 Ultimate Strength Curves For Columns C14 and C15

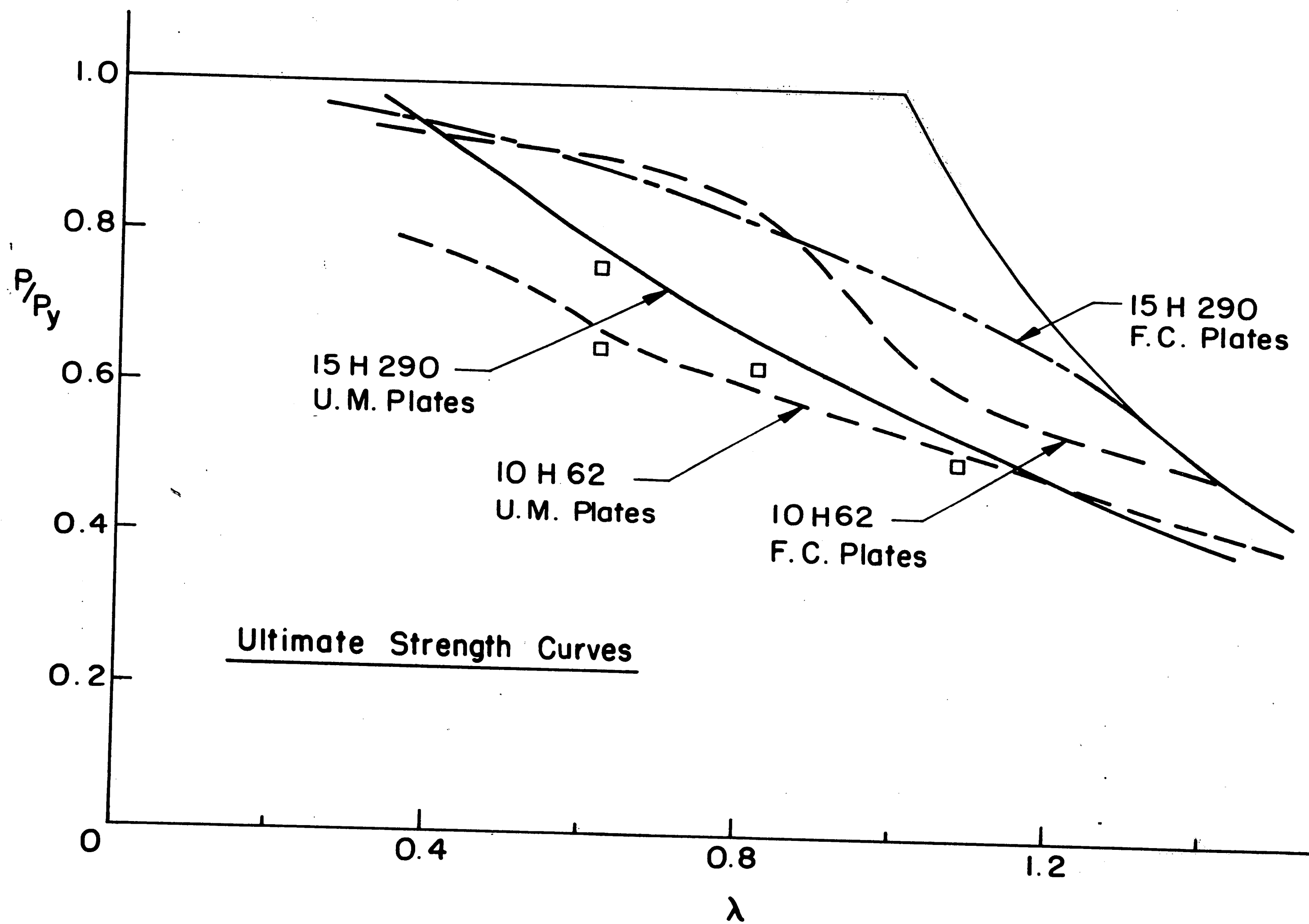


Fig. 42 Ultimate Strength Curves For Fillet Welded Specimens Of Mild Steel

9. REFERENCES

1. Column Research Council  
GUIDE TO DESIGN CRITERIA FOR METAL COMPRESSION MEMBERS, 2nd Edition, John Wiley & Sons, 1966.
2. L. Tall  
RECENT DEVELOPMENTS IN THE STUDY OF COLUMN BEHAVIOR, Jour., Inst. of Engineers, Australia, Vol. 36, Dec. 1964.
3. B. G. Johnston  
BUCKLING BEHAVIOR ABOVE THE TANGENT MODULUS LOAD Trans., ASCE, Vol. 128, Part 1, 1963.
4. N. J. Hoff  
BUCKLING AND STABILITY Jour., Royal Aero. Soc., Vol. 58, Jan. 1964.
5. L. Tall, et.al.  
STRUCTURAL STEEL DESIGN, Ronald Press, 1964.
6. L. S. Beedle, L. Tall  
BASIC COLUMN STRENGTH, ASCE Proc., ST7, Vol. 86, July 1960.
7. F. R. Estuar, L. Tall  
EXPERIMENTAL INVESTIGATION OF WELDED BUILT-UP COLUMNS, Welding Journal, Vol. 42, April 1963.
8. L. Tall  
WELDED BUILT-UP COLUMNS, Fritz Laboratory Report No. 249.29, April 1966.
9. N. R. Nagaraja Rao, M. Lohrmann, L. Tall  
EFFECT OF STRAIN RATE ON THE YIELD STRESS OF STRUCTURAL STEEL, Jour. of Materials (ASTM), Vol.1, No. 1, March 1966.
10. N. R. Nagaraja Rao, F. R. Estuar, L. Tall  
RESIDUAL STRESSES IN WELDED SHAPES, Welding Journal, Vol. 43, July 1964.
11. A. W. Huber, L. S. Beedle  
RESIDUAL STRESS AND THE COMPRESSIVE STRENGTH OF STEEL, Welding Journal, Vol. 33, Dec. 1954.
12. A. W. Huber  
RESIDUAL STRAIN MEASUREMENT, Fritz Laboratory Report No. 220A.17, March 1955.



13. A. W. Huber  
FIXTURES FOR TESTING PIN-END COLUMNS, ASTM  
Bulletin, No. 234, Dec. 1958.
14. WELDING HANDBOOK, 5th Edition, Section 2,  
American Welding Society, 1962.
15. A. W. Huber  
RESIDUAL STRESS IN WIDE-FLANGE BEAMS AND COLUMNS  
Fritz Laboratory Report No. 220A.25, July 1956.
16. M. Lohrmann, N. R. Nagaraja Rao, L. Tall  
RESIDUAL STRESSES IN AUTOMATICALLY WELDED PLATES,  
Fritz Laboratory Report in preparation.
17. F. R. Estuar  
WELDING RESIDUAL STRESSES AND THE STRENGTH OF  
HEAVY COLUMN SHAPES, Ph.D. Dissertation, Lehigh  
University, Aug. 1966.
18. R. K. McFalls, L. Tall  
A STUDY OF WELDED COLUMNS MANUFACTURED FROM FLAME-  
CUT PLATES, Fritz Laboratory Report No. 321.1,  
June 1967.
19. C. H. Yang, L. S. Beedle, B. G. Johnston  
RESIDUAL STRESS AND THE YIELD STRENGTH OF STEEL  
BEAMS, Welding Journal Research Suppl., April 1952.
20. Y. Fujita  
BUILT-UP COLUMN STRENGTH, Ph.D. Dissertation,  
Lehigh University, Aug. 1956.

10. VITA

William Augustin Cranston, the son of William Johnston Cranston, Jr., and Catherine Schatzel Cranston, was born on October 3, 1943, in San Antonio, Texas.

He received his primary education in Kingston, New York, and his secondary education in Newburgh, New York, graduating in June of 1961. He then attended Manhattan College in New York City, obtaining his Bachelor of Engineering degree in Civil Engineering in June of 1965.

He entered Lehigh University in September, 1965, as a research assistant in the Civil Engineering Department, and expects to receive his M. S. degree in October of 1967.